

Skyblazer



Lendon Jackson
AIAA: 1230062

Lendon C. Jackson



Olivia Scharf
AIAA: 1230060

Olivia Scharf



Bhawantha Nilaweera
AIAA: 1081997

Bhawantha N



Matthew Griebe
AIAA: 1230423

Matthew Griebe



Raghav Parikh
AIAA: 998655

Raghav Parikh



Skyler Jacob
AIAA: 807871

Skyler Jacob



Krishna Sitaula
AIAA: 1241011

KS



Brennan Wheatley
AIAA: 124127

Brennan Wheatley



Renaldo Rivera
AIAA: 1241257

Renaldo Rivera



Ethan Seiler
AIAA: 1241013

E Seiler

Advisor: Dr. Ronald Barrett-Gonzalez, AIAA: 022393

Ronald Barrett-Gonzalez

University of Kansas Department of Aerospace Engineering, Lawrence, KS

AIAA Graduate Team Modern Regional Jet Family

Date of Submission: May 13th, 2021

Compliance Matrix

First attempt at Compliance Matrix. The acronym NI stands for “Not Included” in the report at the moment and will be added in the coming reports. The question mark represents doubt for the if the content on the page number listed provides enough compliance.

	Requirement 50-Seat Airplane	Requirement 76-Seat Airplane	Compliance -100	Compliance -200	Page
EIS	2030 for first model and 2031 for second model.		2030	2031	1
Engines	Existing engine(s) or one that is in development that will be in service by 2029. Assumptions must be documented.		GE CF34-3	GE CF34-8C	43
Passenger Capacity (with 30- inch seat pitch)	50	76	50	76	43
Range	2,000 nmi	1,500 nmi	2,000 nmi	1,500 nmi	39
Cruise Mach Number	Minimum Mach 0.78 (Target: Mach 0.80)		0.8		29
Approach Speed	Less than 141 kts		115	141	37
Takeoff Length Over a 50 ft Obstacle (SL ISA + 18°F day)	4,000 ft	6,000 ft	4,000 ft	6,000 ft	80
Landing Length Over a 50 ft Obstacle (SL ISA + 18°F day)	4,000 ft	6,000 ft	4,000 ft	6,000 ft	80
Distance to Climb Up	Less than 200 nmi	-	<200 nmi	<200 nmi	38
Initial Cruise Altitude	FL 320	-	FL320	FL320	1
Takeoff and Landing Altitude	5,000 ft above MSL (ISA + 18°F)		5,000 ft above MSL (ISA + 18°F)		23
Crew No.	2 pilots and at least 1 cabin crew member per 50 passengers.		2 Pilots 1 Cabin Crew	2 Pilots 2 Cabin Crew	43
Pilot/Crew Weight	190 lbs		190 lbs		55
Baggage Weight per Pilot	30 lbs		30 lbs		55
Baggage Volume per Pilot	4 ft ³		4 ft ³		1
Passenger Weight	200 lbs		200 lbs		55
Baggage Weight per Passenger	40 lbs		40 lbs		80-81
Baggage Volume per Passenger	5 ft ³		5 ft ³		1
Seat Width	At least 17.2 inches (Target: 18 inches)		18		43
Aircraft Cross-Section	Stand up height in aisle similar to competitive aircraft. Baggage compartments are serviced ergonomically. Aisle width of at least 18 inches.		Stand Up Ailse Height 7' and Ailse Width 18"		42
Wingspan	At most 36 meters (Target: At most 24 meters)		77 ft		44

Acknowledgments

We would like to thank all of our family members and friends for their support. We would like to thank the entire Skyblazer team for collaborating and working well together to finish this report. We would like to give a special thanks to Dr. Barrett for all of his guidance throughout this project.



Table of Contents

Page #	
Compliance Matrix	ii
Acknowledgments	ii
List of Figures	iv
List of Tables	v
List of Symbols	vi
1....Introduction, Mission Specifications, and Mission Profile.....	1
2....Historical Review and Market Concept of Operations Comparison	3
2.1 50-Seat Regional Jet Historical Review	3
2.2 76-Seat Regional Jet Historical Review	5
2.3 Comparison of Concept of Operations	6
3....Design Optimization Function, Economics Model, Life-Cycle Cost Minimization and Weights	7
3.1 Design Optimization Function.....	7
3.2 Typical Routes, Legs, and Turnaround Time	9
3.3 Current Market Trends	11
4....STAMPED Analysis of Aircraft Regional Jet Market.....	19
4.1 Empty Weight to Takeoff Weight Ratio Market Analysis	19
4.2 Wing Loading Market Analysis.....	20
4.3 Sweep Angle Market Analysis	20
4.4 Wing Loading and Thrust-to-Weight Ratio Market Analysis.....	20
5.... Weight Sizing Code Generation	21
5.1 Aircraft Flight Modes Prescribed to Flight Phase.	21
5.2 Weight Sizing Code for Fuel Burn and Iteration of W_e , W_f , and W_{to}	22
6.... Wing and Powerplant Sizing	22
6.1 Takeoff and Landing Sizing	23
6.2 Climb and Ceiling Sizing.....	23
6.3 Cruise Sizing.....	25
6.4 Power Plant.....	26
6.5 Wing Fuel Volume	26
6.6 Complete Sizing Chart.....	26
6.7 Basic Performance Plots	28
7....Class I Configuration Matrix	30
7.1 Rejected Configurations	31
7.2 Accepted Configurations	32
7.3 Final Configuration Selection.....	33
7.4 Configuration Features and Airline Operations Experts' Observations.....	34
8.... V-n Gust and Maneuver Diagram and Flight Envelope	37
9.... Payload-Range and Fuel Burn	38
10.. Design and Sizing	39
10.1 Cockpit Layout and Design	40
10.2 Fuselage Layout.....	42
10.3 Engine Selection and Installation.....	44
10.4 Wing Layout	44
10.5 High Lift Devices.....	46
10.6 Empennage Sizing	46
10.7 Landing Gear Designs.....	50
11.. Weight and Balance	53
11.1 CG Excursion and Effects on Static Margin and Trim Drag	55
11.2 Items to Account for Static Margin and CG Excursion	55
12.. Advanced CAD.....	56
12.1 Substructure	59
13.. Aircraft Systems	61
13.1 Flight Control Systems	61
13.2 Propulsion Systems.....	63
13.3 Fuel Systems	63
13.4 Hydraulic System.....	64
13.5 Electric Systems.....	65
13.6 Escape System, Fire Detection, and Suppression System	67
13.7 Pressurization System	67
13.8 Pneumatic System.....	68
13.9 Oxygen System.....	69
13.10 Cabin Sterilization System	69
13.11 Cockpit Instrumentation	69
13.12 De Icing Systems.....	70
13.13 Window Rain, Fog, and Frost Control Systems	70
13.14 Lavatory, Galley, Water, and Waste Systems	70
13.15 Safety and Survivability	71
Ground Equipment and Servicing Vehicles Compatibility	71
13.16 Camera System.....	73
14.. Class II Stability and Control.....	73
15.. Performance and Acoustics.....	80
15.1 Takeoff Performance	80
15.2 Stall Performance.....	80
15.3 Drag Polar and Wetted Area	81
15.4 Acoustics.....	84
16.. Cost Analysis	85
References.....	87



List of Figures

	Page
Figure 1-1: Proposed Mission Profile Skyblazer-100 Series.....	2
Figure 1-2: Proposed Mission Profile of the Skyblazer-200 Series.....	2
Figure 2-1: De Havilland Comet 1 [2]	3
Figure 2-2: Embraer ERJ145 [5].....	3
Figure 2-3: Bombardier CRJ100 [7]	4
Figure 2-4: Bombardiers CRJ550 [8].....	4
Figure 2-5: Fairchild Dornier 428JET [9]	4
Figure 2-6: Embraer E170 [11]	5
Figure 2-7: Bombardier CRJ700 [10]	5
Figure 2-8: Mitsubishi SpaceJet M100 [14].....	5
Figure 3-1: Regional Jet and Turboprop Routes of Four Major US Airlines [18].....	9
Figure 3-2: Embraer 170/190 Ground Operations Example Diagram [23].....	10
Figure 3-3: Turn Around Time for Typical Jet vs Skyblazer Series	11
Figure 3-4: US Fleet 2020 RJ 50-Seat Market Ownership	11
Figure 3-5: US Fleet 2020 RJ 76-Seat Market Ownership	11
Figure 3-6: Historical Trend of American Airlines Direct Operating Costs (DOC) [24]	13
Figure 3-7: Historical Trend of American Airlines Fuel and Personnel Costs [24].....	14
Figure 3-8: Total Stage Time Comparison of Average RJ, 30%+ High L/D RJ, and Skyblazer Family [25]	15
Figure 3-9: DOC Comparison of Conventional, Aerodynamically Advanced and Skyblazer Series RJ's[26][27][28].....	16
Figure 3-10:Relative Fleet and Flight Crew Sizes to Accommodate a Typical Regional Jet Route Structure [26][27][29].....	17
Figure 3-11: SkyBlazer Regional Jet Design: A New Approach to Reducing Acquisition, Direct Operating and Life Cycle Costs [24].....	18
Figure 4-1: Empty Weight to Takeoff Weight Ratio Market Trend Through Time.....	19
Figure 4-2: Wing Loading Market Trend Through Time	20
Figure 4-3: Sweep Angle Market Trend Through Time	20
Figure 4-4: Wing Loading and Thrust-to-Weight Ratio Market Trend Through Time	21
Figure 6-1: Skyblazer 100 Drag Polars	24
Figure 6-2: Skyblazer 200 Drag Polars	25
Figure 6-3: Skyblazer 100 Sizing Chart.....	27
Figure 6-4: Skyblazer 200 Sizing Chart.....	27
Figure 6-5: Skyblazer-100 Performance Plots	28
Figure 6-6: Skyblazer-200 Performance Plots	29
Figure 7-1: Configuration Matrix for Class I Design	30
Figure 7-2: Low Wing/Low Engines	31
Figure 7-3: Blended Wing Aft Engines	31
Figure 7-4: Low Wing Duel Tail	31
Figure 7-5: High Wing Canard	31
Figure 7-6: Infinity Wing	32
Figure 7-7: Blended Wing High Engines	32
Figure 7-8: High Wing	32
Figure 7-9: High Wing/High Engines.....	33
Figure 7-10: Low Wing/Aft Engines	33
Figure 7-11: High Wing/ High Engine Final Selection	34
Figure 7-12: Easy Line Maintenance for Engine at 10 ft off Ramp like Skyblazer, DC-9, EMB-145, and CRJ [31]	34
Figure 7-13: Skyblazer-200 Cabin Door Locations for Normal and Emergency Operations.....	35
Figure 7-14: C-17 Globemaster II Landing Gear and Fuel Sponsons [32].....	35
Figure 7-15: Number of Baggage Unloaders with Manual vs. Sliding Carpet [33].....	36
Figure 7-16: Continuous Nose-to-Tail Magic Carpet System	36
Figure 8-1: 50-Seat V-n Maneuver and Gust Diagram	37
Figure 8-2: 76-Seat Flight Envelope.....	38
Figure 9-1: Payload-Range Diagram for Varying Cruise Velocities	39
Figure 10-1: Cockpit Layout	40
Figure 10-2: 95 th and 20 th Percentile Male and Female in Cockpit	40
Figure 10-4: Pilot Maximum Viewing Angles	41
Figure 10-4: Cockpit Side View	41
Figure 10-5: Skyblazer vs. FAR 25 Recommended Cockpit Viewing Angles	41
Figure 10-6: Fuselage Cross Section	42
Figure 10-7:50 Seat 2x2 Cabin Layout Top view..	43
Figure 10-8:76 Seat 2x2 Cabin Layout Top view..	43
Figure 10-10: GE CF34-3 [34]	44
Figure 10-10: GE CF34-8C [35].....	44
Figure 10-11: Three-View of the Engine Mounting Structure	44
Figure 10-12: Integrated Winch System and Maintenance	44
Figure 10-13: Wing Front and Isometric View.....	45
Figure 10-14: Upper Surface Wing Blowing.....	46
Figure 10-15: Skyblazer-100 AC and CG Location Plot with Horizontal Tail Area	49



Figure 10-16: Skyblazer-200 AC and CG Location Plot with Horizontal Tail Area.....	49	Figure 13-12: Cockpit Oxygen.....	69
Figure 10-17: Yawing Moment Coefficient Plot with Vertical Tail Area.....	49	Figure 13-13: Cockpit.....	69
Figure 10-18: 76-Seater Side View and Clearance Angle.....	50	Figure 13-14: Wing and Engine Cowl De Icing Method.....	70
Figure 10-19: 50-Seater Side View and Clearance Angle.....	50	Figure 13-15: Lavatory Layout and Galley	71
Figure 10-20: Landing Gear Front View.....	51	Figure 13-17: Traffic Alert and Collision Avoidance System	71
Figure 10-21: Landing Gear Placement Method.....	51	Figure 13-17: Enhanced ground proximity warning system [42]	71
Figure 10-22: Nose-Wheel Strut Layout.....	53	Figure 13-18: Service Vehicle Compatibility	72
Figure 11-1: 50-Seat Class II CG Excursion Diagram	54	Figure 13-19: Embraer 190 vs. Skyblazer Flight line Footprint Comparison.....	72
Figure 11-2: 76-Seat Class II CG Excursion Diagram	54	Figure 13-20: Skyblazer vs. Embraer 190 Terminal Packing	73
Figure 12-1: Skyblazer 100 Three-View	56	Figure 14-1: Skyblazer-100 AAA Trim Diagram During Cruise	76
Figure 12-2: Skyblazer 200 Three-View	56	Figure 14-2: Skyblazer-200 AAA Trim Diagram during Cruise	76
Figure 12-3: Situational Rendering of 100 Series ..	57	Figure 14-3: Skyblazer-100 AAA Short Period Frequency Requirements during Cruise	77
Figure 12-4: Situational Rendering of 200 Series ..	57	Figure 14-4: Skyblazer-200 AAA Short Period Frequency Requirements during Cruise	77
Figure 12-5: Exploded View of Series 100 and 200	58	Figure 14-5: Skyblazer-100 AAA Dutch Roll Frequency and Damping Ratio Requirements during Cruise.....	78
Figure 12-6: Skyblazer 100 and 200 Series Substructure	59	Figure 14-6: Skyblazer-200 AAA Dutch Roll Frequency and Damping Ratio Requirements during Cruise.....	79
Figure 12-7: Fuselage Substructure for 50-Seat and 76-Seat	59	Figure 15-1: Skyblazer Series Schrenk's Approximation Plot for Clean Condition.....	80
Figure 12-8: Wing Substructure	60	Figure 15-2: 50-Seater Perimeter Cross-section Analysis	82
Figure 12-9: Horizontal Tail Substructure	60	Figure 15-3: 76-Seater Perimeter Cross-section Analysis	82
Figure 12-10: Vertical Tail Substructure.....	60	Figure 15-4: 50 Seat and 76 Seat Variant Wetted Area	83
Figure 12-11: Engine Mount Substructure.....	61	Figure 15-5: 50 Seat Variant Wetted Area	83
Figure 13-1: Flight Control Systems Layout Diagram	62	Figure 15-6: Skyblazer Acoustic Refraction.....	84
Figure 13-2: Right Side Fuel System	63	Figure 15-7: EMB-190 Acoustic Refraction.....	84
Figure 13-3: Left Side Fuel System	63	Figure 15-8 Stage 5 Airplane Noise Standards [44]	84
Figure 13-4: Fuel System Layout Diagram Top View	64	Figure 16-1: Aircraft Price vs Units Manufactured [45][46]	[47][48]
Figure 13-5: Hydraulic System Layout Diagram ...	65	85
Figure 13-6: Hydraulic System Layout Diagram ...	65		
Figure 13-7: Syblazer 100 and 200 Electrical System Load Summary	66		
Figure 13-8: Electrical System Layout Diagram.....	66		
Figure 13-9: Escape System and Fire Extinguisher locations	67		
Figure 13-10: Pressurization System Schematic	68		
Figure 13-11: Pneumatic System Schematic	68		

List of Tables

	Page #
Table 1-1: Regional Jet Family Design Specifications [1].....	1
Table 1-2: Additional Requirements and Objective Design Criteria [1]:	2
Table 2-1: 50-Seat Regional Jet Comparison.....	6
Table 2-2: 76-Seat Regional Jet Comparison.....	6
Table 3-1: Design Requirements	7
Table 3-2: Specified Objectives.....	8
Table 3-3: Ancillary Objectives.....	8
Table 5-1: Flight Mode Associated with Flight Phase	21
Table 5-2: Aircraft Fuel Fractions	22



Table 5-3: Weights for Skyblazer 100 and 200 Series	22	Table 13-1: Actuator Sizing For Control Surface Forces for Both Aircraft	61
Table 6-1: Fuel Volume	26	Table 14-1: Skyblazer Series Determined AAA Stability Metrics	74
Table 9-1: Fuel Burn Comparison	39	Table 14-2: Allowable Short Period Damping Ratios for Dynamic Longitudinal Stability [43]	74
Table 10-1: Skyblazer 100 and 200 Series Salient Characteristics	40	Table 14-3: Allowable Phugoid Damping Ratios for Dynamic Longitudinal Stability [43]	74
Table 10-2: Horizontal and Vertical Tail Volume Coefficients of Similar Aircraft	47	Table 14-4: Time to Double Amplitude for Roll Mode Lateral-Directional Stability [43]	74
Table 10-3: Skyblazer Series Projected Empennage Characteristics	47	Table 14-5: Time to Double Amplitude for Spiral Mode Lateral-Directional Stability [43]	74
Table 10-4: Empennage Selected Sizing Values	48	Table 14-6: Skyblazer Series Class II Longitudinal Stability and Control Derivatives	75
Table 10-5: Critical Engine Out Rudder Deflection Values	50	Table 14-7: Skyblazer Series Class II Lateral-Directional Stability and Control Values	75
Table 10-6: Landing Gear Wheel Dimensions	50	Table 14-8: Ride Comfort Index Values for Skyblazer Series and Competing Regional Jet Aircraft	79
Table 10-7: Landing Gear Loads	51	Table 15-1: Class II Performance for the Skyblazer Series	80
Table 10-8: Determined Static and Dynamic Tire Loads for the Skyblazer Series	52	Table 15-2: Wing Wetted Area Characteristics	83
Table 10-9: Landing Gear Strut and Tire Deflection for the Skyblazer Series	52	Table 15-3: Empennage Wetted Area Characteristics	83
Table 10-10: Tire Selection and Specifications for the Skyblazer Series	53	Table 15-4: Total Wetted Area	83
Table 11-1: : 50-Seat CG Excursions and Weights for Load Cases	53	Table 16-1: Skyblazer Cost and Price	85
Table 11-2: 76-Seat CG Excursions and Weights for Load Cases	53	Table 16-2: Skyblazer General Costs in Millions of Dollars	86
Table 11-3: 50-Seat Weight and Balance Sizing	55	Table 16-3: Skyblazer Direct Operating Cost in Dollars Per Nautical Mile	86
Table 11-4: 76-Seat Weight and Balance Sizing	55	Table 16-4: Skyblazer Direct Operating Cost in Millions of Dollars	86
Table 12-1: CAD Model Materials	58	Table 16-5: Potential Profit of Skyblazer Aircraft	86
Table 12-2: Fuselage Characteristics	59		
Table 12-3: Wing Substructure Characteristics	60		
Table 12-4: Horizontal Tail Substructure Characteristics	60		
Table 12-5: Vertical Tail Substructure Characteristics	60		

List of Symbols

<u>Symbols</u>	<u>Description</u>	<u>Units</u>
A	Aspect ratio	~
AO _k	Ancillary design objectives	~
AR	Aspect ratio	~
b	Span	ft
BFL	Balanced Field Length	ft
\bar{c}	Mean geometric chord	ft
c _j	Thrust specific fuel consumption	lb/(lb-hr)
C	Coefficient	~
C _D	Coefficient of drag	~
C _L	Coefficient of lift	~
C _m	Pitching Moment Coefficient	~
d	Diameter	ft
d _i	Distance	ft
e	Oswald Efficiency Factor	~
F	Pressure	psi
h	Height	ft



i	Incidence angle	deg
k	Feedback Gain	deg/deg
K	Kinetic Energy	ft-lbf
l	Length	ft
L/D	Lift-to-Drag Ratio	~
M	Mach speed	Mach
M _{ff}	Mission Fuel Fraction	~
n	Load Factor	g's
\tilde{N}	Landing Gear Load Factor	~
N _D	Critical Induced Yawing Moment	ft-lb
O _j	Specified design objectives	~
P	Load	lbf
\bar{q}	Dynamic Pressure	slugs/ft/s ²
r	Radius	in
R	Range	nmi
R _i	Design requirements	~
s	Field Distance	ft
\acute{s}	deflection	in
S	Wing area	ft ²
SR	Specific Range	nmi/lbf
t	Time	sec
t/c	thickness-to-chord ratio	~
T	Thrust	lb
V	True air speed	kts
\bar{V}	Volume coefficient	~
w	Width	ft
W	Weight	lb
X	CG distance to quarter-chord of the MGC	ft
\bar{X}	Location from Leading Edge of the Wing MGC	~
y	Semispan	ft
Yr	Calendar Year	yr

<u>Greek Symbols</u>	<u>Description</u>	<u>Units</u>
α	Angle of Attack	deg
$\dot{\alpha}$	Angle of Attack Rate	rad/s
β	Sideslip Angle	deg
$\dot{\beta}$	Sideslip Angle Rate	deg
Γ	Anhedral Angle	deg
δ	Pressure ratio	~
δa	Change in Aileron Deflection	deg
δe	Change in Elevator Deflection	deg
δr	Change in Rudder Deflection	deg
Δ	Change in	deg
ϵ	Downwash	deg
ζ	Damping Ratio	~
η	Efficiency	~
λ	Taper ratio	~
Λ	Sweep angle	deg
ρ	Density	slug/ft ³
σ	Air density ratio	~
τ	Wing Thickness-to-Chord Ratio	~
Ψ	Dihedral Angle	deg
ω_n	Natural Frequency	rad/s



<u>Subscripts</u>	<u>Description</u>	<u>Units</u>
a	Maneuver	~
ac	Aerodynamic Center	~
alt	Altitude	~
A	Aircraft	~
b	Designed Maximum Gust Intensity	~
c	Cruise	~
cg	Center of Gravity	~
cl	Clearance	~
cr	Critical	~
d	Dive	~
dr	Dutch Roll Mode	~
eng	Engine	~
E	Empty	~
f	Fuselage	~
F	Fuel	~
g	gravity	~
h	Horizontal tail	~
is	Inboard Sweep	~
l	Rolling Moment	~
L	Landing	~
max	Maximum	~
mc	Minimum Control	~
min	Minimum	~
M	Main Landing Gear	~
MD	Dynamic Main Gear	~
MDT	Main Dynamic Tire	~
MST	Main Static Tire	~
n	Yawing Moment	~
ND	Dynamic Nose Gear	~
NDT	Nose Dynamic Tire	~
NS	Static Nose Gear	~
NST	Nose Static Tire	~
o	Zero-Lift	~
oe	Operating Empty	~
os	Outboard Sweep	~
out	Outer	~
ph	Phugoid Mode	~
pl	Payload	~
q	Pitch Rate	~
r	Yaw Rate	~
R	Roll Mode	~
shock	Shock Absorption	~
sl	Static Loaded	~
sp	Short Period Mode	~
ss	Strut Stroke	~
S1	Stall	~
SL	Sea Level	~
t	Touchdown	~
total	Total	~
tire	Tire	~
TO	Take-off	~
TOFL	Takeoff field length	~



TO(1engine)	Take-off OEI	~
u	Forward Flight	~
v	Vertical tail	~
ui	Unloaded Inflation	~
w	Wing	~
wf	Wing-Fuselage	~
y	Side Force	~
2D	Two-Dimensional	~
2S	Double Amplitude Spiral Mode	~
25%	25% Growth	~

<u>Abbreviations</u>	<u>Description</u>	<u>Units</u>
AC	Aerodynamic Center	~
ADA	Aeronautical Development Agency	~
AEO	All Engines Operating	~
AIAA	American Institute of Aeronautics and Astronautics	~
BFL	Balanced Field Length	~
CAD	Computer Aided Design	~
CFR	Current Federal Regulations	~
CG	Center of Gravity	~
CGR	Climb Gradient Requirement	~
CTOL	Conventional Take-Off and Landing	~
DOC	Direct Operating Cost	~
EIS	Entry Into Service	~
FAA	Federal Aviation Administration	~
FAR	Federal Aviation Regulation	~
FL	Flight Level	~
GD	Gear Down	~
GE	General Electric	~
GOF	General Optimization	~
GU	Gear Up	~
HT	Horizontal Tail	~
ICAO	International Civil Aviation Organization	~
IFR	Instrument Flight Rules	~
ISA	International Standard Atmosphere	~
LE	Leading Edge	~
MGC	Mean Geometric Chord	~
MSL	Mean Sea Level	~
MTOW	Maximum Take-Off Weight	~
O	Objective	~
OF	Optimization Function	~
OEI	One Engine Inoperative	~
R	Requirement	~
RFP	Request for Proposal	~
RJ	Regional Jet	~
ROC	Rate-of-Climb	~
ROWF	Relative Objective Weighting Function	~
SL	Sea Level	~
STAMPED	Statistical Time and Market Predictive Engineering Design	~
STD	Standard Deviation	~
USB	Upper Surface Blowing	~
VFR	Visual Flight Rules	~
VT	Vertical Tail	~



1 Introduction, Mission Specifications, and Mission Profile

The objective of this report is to document the design of a modern regional jet family. This includes a 100 series (50-seat) and a 200 series (76-seat) aircraft. This design request for a new series of regional jets was announced due to a predicted rise in domestic flights. This regional jet family must follow the US domestic airline “Scope Clause” agreements. The goal of this regional jet family series is more profitable with lower environmental impact than the existing 50-seat regional jet aircraft.

Table 1-1 contains design specifications for a regional jet family and is a simplified table of requirements and objectives outlined in the AIAA Request for Proposal as shown. This regional jet family consists of a 50-seat and 76-seat aircraft version. The design specifications include entry into service, engines, passenger capacity, performance characteristics, number of crew, weights, associated volumes, seat width, aircraft cross-section, and wingspan. In Table 1-1, a dash indicates a nonapplicable design specification. Table 1-2 contains additional requirement and objective design criteria.

Table 1-1: Regional Jet Family Design Specifications [1]

	50-Seat Airplane	76-Seat Airplane
EIS	2030 for first model and 2031 for second model.	
Engines	Existing engine(s) or one that is in development that will be in service by 2029. Assumptions must be documented.	
Passenger Capacity (with 30- inch seat pitch)	50	76
Range	2,000 nmi	1,500 nmi
Cruise Mach Number	Minimum Mach 0.78 (Target: Mach 0.80)	
Approach Speed	Less than 141 kts	
Takeoff Length Over a 50 ft Obstacle (SL ISA + 18°F day)	4,000 ft	6,000 ft
Landing Length Over a 50 ft Obstacle (SL ISA + 18°F day)	4,000 ft	6,000 ft
Distance to Climb Up	Less than 200 nmi	-
Initial Cruise Altitude	FL 320	-
Takeoff and Landing Altitude	5,000 ft above MSL (ISA + 18°F)	
Crew No.	2 pilots and at least 1 cabin crew member per 50 passengers.	
Pilot/Crew Weight	190 lbs.	
Baggage Weight per Pilot	30 lbs.	
Baggage Volume per Pilot	4 ft ³	
Passenger Weight	200 lbs.	
Baggage Weight per Passenger	40 lbs.	
Baggage Volume per Passenger	5 ft ³	
Seat Width	At least 17.2 inches (Target: 18 inches)	
Aircraft Cross-Section	Stand up height in aisle similar to competitive aircraft. Baggage compartments are serviced ergonomically. Aisle width of at least 18 inches.	
Wingspan	At most 36 meters (Target: < 24 m)	

Table 1-2: Additional Requirements and Objective Design Criteria [1]:

○ Economic Missions
▪ [R] Show fuel burn performance per trip and per seat and compare with the appropriate competitive aircraft at 500 and 1,000 nmi
○ [R] Meet 14 CFR 25.121 Climb Gradient Requirements
○ Certifications
▪ [R] Capable of VFR and IFR flight with an autopilot
▪ [R] Capable of flight in known icing conditions
▪ [R] Meets applicable certification rules in FAA 14 CFR Part 25
• All missions below assume reserves and equipment required to meet applicable FARs
▪ [O] Provide systems and avionics architecture that will enable autonomous operations
• Provide a market justification for choosing to either provide or omit this capability
• Determine how the design would change

Figure 1-1 below depicts a possible mission profile for the 50-seat airplane design specification. The profile is comprised of ten mission phases. The lengths of these segments are arbitrary and are primarily used to track the overall flow of the mission. Mission phase seven in the profile is the divert to alternate for 100 nmi due to a balked landing. Mission phase eight is an additional 45 minute loiter leg while waiting to begin final descent and landing.

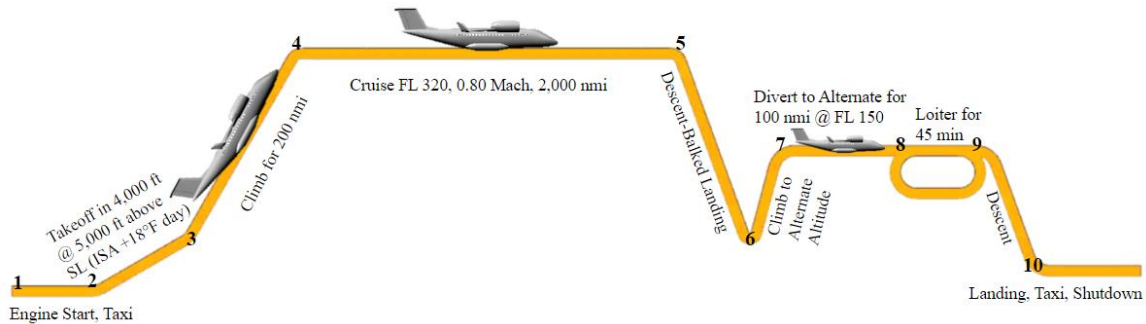


Figure 1-1: Proposed Mission Profile Skyblazer-100 Series

Figure 1-2 below depicts a possible mission profile for the 76-seat airplane design specification. The aircraft range decreased as the size of the vehicle increased. The takeoff distance also increased to compensate for the increased weight of the 76-seat aircraft compared to the 50-seat.

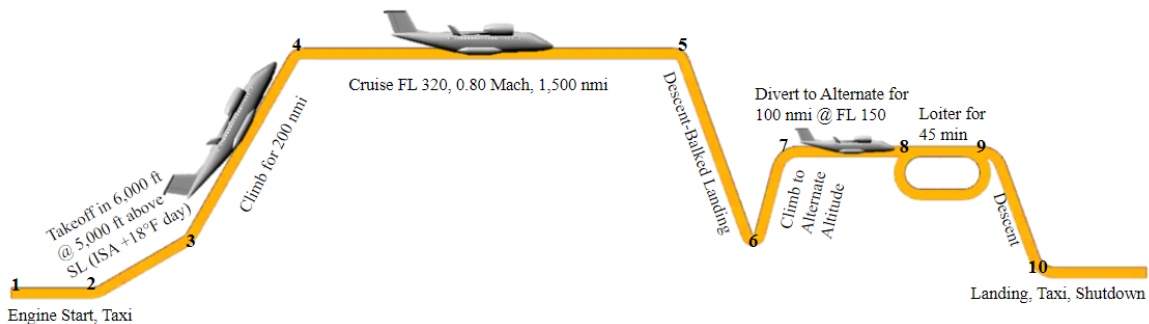


Figure 1-2: Proposed Mission Profile of the Skyblazer-200 Series

2 Historical Review and Market Concept of Operations Comparison

The current regional jet market is based upon aircraft designs with origins in the late 1980s and early 1990s. The industry forecasts that in the next 20 years nearly 2,000 new regional aircraft will be needed to meet the demand of regional travel while the current aircraft in the market begin to age out of service. 50-seat capacity regional jets such as those designed and manufactured in the 1980s were no longer marketable, as the industry moved towards optimizing passenger capacity to decrease the number of flights. However, the U.S. domestic airline “scope clause” opens the opportunity for more economically sound 50-seat aircraft to become more prevalent in the industry. 50-seat and 76-seat regional jets are climbing in popularity for customers with commuter jumps and shorter-range flights; this helps save money by filling aircraft rather than having empty seats on a larger jet. A historical review of regional jets is discussed to provide a reference for the trends and developments through time. A comparison of current regional jet market leaders is also shown with general characteristics to orient the reader.

2.1 50-Seat Regional Jet Historical Review

With its first flight in 1949, the British manufactured De Havilland DH106 Comet was the world’s first commercial jet airliner to enter service [2]. Twenty thousand pounds of thrust along with other technological and performance advancements allowed for the Comet to lead the commercial transport market post World War II. After two deadly crashes, investigation found a structural design flaw. This structural failure resulted from repeated pressurization which caused the fuselage to abruptly split [3]. After this investigation, the Comet or any of its successors would never carry another passenger again, leaving the market open to other developments in the United States.



Figure 2-1: De Havilland Comet 1 [2]

Development of the ERJ145 began in 1995 with certification and entry into service in 1996. With over 20 years of operation and servicing 36 airlines in 26 countries, this aircraft has logged over 26 million flight hours [4]. In total, over 1,200 aircraft based off the ERJ145 platform



Figure 2-2: Embraer ERJ145 [5]

have been delivered worldwide. This has established the ERJ program to be one of the most successful in the aircraft industry [4].

In the year 1991, the first of three CRJ100 prototypes, designed and manufactured by Bombardier Aerospace, conducted its maiden flight with entry into service the following year of 1992 with Lufthansa [6]. The CRJ200 variant was later established and retained all the features of the CRJ100 but used improved GE engines which resulted in a slightly increased range. In 2006, Bombardier Aerospace concluded producing the CRJ100 and its variant CRJ200, however most CRJ100s and 200s remain in service to date. This has established the CRJ series as a market leader over the past 20 plus years acting as a competitor to Embraer and the ERJ145.



Figure 2-3: Bombardier CRJ100 [7]

The CRJ550 is Bombardier’s newest aircraft type and will be the newest 50-seat regional jet in the market upon its entry into service. In 2019, Bombardier’s president described the CRJ550 as “the only solution in North America that can replace the existing fleet of ageing 50-seaters, a market of over 700 aircraft” [8]. This implies that the CRJ 550 will be projected to be a future market leader as other aircraft begin to age out of service. The CRJ550 has also been developed for logistical purposes for United Airlines. Due to labor contracts, United can only fly a finite number of jets that have over 50 seats at once, and the airlines have reached it cap, thus the development of this smaller capacity regional airliner.



Figure 2-4: Bombardiers CRJ550 [8]

The Fairchild Dornier 428Jet had a first flight scheduled for 2001 before it was cancelled. The aircraft was designed for 44 seats but proved inferior in the market to a 50-seat configuration; this caused the cancellation due to lower profits for less seats but similar operating costs. It was originally designed to compete against the Bombardier CRJ and Embraer E-Jet family.



Figure 2-5: Fairchild Dornier 428JET [9]

2.2 76-Seat Regional Jet Historical Review

Based in Canada, Bombardier created a CRJ700 series of regional jets with its first flight in 1999 and introduction into service in 2001 with production still continuing in 2020. Bombardier originally designed the CRJ700 to have a small commuter for shorter range flights that could compete with the Embraer 170. The CRJ700 was designed with three variations of different passenger seating arrangements, and there are also three fuel to weight options including standard, extended range, and long range. In 2007, the aircraft was modified to increase passenger comfort by enlarging the windows, increasing baggage storage, and adding better lighting. The CRJ700 has been modified through its 20 years of being service but has remained a strong competitor in the regional jet market due to its popularity by many large airlines, including Delta as shown in Figure 2-7.



Figure 2-7: Bombardier CRJ700 [10]

Embraer has a family of four E-Jets introduced in 1999 with production starting in 2002. The E170 and E175 models seat 72–78 passengers with the E175 being a slightly stretched version of the E170. The E-Jets currently lead the market in regional jets with vehicles in service around the globe in 35 countries with 53 different customers [12]. The E170 leads the market in operating costs with a fuel consumption proportional to the aircraft weight. Some other highlighted features include high cruising speeds with a maximum of 0.82M and one of the most spacious single-aisle interiors for a regional aircraft.



Figure 2-6: Embraer E170 [11]

Looking forward, Mitsubishi has a series of regional jets called SpaceJet with the M90 having its first flight in 2015. The newest M100 model is a prospective regional jet that has not been introduced into service due to financial losses within the company. However, with a new Pratt & Whitney GTFTM PW1200G engine and improved aerodynamic design, the lowered fuel consumption, and decreased operating costs create a competitive regional jet design [13]. The main goal of the M100 is a more comfortable passenger experience to better meet the needs of the customer with increased personal space, storage capacity, and available amenities.



Figure 2-8: Mitsubishi SpaceJet M100 [14]

2.3 Comparison of Concept of Operations

The concept of operations for some top regional jets in the market are shown in Table 2-1 and Table 2-2 below for the 50 and 76 seat regional jet categories respectively. The regional jets are also compared against the RFP requirements to show an evaluation of the market competition.

Looking at the 50-seat regional jet concept of operations comparison in Table 2-1, none of the current market aircraft meet the RFP requirement for maximum range or field lengths for landing and takeoff. However, the maximum service ceiling is met by all aircraft. The Bombardier CRJ550 is the only aircraft with a lower maximum cruise speed.

Table 2-1: 50-Seat Regional Jet Comparison



Aircraft	Bombardier CRJ100 [15]	Embraer ERJ145 [4]	Bombardier CRJ550 [16]	RFP Requirement [1]
Max Service Ceiling (ft)	41,000	37,000	41,000	32,000
Max Cruise Speed (Mach)	0.81	0.78	0.70	0.8
Max Range (nmi)	1,650	1,550	1,378	2,000
Max Passengers	50	50	50	50
Takeoff Distance (ft)	6,290	7,448	5,265	4,000
Landing Distance (ft)	4,850	4,593	5,039	4,000

For the 76-seat regional jets, it is observed in Table 2-2 that most of the RFP requirements are already met by existing aircraft on the market. However, the maximum passenger specification are higher than the required 76 passengers, and the maximum cruise speed for the Bombardier CRJ700 does meet the 0.8 Mach speed requirement. All of the other aircraft concept of operations meets or surpass the RFP requirements.

Table 2-2: 76-Seat Regional Jet Comparison



Aircraft	Embraer E170 [12]	Bombardier CRJ700 [17]	Mitsubishi M100 [13]	RFP Requirements [1]
Max Service Ceiling (ft)	41,000	41,000	39,000	32,000
Max Cruise Speed (Mach)	0.82	0.70	0.78	0.8
Max Range (nmi)	2,150	1,702	1,910	1,500
Max Passengers	78	78	84	76
Takeoff Distance (ft)	5,294	5,265	5,770	6,000
Landing Distance (ft)	4,027	5,040	5,090	6,000

3 **Design Optimization Function, Economics Model, Life-Cycle Cost Minimization and Weights**

3.1 **Design Optimization Function**

An optimization function is a preliminary design method which uses mathematical formulation of design parameters to support a selection of an optimal configuration or design among alternatives. The development of the general optimization function (GOF) is based off of three weighting functions. Requirements (R_i), objectives based on specified design objectives (O_j), and objectives based on ancillary objectives (AO_k). After determining each of these weighting functions, they can be applied to the GOF equation below.

$$\text{General Optimization Function} = \text{GOF} = \prod_1^l R_i \left(\frac{1}{m} \sum_1^m O_j + \frac{1}{n\text{ROWF}} \sum_1^n \text{AO}_k \right) \quad \text{Eqn. 3.1}$$

Table 3-1: Design Requirements

R ₁	EIS, year
R ₂	Passenger Capacity
R ₃	Range, nmi
R ₄	Cruise, M
R ₅	Seat Width, in
R ₆	Aisle Width, in
R ₇	Span (Folded), ft
R ₈	Approach Speed, kts
R ₉	Max Takeoff Field Length, ft
R ₁₀	Max Landing Length, ft
R ₁₁	Cruising Altitude, ft
R ₁₂	Meet 14 CFR 25.121 Climb Gradient Requirements
R ₁₃	Capable of VFR and IFR Flight and Autopilot
R ₁₄	Capable of Flight in Known Icing Conditions
R ₁₅	Meets Applicable Certification Rules in FAA 14 CFR Part 25

The requirement weighting functions were developed based off the required design characteristics provided in the request for proposal [1]. Requirements are design qualities that must be met in order to have a competitive design which achieves each requirement. As a result, requirements are treated in a binary manner as seen in the equation below. Table 3-1 to the right includes each requirement that will be used in the optimization.

$$R_i(\text{binary}) = \begin{cases} 0 & \text{if criterion not met} \\ 1 & \text{if criterion met} \end{cases}$$

Unlike requirement functions, design and ancillary objectives are design characteristics that do not need to be met in order for the configuration to be considered for selection. Instead, these objectives act as configuration advancements and could make the design more competitive than a baseline design that simply meets the design requirements. Specified design objectives are objectives that can be found in the request for proposal, whereas ancillary objectives are formed by any additional design considerations taken into account that would make the design more competitive in the market. The ancillary objective function also requires a relative objective weighting factor (ROWF). This factor is placed on the ancillary objective to weight the

importance of the specified design objective with relation to the importance of the ancillary objective itself. Both design and ancillary objectives use linear grading methods.

Table 3-2: Specified Objectives

O ₁	Target Mach
O ₂	Target Seat Width
O ₃	(Span) Max ICAO Code B
O ₄	Autonomous Capabilities
O ₅	Maximize Structural Commonality Between -100 &-200
O ₆	Good Aesthetics
O ₇	Enhances Reliability WRT SOTA
O ₈	Reduced MRO load WRT SOTA
O ₉	Minimize DOC
O ₁₀	Minimize Production Costs

$$O_j = \begin{cases} 0 & \text{if worst in meeting objective} \\ \text{Linearly varying} & \text{if neither worst or best} \\ 1 & \text{if best in meeting objective} \end{cases}$$

$$AO_k = \begin{cases} 0 & \text{if worst in meeting objective} \\ \text{Linearly varying} & \text{if neither worst or best} \\ 1 & \text{if best in meeting objective} \end{cases}$$

After defining each requirement, specified objective, and ancillary objective, the ROWF shown in Eqn. 3.2 and GOF shown in Eqn. 3.3 have now been established and can be applied to later configurations as they are developed.

$$\text{ROWF} = \frac{\text{Importance of Spec'd Design Objectives}}{\text{Importance of Ancillary Design Objectives}} = \frac{2}{1} = 2 > \epsilon > 0 \quad \text{Eqn. 3.2}$$

$$\text{General Optimization Function} = \text{GOF} = \prod_{i=1}^{15} R_i \left(\frac{1}{10} \sum_{j=1}^{10} O_j + \frac{1}{16 * 2} \sum_{k=1}^{16} AO_k \right) \quad \text{Eqn. 3.3}$$

Table 3-3: Ancillary Objectives

AO ₁	Reduce total fuel burn to most efficient in class
AO ₂	Minimize Time of Ground per turn
AO ₃	Under FAA 90 second Evacuation requirement
AO ₄	Rapid Cabin Sterilization
AO ₅	Exceed Most stringent EASA noise regulations for RJ's
AO ₆	Special accommodations for business travelers
AO ₇	Allow passengers to have ready access to all luggage without wait
AO ₈	Allow path for growth of the physical dimensions of the traveling public
AO ₉	Operate from austere airports with neither jetways nor air-stairs
AO ₁₀	Allow for rapid powerplant inspection, LRU replacement, drop
AO ₁₁	Enable all normal ground operations with engines running
AO ₁₂	Minimal to no de-icing dispatch delays
AO ₁₃	Powerplants reachable without special requirement
AO ₁₄	Minimize number of engine start cycles per operational day
AO ₁₅	Allow for powerplant diameter growth with time without significant aircraft changes
AO ₁₆	ADA compliant cabin section ingress and egress from ground without special equipment

3.2 Typical Routes, Legs, and Turnaround Time

Figure 3-1 below contains an image of the United States mainland superimposed with aircraft routes of four major commercial airline companies. The cities displayed on the map host large airports and hubs. The solid-colored curves represent a regional jet route of a particular airline company. The map depicts the reliance that the commercial market has on regional jet airliners. These routes were likely influenced by customer demand and how to maximize the number of passengers aboard each airplane.



Figure 3-1: Regional Jet and Turboprop Routes of Four Major US Airlines [18]

A journal article studied the rise in regional jet flights in the market and its implication on the aviation market [19]. The study observed route densities of regional jets, turboprops, and traditional jets (narrow body and wide body) and observed similarities and differences in flight patterns in the United States and Europe. Geographical location and current infrastructure were considered for the United States and Europe. Turboprops were typically found to support major airport hubs by connecting to smaller surrounding airports because they have much lower range and endurance capabilities. The introduction of regional jets allowed a wider variety of flight routes between

airports. The study includes a figure from the National Air Space System regarding route changes from 1992 to 2001 due to the rise of regional jets in the United States. It showed 43.2% of routes were new routes established by regional jets, while the remaining percent was split equally between replacing traditional jet routes, replacing turboprop routes, and supplementing traditional jet routes. The article concluded that the rise in regional jets could cause congestion problems at airports and add conflict when competing for land space. In 2008, the Regional Airline Association reported that half of all flights in the US were regional jets [20]. Additionally, these regional jets flew on average 461 miles per flight, which is 23% further than a regional jet in 2003 [20]. This allows travel to small airports that could be further away and allow more direct flights.

A regional jet could have 1 to 5 legs per day in a multi-day trip [21]. This varies due to airline company and duration of each leg. A regional jet pilot, Capt. Justin Dahan, documented what a typical day/ trip of his career is like [22]. He was based out of Charlotte, NC, and has flown the Bombardier CRJ-200, CRJ-700, and CRJ-900 regional jets. He writes about being on a three-day trip and on the second day they completed four legs on a CRJ-700. He and his crewmates traveled between Charlottesville, VA, Charlotte, NC, Ft. Walton Beach, FL, and Greensboro, NC. He included details such as switching planes, meeting other crews, and being evaluated by a check airman on a leg of his trip (a yearly thing done to observe pilots for safety practices and performance). His account shows insight into the daily operations of regional jets as well as regional jet trips.

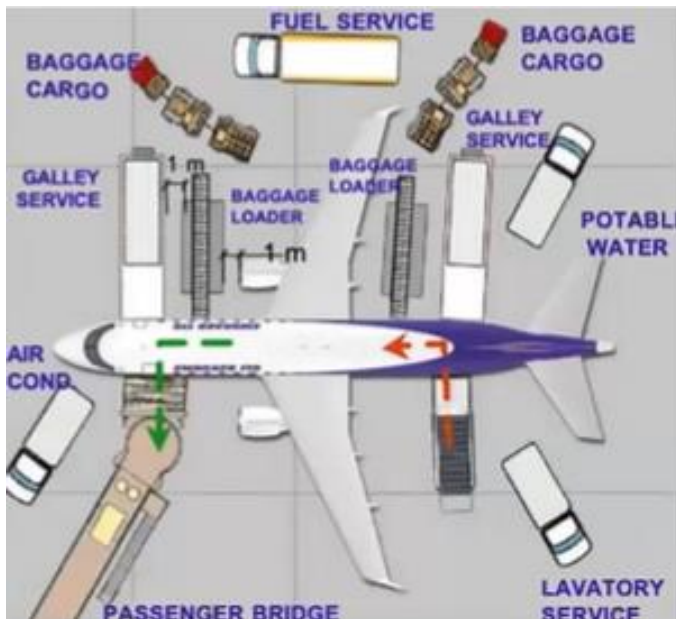


Figure 3-2: Embraer 170/190 Ground Operations Example Diagram [23]

Figure 3-2 to the left shows an Embraer 170/190 regional jet aircraft and its strategic positioning during the turnaround process. All the available services and equipment are staged efficiently to perform various tasks simultaneously handling both customer service demands, maintenance, and preparing for the next departure. This articulates the importance of aircraft design for ground operations and services. This management of ground services is significant to reducing the time an aircraft is spent on the ground and benefits

efficiently to perform various tasks simultaneously handling both customer service demands, maintenance, and preparing for the next departure. This articulates the importance of aircraft design for ground operations and services. This management of ground services is significant to reducing the time an aircraft is spent on the ground and benefits

efficiently to perform various tasks simultaneously handling both customer service demands, maintenance, and preparing for the next departure. This articulates the importance of aircraft design for ground operations and services. This management of ground services is significant to reducing the time an aircraft is spent on the ground and benefits

both the airline company and traveling customers. As for regional jets, fewer services and operations may be required. Combining or even eliminating services could potentially remove time spent on the ground. Figure 3-3 compares estimated turnaround time actions for a typical regional jet and proposed turnaround time actions for the Skyblazer series. With the Skyblazer series, the proposed turnaround time can be approximately halved with the selected configuration.

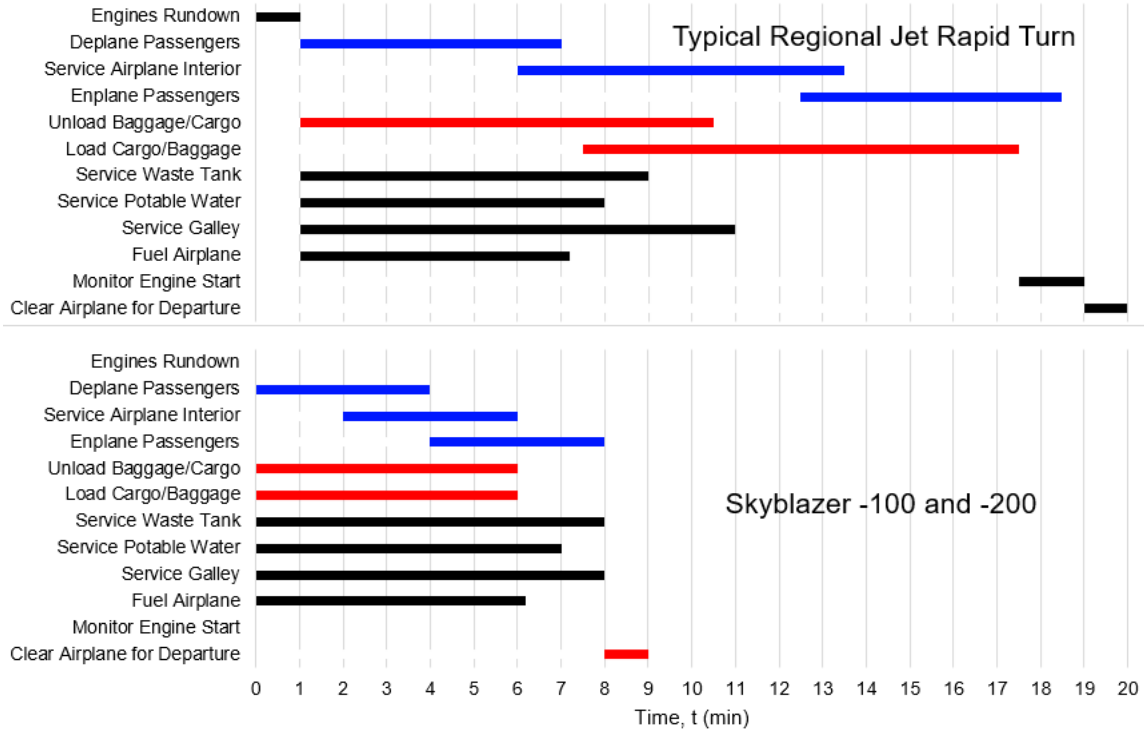


Figure 3-3: Turn Around Time for Typical Jet vs Skyblazer Series

3.3 **Current Market Trends**

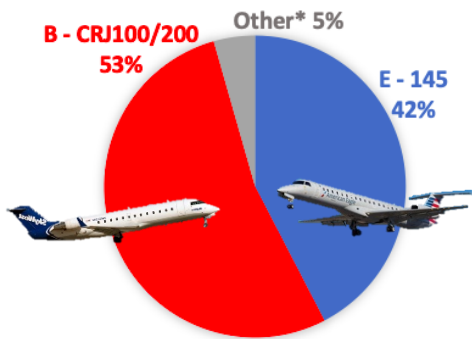


Figure 3-4: US Fleet 2020 RJ 50-Seat Market Ownership

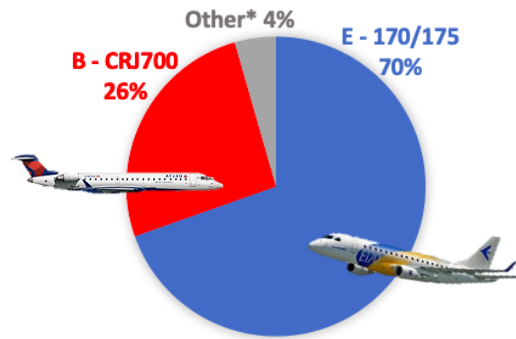


Figure 3-5: US Fleet 2020 RJ 76-Seat Market Ownership

Currently over 1,100 50-seat variants and 1,100 76 seat variants exist on the market. These fleets are almost entirely made up of aircraft designed and manufactured by Embraer and Bombardier. The market breakdown is shown in Figure 3-4 and Figure 3-5 . Bombardier left the RJ market and sold the program to the Mitsubishi Aircraft Corporation. This leaves a gap for other companies to begin to compete with the market left open by their absence. The estimated number of regional jets made by other companies may be undersized due to the inclusion of companies that only manufactured more than two aircraft of that type. The Skyblazer plan is to manufacture a much larger number of these aircraft in our scope, those companies are not considered competitors that hold enough of a market share to consider in analysis. This analysis allows a comparison between the designs of these aircraft to determine what they are optimized for.

Most of these aircraft are located within the United States and are reaching half of their expected life cycles. This aging fleet is causing several companies to begin looking for replacement aircraft to provide the U.S. travelers with a new model for flight allowing them to sell the aging fleet to other sources including airlines in other countries or shipping companies. Knowing this, the Skyblazer team can begin to assume the total possible aircraft expected to sell to other companies and determine a competitive market price to meet. Due to the bounds described within the RFP, the market was restricted to RJ that could seat 50 or 76 people and their remodels. The Scope Clause Airlines sign must also be considered when determining the market capacity in the U.S. This limits the number of RJs that an airline can have by the number of seats within the aircraft, many of the larger airlines are able to have an unlimited number of 50-seat regional jets they can operate. This is not the case for 76-seat versions. With Bombardier no longer manufacturing aircraft, repairs will begin to get more expensive driving upkeep costs higher. The best way for airlines to combat this will be through selling those aircraft earlier and replacing them with a new line that will last longer. Mitsubishi and Embraer currently have over 150 orders for their respective 76-seat models. While this means the market for the 50-seat aircraft will probably be easier to reach, the 76-seat market will be able to have

competition if there is a competitive new model. To determine the market cap more accurately, the growing operating costs need to be analyzed.

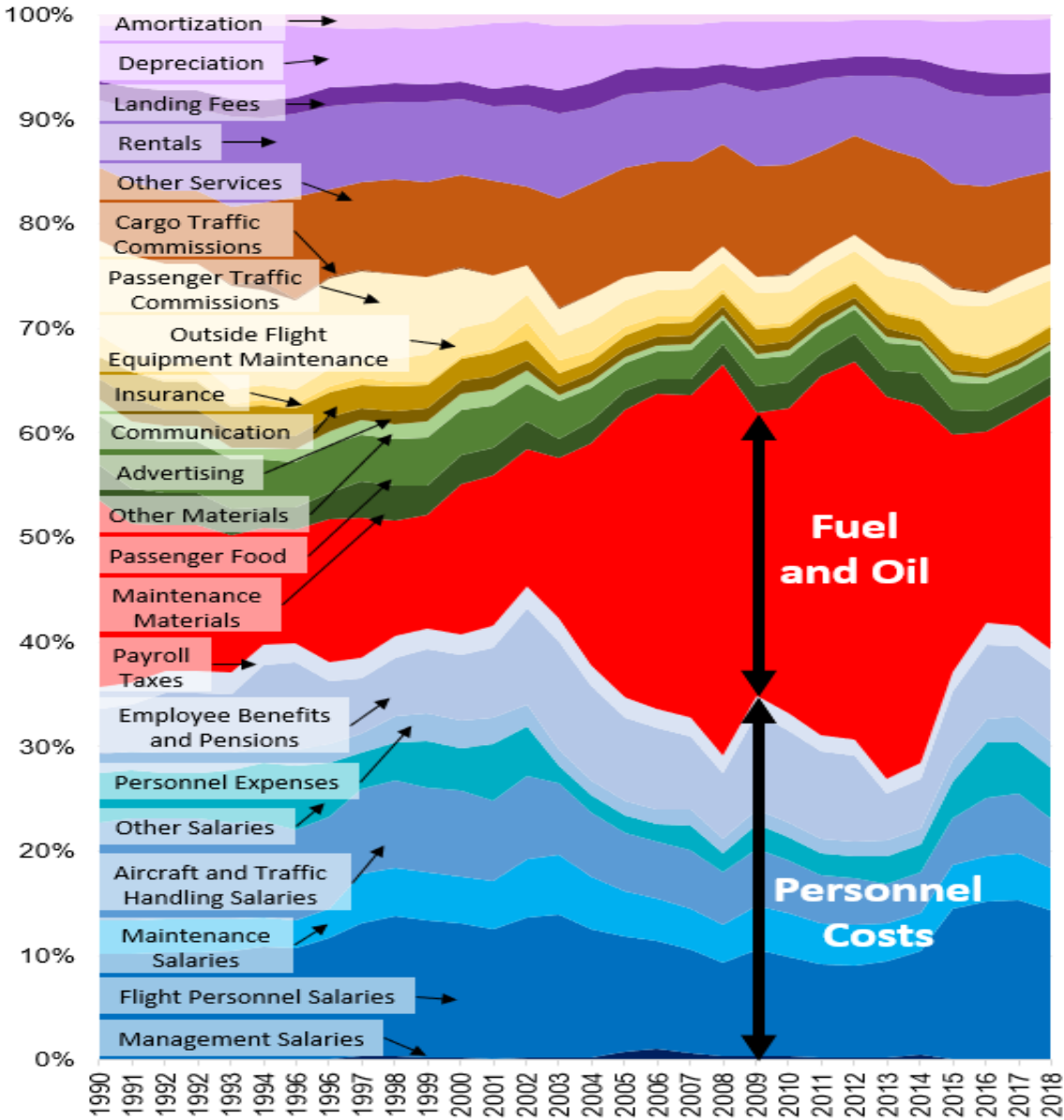


Figure 3-6: Historical Trend of American Airlines Direct Operating Costs (DOC) [24]

Figure 3-6 relates the percent American Airlines spent on direct operating cost (DOC) for each major financial consideration to the year in which it was spent. Much information can be derived from this chart to provide the design team crucial cost considerations for the development of the design, and the potential post acquisition costs

should be designed to be as low as possible. These were acquired from the US Department of Transportation [24]. Within this chart showing a breakdown of major costs within American Airlines DOC's, one unsurprising factor is the large variability of fuel cost from decade to decade depending on political and economic situations. Airlines have shown to continue to streamline the aerodynamics of their design to cut down on the potential fuel and oil costs associated with their aircraft. A feature that was shocking enough to direct the team's attention to other design details is the total size of salaries and associated employee costs. As far as the Skyblazer team is aware, airlines spend no visible resources optimizing these costs over fuel costs and with current Worker Union and political trends it is quite possible for these costs to rise even faster than that of oil and fuel. With this in mind, the team decided to dig deeper into the employee costs airlines often pay before spending time designing an aircraft to reduce these costs.

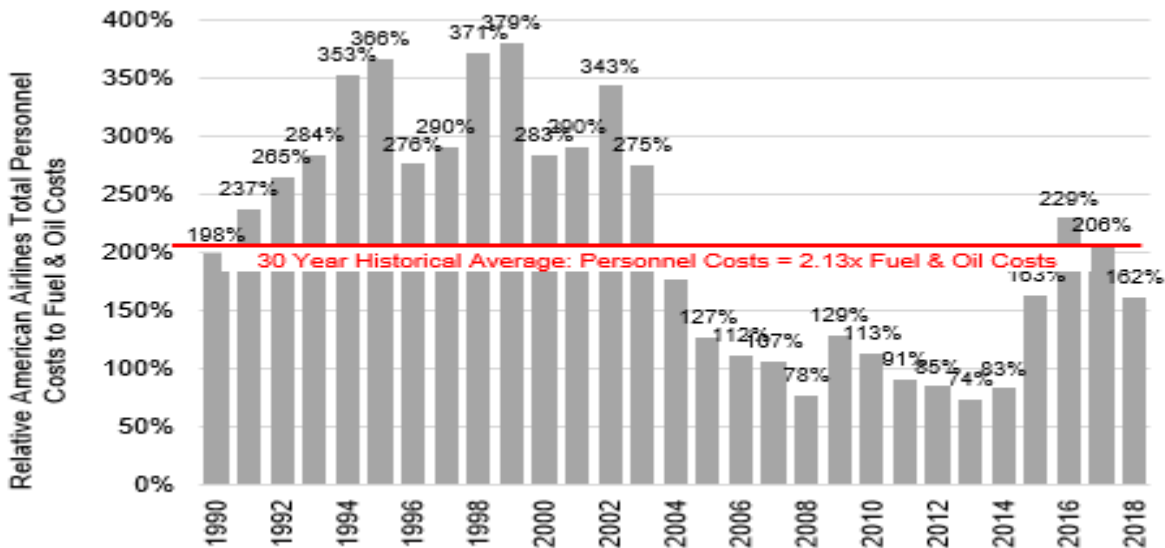


Figure 3-7: Historical Trend of American Airlines Fuel and Personnel Costs [24]

Parsing the DOC's down to just personnel and fuel expenditures led to an interesting find. details that out of the past 30 years, only 5 of them had fuel costs equal to or greater than total salary costs and with personnel costs being 2.13 times greater than fuel and oil costs on average trending lower more recently. This means if an equivalent percent savings is found in personnel and fuel, it would be more valuable to the company to focus on reducing personnel costs more than fuel costs.

Another major consideration that must be made is that studies are showing pilots are beginning to retire at an rate previously unseen. Between Delta, America, Alaska Air, Southwest, and United, an average of over 40% of their pilots will retire by 2026. This means that with current fleet sizes in mind, airlines will either have to overwork

their pilots and planes to serve the same number of passengers, or they will not be able to support the amount of passengers who want a flight and create a rise in ticket prices. This should push aircraft designers to design a plane that attempts to allow a pilot to serve a larger number of passengers each day. This research has been well documented over the last 5 years by many companies and Covid policy changes has only exacerbated this issue. This has led many pilots to retire or leave the fleet earlier than intended with almost all flight being ground for most of a year. In order to ensure that Skyblzer can be operated by a smaller number of pilots for the same number of passengers, the motivation is designing an aircraft that focuses on increasing the number of flights turns per day. This will also increase the salary for the RJ pilots potentially increasing the demand for smaller fleets in order to save on salary costs.

SkyWest Airlines Data
 13 hr Flight Day
 2,400 flights/day
 452 aircraft in fleet
 5.3 flights/day average
 138 nmi/stage average

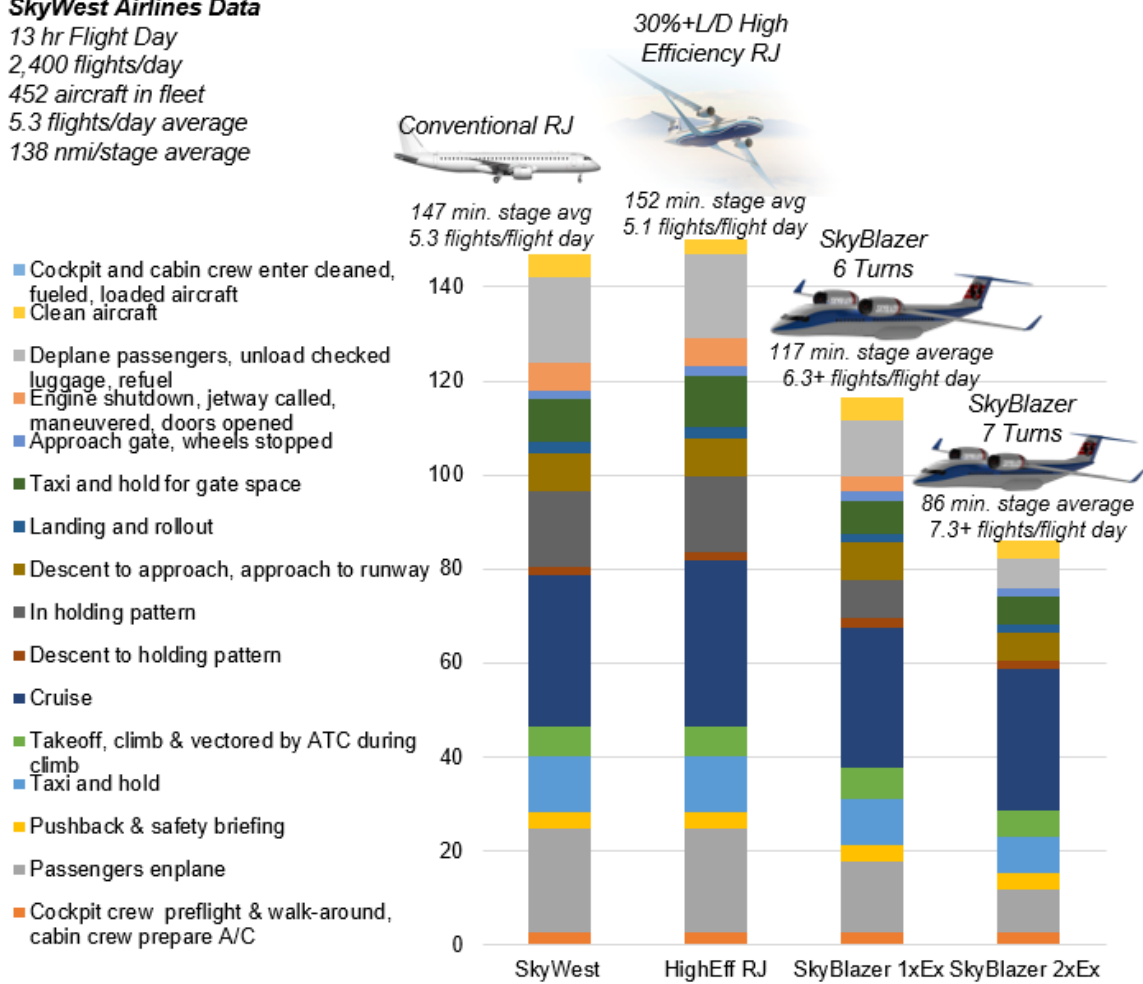


Figure 3-8: Total Stage Time Comparison of Average RJ, 30%+ High L/D RJ, and Skyblazer Family [25]

Figure 3-8 breaks down the time required for specific tasks when preparing a for a turn around and how the Skyblazer Series aircraft can potentially achieve 1-2 more turnarounds per day. This allows for more yearly profit per aircraft and a smaller fleet for the same number of total passengers, offering a solution to the pilot crisis and potentially increasing the company's profit margins.

Figure 3-9 lays out the expected cost difference between the traditional RJ aircraft of today, the currently anticipated highly efficient fuel burn aircraft, and the Skyblazer aircraft. While the high efficiency aircraft

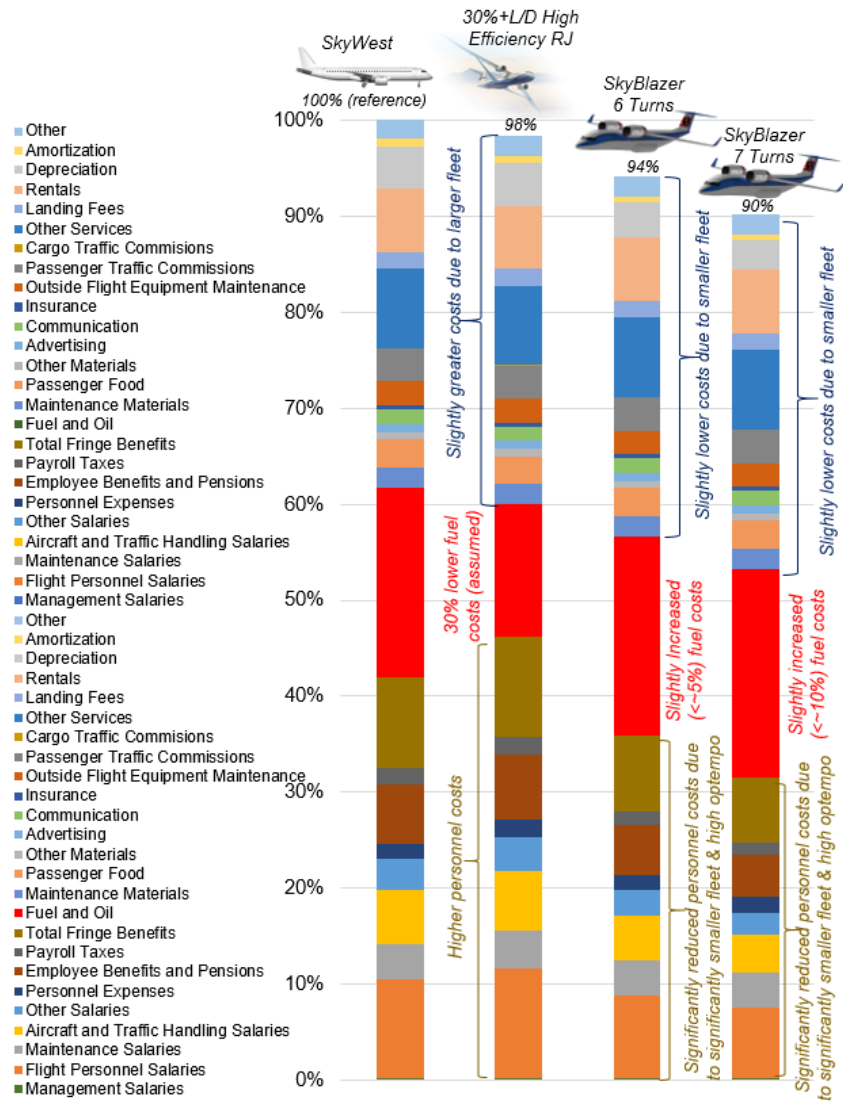


Figure 3-9: DOC Comparison of Conventional, Aerodynamically Advanced and Skyblazer Series RJ's[26][27][28]

estimate a cost savings of 2% or more as shown, the additional personnel and fleet costs associated with them outweigh most of that gain. The Skyblazer series hopes to prove a larger financial gain through reducing the necessary fleet and personnel costs while slightly increasing the fuel costs. This leads to a financial savings of up to 6% per year with only a single more flight turns per day and up to 10% with 2 more flight turns per day. This is an expected saving of 3-5 times more than the potential savings from decreased fuel burn alone. Figure 3-10 also shows that the airlines would need 83% or 71% of the amount of aircraft currently needed to provide the same number of



passengers with flights. Meaning fewer pilots required to work at the same time and potentially less overworked pilots. This means ticket prices can be decreased, and our aircraft can be more competitive with the competition.

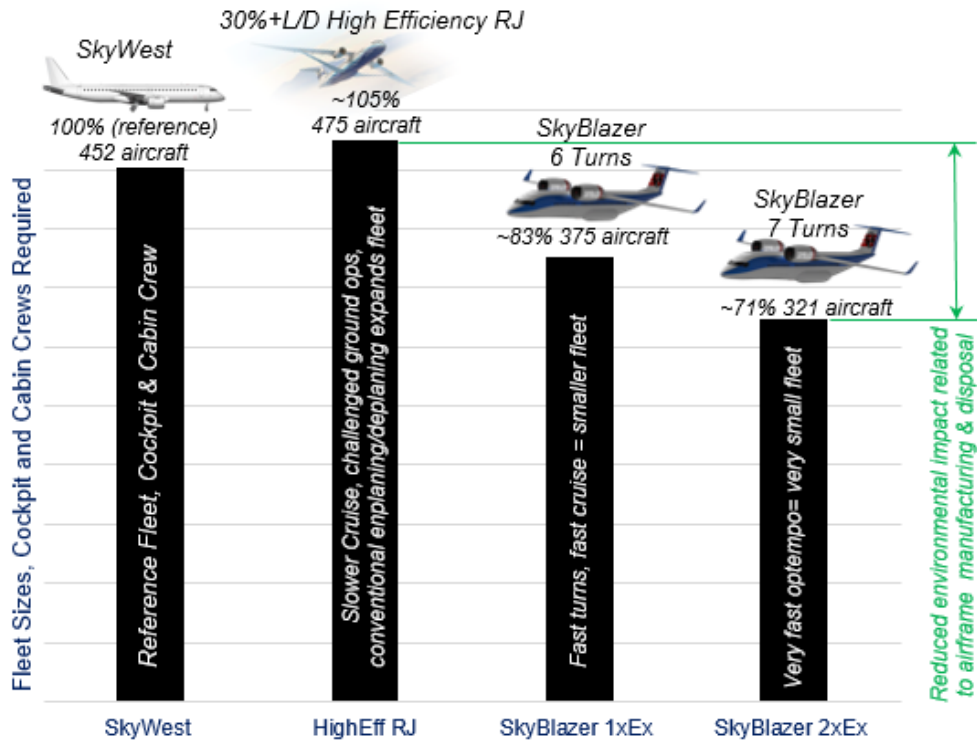


Figure 3-10: Relative Fleet and Flight Crew Sizes to Accommodate a Typical Regional Jet Route Structure [26][27][29]

Figure 3-11 outlines the entirety of the operation plan Skyblazer aims to achieve in a simple chart detailing the design points the team plans to focus on as down selection of planforms occurs and narrow in on a potential solution to the issues presented within the market.

Decreasing fuel burn is still a priority to the team, but not at the expense of a greater increase in salary costs than the fuel cost reduction allows for. This allows the team to optimize the design for a decrease in cost and an increase in profit.

“There are three ways to grow your capacity as an airline, buy more planes, increase the number of seats available on current aircraft, and lastly increase utilization”.
 - Ms. Abriell Jackson, Senior Financial Planning Manager, American Airlines

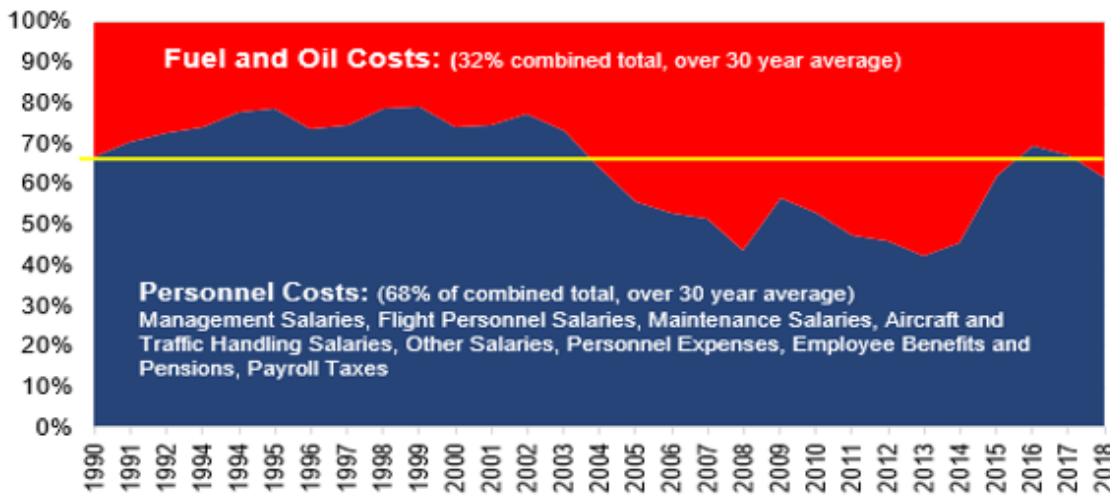


Conventional Approach seen in past AIAA Airliner Proposals:

- Stretch AR to limits & cruise slower to increase L/D & SR to minimize fuel burn

Inducing:

- Higher personnel costs
- Higher stage time
- Fewer movements per A/C/yr
- Lower profits
- Higher ticket prices
- Larger fleet requirements for given route structure, with adverse environmental impact



SkyBlazer Approach:

- Keep fuel burn low, but reduce personnel costs for given fleet operations by enabling 1 – 2x more aircraft movements per flight day per aircraft, reducing fleet size & environmental impact

- Cruise slightly faster, accept small drag penalty to save stage time and save far more in DOC
- Employ known technologies, reducing program risk & maintenance load
- Use no complicated wing-fold which could induce certification, dispatch reliability & MRO issues
- Use flight-proven, fielded advanced high lift systems enabling shorter runway ops
- Use shorter runways at large hubs, fly in to smaller airports at spoke tips
- Shorten or avoid completely holding pattern delays by opening up shorter runways
- Use earlier exits from runways on landing, saving time
- Deconflict ramp with high wing, high engines, allowing unimpeded access to aircraft
- Configure engines well above personnel and vehicle max. heights, allowing deconfliction
- Keep engines at DC-9/MD-8x/B717 height, allowing use of existing ramp equipment
- Minimize cabin floor off ground, allowing integral stairs
- Enplane and deplane passengers via multiple doors
- Use entrance luggage storage bins to deconflict overhead luggage space
- Enable double-hose refueling, cutting refueling time in half
- Use nose-to-tail cargo belt allowing rapid checked baggage loading and unloading

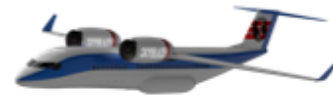


Figure 3-11: SkyBlazer Regional Jet Design: A New Approach to Reducing Acquisition, Direct Operating and Life Cycle Costs [24]

4 STAMPED Analysis of Aircraft Regional Jet Market

To predict where the market will be in 2030 and create a competitive regional jet for that time, various characteristics are plotted through time to see how they have trended over the years including a market analysis of various similar regional jets for comparison. Each trend is plotted throughout the years from 1950 to the 2020 current market. The linear trend for the aircraft is in blue with the trendline equation shown in the corner of each plot. The equation is used to plot the +1 and -1 standard deviation lines in orange and grey respectively. The standard deviations show how conservative and aggressive each characteristic can be and provide a range of possible values to help realistically spec our regional jets designs. The 50-seat regional jets are on the left with the 76-seat regional jets shown on the right with the trendlines forecasting into the year 2030 for an accurate prediction of each aircraft characteristic. Other characteristics were plotted but not shown such as span loading, aspect ratio, range, takeoff and landing field lengths, and cruise speed.

4.1 Empty Weight to Takeoff Weight Ratio Market Analysis

Observed in Figure 4-1, it is shown that the ratio of empty weight to takeoff weight has significantly decreased over time for 50-seat aircraft while 76-seat aircraft have increased. To stay on trend for 2030, a 50-seat regional jet would have an empty weight to takeoff weight ratio around the value of 0.56. In the 76-seat regional jet market, it is observed that the ratio of empty weight to takeoff weight is trending towards a value of 0.57 in the 2030 market.

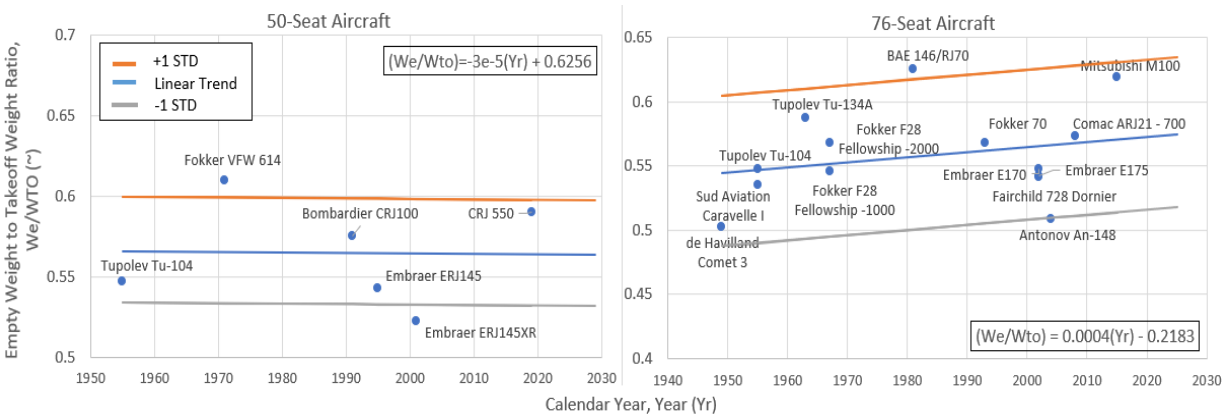


Figure 4-1: Empty Weight to Takeoff Weight Ratio Market Trend Through Time



4.2 Wing Loading Market Analysis

When trending wing loading through time, it is shown in Figure 4-2 that wing loading has increased through the years. The regional jet released in 2030 would have a wing loading of 110 lbf/ft² to stay on trend with competing 50-seat regional jets and a wing loading of 120 lbf/ft² to compete with 76-seat regional jets.

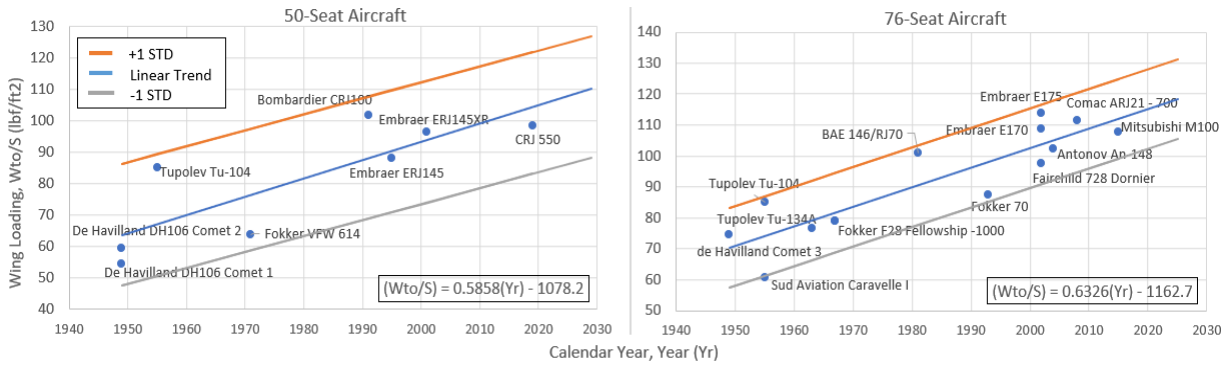


Figure 4-2: Wing Loading Market Trend Through Time

4.3 Sweep Angle Market Analysis

Shown in Figure 4-3, the trend shows a slight decrease in sweep angle over time for 50-seat regional, but there is almost no change. This indicates that the market has settled. On the other hand, the 76-seat regional jet market has slightly increased sweep angle over time. 50-seat regional jets released in 2030 would have a sweep angle of about 25° to stay around the market average based on the trends while a 76-seat regional jet is around 27°.

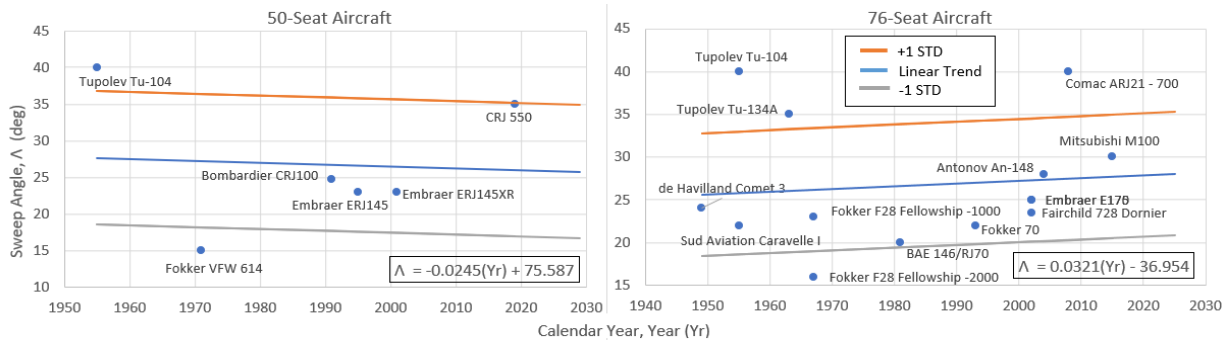


Figure 4-3: Sweep Angle Market Trend Through Time

4.4 Wing Loading and Thrust-to-Weight Ratio Market Analysis

The wing loading plotted against the thrust-to-weight ratio is shown in Figure 4-4 below. The black box indicates the standard deviation occurring around the most recent data. To stay on trend with regional jets in the 2030 market, the Skyblazer Series should stay within the standard deviation to remain on trend and competitive.



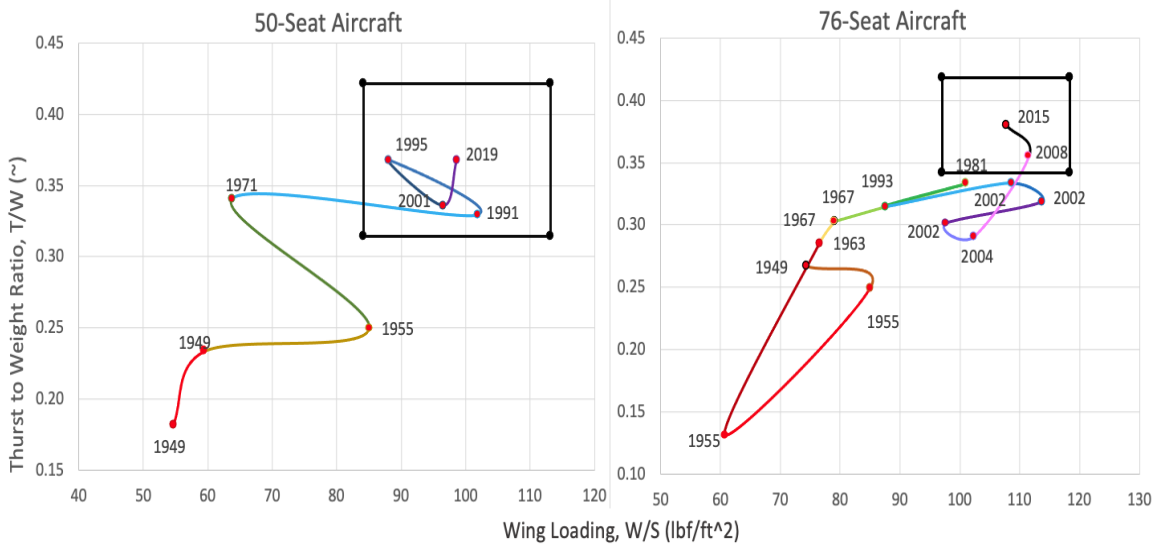


Figure 4-4: Wing Loading and Thrust-to-Weight Ratio Market Trend Through Time

5 Weight Sizing Code Generation

The purpose of this chapter is to size the aircraft to the mission requirements listed in the RFP. This section will also discuss aircraft characteristics to improve performance and design. The following airplane design parameters will be determined for the series 100 and series 200:

- Take-off Weight (W_{TO})
- Empty Weight (W_E)
- Mission Fuel Weight (W_F)
- Maximum Take-off Thrust (T_{TO})
- Wing Area (S) and Aspect Ratio (AR)
- Maximum Cruise Lift Coefficient ($C_{LMAX,C}$)
- Maximum Take-off Lift Coefficient ($C_{LMAX,TO}$)
- Maximum Landing Lift Coefficient ($C_{LMAX,L}$)

5.1 Aircraft Flight Modes Prescribed to Flight Phase

The flight modes prescribed to each flight phase are displayed in Table 5-1.

Table 5-1: Flight Mode Associated with Flight Phase

Flight Phase	Flight Mode	Flight Phase	Flight Mode
1. Taxi	• Gear Down	6. Climb to Alternate	• Take-Off Flaps
2. Take off	• CTOL • Take-Off Flaps	7. Divert to Alternate	• Flap Retraction • Clean Configuration
3. Climb	• Gear Up • Take-Off Flaps	8. Loiter	• Clean Configuration
4. Cruise	• Flap Retraction • Clean Configuration	9. Descend	• Approach Flaps • Gear Down
5. Descend, Bailed Landing	• Approach Flaps • Gear Down	10. Landing	• CTOL

5.2 Weight Sizing Code for Fuel Burn and Iteration of W_e , W_f , and W_{to}

Aircraft fuel fractions for each flight leg were determined using the processes outlined in Jan Roskam's *Airplane Design Part I: Preliminary Sizing of Airplanes*. All fuel fractions are tabulated in Table 5-2.

Table 5-2: Aircraft Fuel Fractions

W_{i+1}/W_i	Segment	Fuel Fraction [R] – Roskam Estimation [30] [E] - Estimation [C] - Calculated
W_1/W_{TO}	Engine Start, Warm Up	0.99 [R]
W_2/W_1	Taxi	0.999 [R]
W_3/W_2	Take-off	0.995 [R]
W_4/W_3	Climb	0.98 [R]
W_5/W_4	Cruise - Series 100/Series 200	0.8625/0.8950 [C]
W_6/W_5	Climb to Alternate	0.98 [E]
W_7/W_6	Divert to Alternate	0.98 [E]
W_8/W_7	Loiter	0.9788 [C]
W_9/W_8	Descent	0.99 [R]
W_{10}/W_9	Landing, Taxi, Shutdown	0.992 [R]
M_{ff}	Mission Fuel Fraction - Series 100/ 200	0.7534/0.7817 [C]

Take-off weights for 100 Series and 200 Series aircraft were estimated using the average take-off weight found in STAMPED trends for 50-seat and 70-seat configurations. A MATLAB code was generated to calculate the empty weight and fuel weight of the 100 and 200 series aircraft using the weight fractions listed above. The weights are tabulated in Table 5-3.

Table 5-3: Weights for Skyblazer 100 and 200 Series

	100 Series Aircraft	200 Series Aircraft
Take-off Weight, W_{to}	55,000 lbs.	71,000 lbs.
Empty Weight, W_e	28,774 lbs.	36,603 lbs.
Fuel Weight, W_f	13,565 lbs.	15,496 lbs.

6 Wing and Powerplant Sizing

To size the wing and powerplant design points, aircraft parameters were rapidly estimated. These main parameters include wing area, takeoff thrust, takeoff power, and maximum lift coefficients for takeoff, landing, and inflight. These parameters have been estimated and optimized to achieve performance requirements and objectives such as stall speed, cruise speed, and field lengths.

The design point was determined by defining boundaries on sizing charts. Optimizing the relationship results in smaller wing and engine sizes. The smaller wing and powerplant sizes can result in higher performance.

The design point is determined by calculating the wing loading and thrust-to-weight ratio under the limiting flight condition as shown in Eqn. 6.1.

$$\frac{W}{S} \Big|_{\text{lim}} = \frac{1}{2} \rho V^2 C_{L\text{max}} \Big|_{\text{LimitingFlightCondition}} \quad \text{Eqn. 6.1}$$

6.1 Takeoff and Landing Sizing

Take off sizing is dependent on the takeoff distance shown in Eqn. 6.2 for reference. Takeoff distances are affected by the takeoff weight, takeoff speed, thrust-to-weight ratio, aerodynamics drag coefficient, ground friction coefficient, and lastly pilot technique.

$$\left(\frac{T}{W}\right)_{\text{TO}} = \frac{37.5 \left(\frac{W}{S}\right)_{\text{TO}} (\text{lb/ft}^2)}{S_{\text{TOFL}}(\text{ft}) \sigma C_{L\text{maxTO}}} \quad \text{Eqn. 6.2}$$

When solving for takeoff thrust-to-weight ratio, the independent variable is the wing loading which runs across the horizontal axis. The S_{TOFL} differs between the 50-seat and 76-seat required takeoff distances which are 4,000 ft and 6,000 ft respectively. Sigma, σ , represents the air density ratio and was calculated at 5,000 ft above mean seal level and with ISA +18°F as required in the RFP [1]. Lastly, three $C_{L\text{maxTO}}$ values are plotted to serve as boundaries for the specific design point in order to provide an idea of what $C_{L\text{maxTO}}$ values are required to achieve specified requirements.

Landing distances are affected by landing weight, approach speed, deceleration methods used, flying qualities of the airplane, and pilot technique.

$$\frac{W}{S} = \frac{\frac{1}{2} \rho V_{\text{SL}}^2 C_{L\text{max}} \Big|_L}{\left(\frac{W_L}{W_{\text{TO}}}\right)} \quad \text{Eqn. 6.3}$$

Eqn. 6.3 on the right was used to determine the wing loading for landing sizing. It is also used to find the required wing area using the takeoff weight.

Following the same methods used to calculate wing loading values for takeoff, three $C_{L\text{maxL}}$ values were plotted to serve as boundaries for the specific design point in order to provide an idea what $C_{L\text{maxL}}$ values are required to achieve the specified landing field lengths of 4,000 ft and 6,000 ft for the respective aircraft configuration.

6.2 Climb and Ceiling Sizing

Climb sizing follows the FAR 25 guidelines and requirements for the different segments of flight and for One Engine Inoperative (OEI) and All Engines Inoperative (AEI) situations. The thrust-to-weight ratio is calculated for each segment using Climb Gradient Requirement (CGR), number of engines, and lift-to-drag ratio. The lift-to-drag ratio is dependent on the drag polar equations.

There are six main configurations that define the various phases of flight for the aircraft. Each configuration has a different amount of drag depending on the landing gear and flaps. These drags are quantified in a drag polar equation as shown next to the curve in the drag polar plots below. It is observed that the landing gear down and flaps out create more drag than the clean configurations or landing gear up.

The drag polars are plotted for each configuration for each aircraft shown below with the Skyblazer 100 in Figure 6-1 and the Skyblazer 200 in Figure 6-2. The coefficient of lift is plotted at higher values on the 50-seat aircraft chart due to requiring higher C_{LmaxTO} and C_{LmaxL} values. The drag polars plotted each have a respective equation that is a function of C_L .

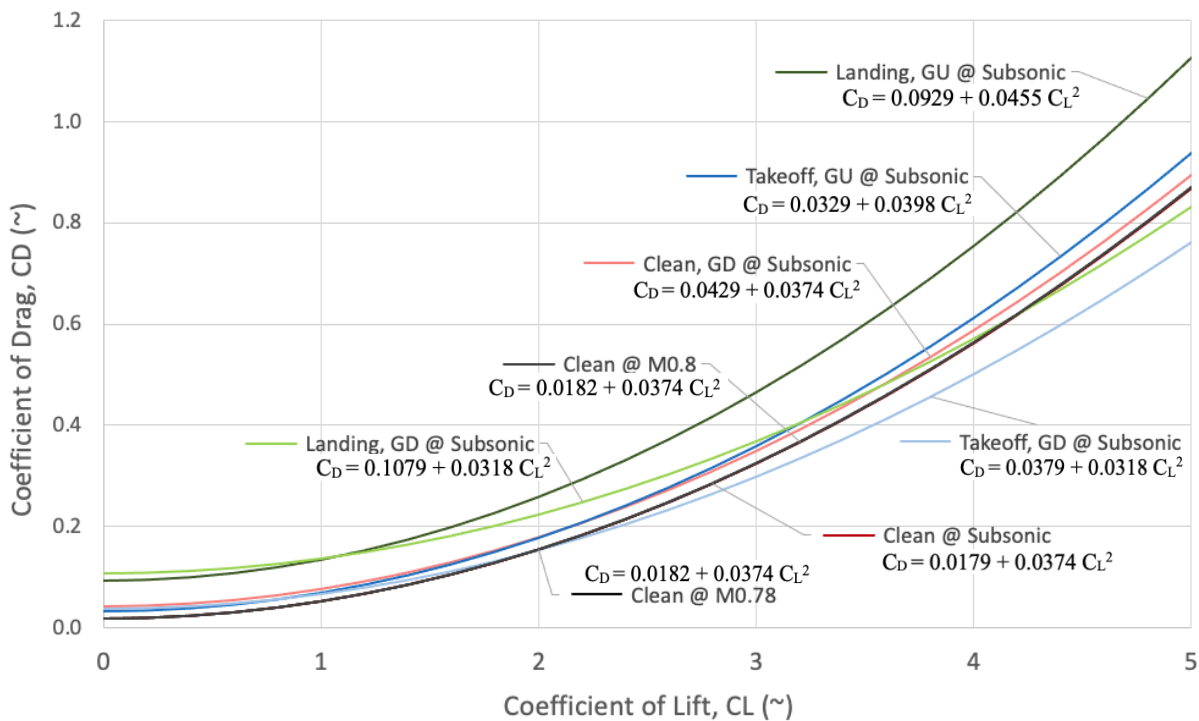


Figure 6-1: Skyblazer 100 Drag Polars

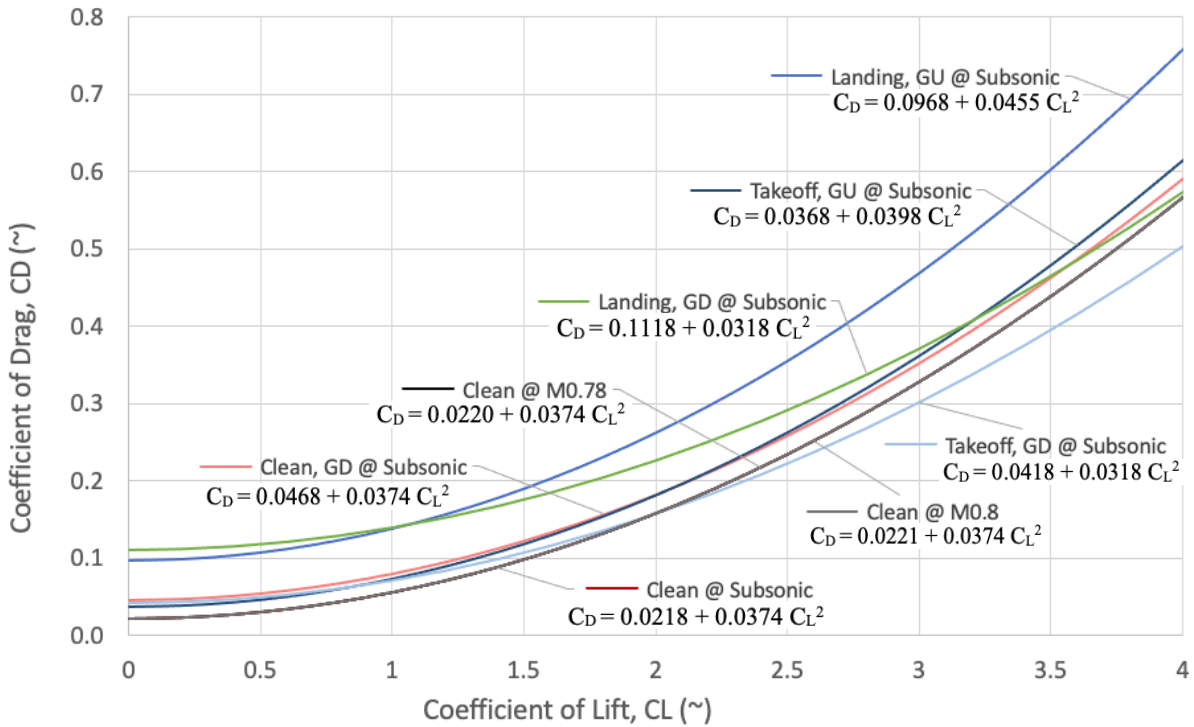


Figure 6-2: Skyblazer 200 Drag Polars

The ceiling sizing calculation for thrust-to-weight ratio is dependent on many variables as shown to the right in Eqn. 6.4. It is also noted that the equation is translated to altitude using the ratio of air density and pressure between 32,000 ft and standard sea-level. The ceiling requirement sizes the aircraft wing loading and thrust-weight-ratio capabilities to fly at cruise altitude.

$$\left. \frac{T}{W} \right|_{alt} = \frac{\left(\frac{0.031 + 0.441 \left(\frac{2n(W/S)}{\rho V^2} \right)^2}{\sqrt{M^2 - 1}} \right)}{\frac{2n(W/S)}{\rho V^2}} \quad \text{Eqn. 6.4}$$

6.3 Cruise Sizing

Cruise sizing is based on cruise conditions such as altitude, density, and speed. It is also dependent on the drag polar for aircraft cruise configurations. The thrust-to-weight equation for cruise is shown on the right.

$$T_{altitude} = T_{SL} \sqrt{\sigma} \sqrt{\delta} \quad \text{Eqn. 6.5}$$

$$\frac{T}{W} = \left(C_{D0} + \frac{\left(\frac{W}{qS} \right)^2}{\pi A e} \right) \bar{q} \frac{S}{W} \quad \text{Eqn. 6.6}$$

6.4 Power Plant

Using thrust to weight ratio found in sizing charts and the specified takeoff weight, the required takeoff thrust for the aircraft could be determined leading to

$$T_{TO} = \frac{T}{W} * W_{to} \quad \text{Eqn. 6.7}$$

the selection of engines. Using the relationship on the right in Eqn. 6.7, the takeoff thrust required for the 50-seat and 76-seat configurations are 17,458 lbf and 25,000 lbf respectively.

$$\tau_w = (t/c)_t / (t/c)_r \quad \text{Eqn. 6.8}$$

6.5 Wing Fuel Volume

The wing fuel volume was calculated along with the wing loading. It was based on the thickness to chord ratios for the tip and root shown in Eqn.

$$V_{WF} = 0.54 \left(\frac{S^2}{b} \right) \left(\frac{t}{c} \right)_r \left((1 + \lambda_w \tau_w^{1/2} + \lambda_w^2 \tau_w) / (1 + \lambda_w)^2 \right) \quad \text{Eqn. 6.9}$$

6.8. This ratio is then applied to Eqn. 6.9

with other wing characteristics to get an estimated wing fuel volume. Considering a supercritical airfoil, the thickness to chord ratio was determined to be 14%. The thickness to chord ratio will remain consistent from the root to the tip as the same airfoil will be used throughout the entirety of the wing. This will result in a τ_w of 1. With a wing area of 478 ft² and a span of 77 ft, the wing fuel volume is calculated to be 167 ft³ which converts to 1,249 gallons of fuel. This serves as a suitable fuel volume for both series of aircraft shown in Table 6-1 below. The 76-seat aircraft will have the same wing size on its configuration.

Table 6-1: Fuel Volume

	Fuel Weight, W_f	Fuel in Gallons	Fuel Volume Needed	Available volume
Skyblazer 100 Series	13,565 lbs.	2,033 gal	272 ft ³	167 ft ³
Skyblazer 200 Series	15,496 lbs.	2,323 gal	311 ft ³	

6.6 Complete Sizing Chart

Overall, the Skyblazer series are shown to meet all of the sizing requirements based on its location with respective guidelines and trends as calculated and shown in Figure 6-3 and Figure 6-4 for the 50-seat 76-seat version respectively. All of the requirements are shown to be met, as the design location is above and within all of the boundaries on the plot as shown as the black circles. The vertical red lines shown on the graph are the maximum landing C_L boundaries, and the aircraft is to the left of them which indicates meeting the requirement. The blue diagonal lines are the maximum takeoff C_L boundaries, and the aircraft is above the requirement. The horizontal lines are defined by the FAR 25 climb requirements, and higher than this meets the requirement. The curved lines



in yellow are the ceiling and climb boundaries and are met with the aircraft location shown as a black dot is above those lines.

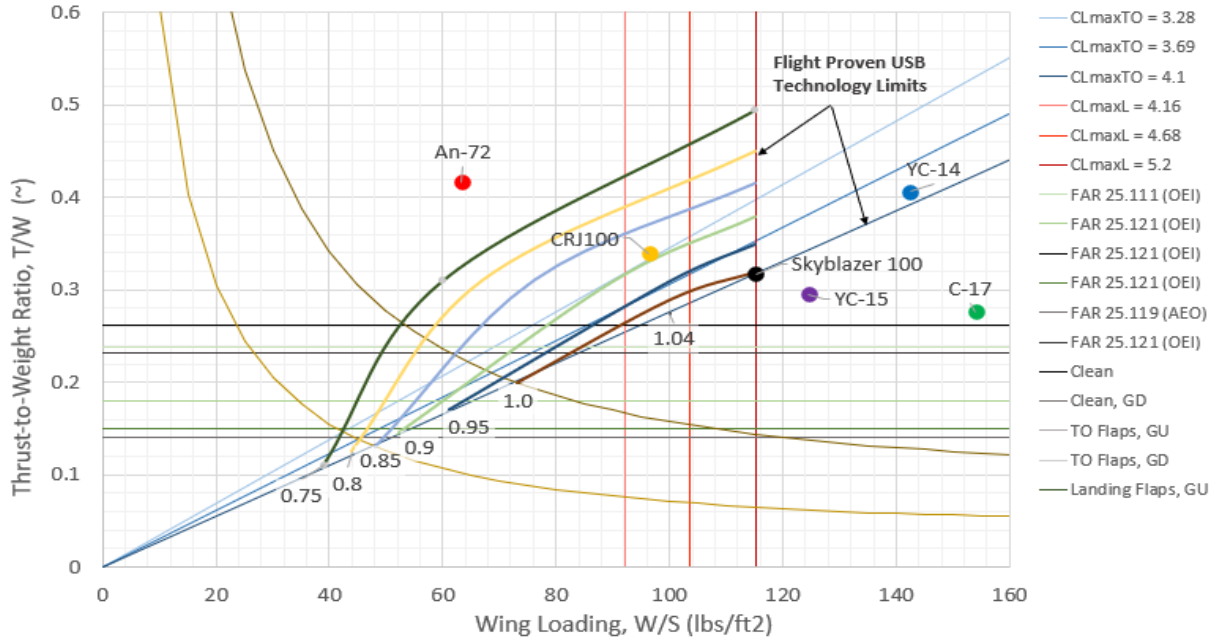


Figure 6-3: Skyblazer 100 Sizing Chart

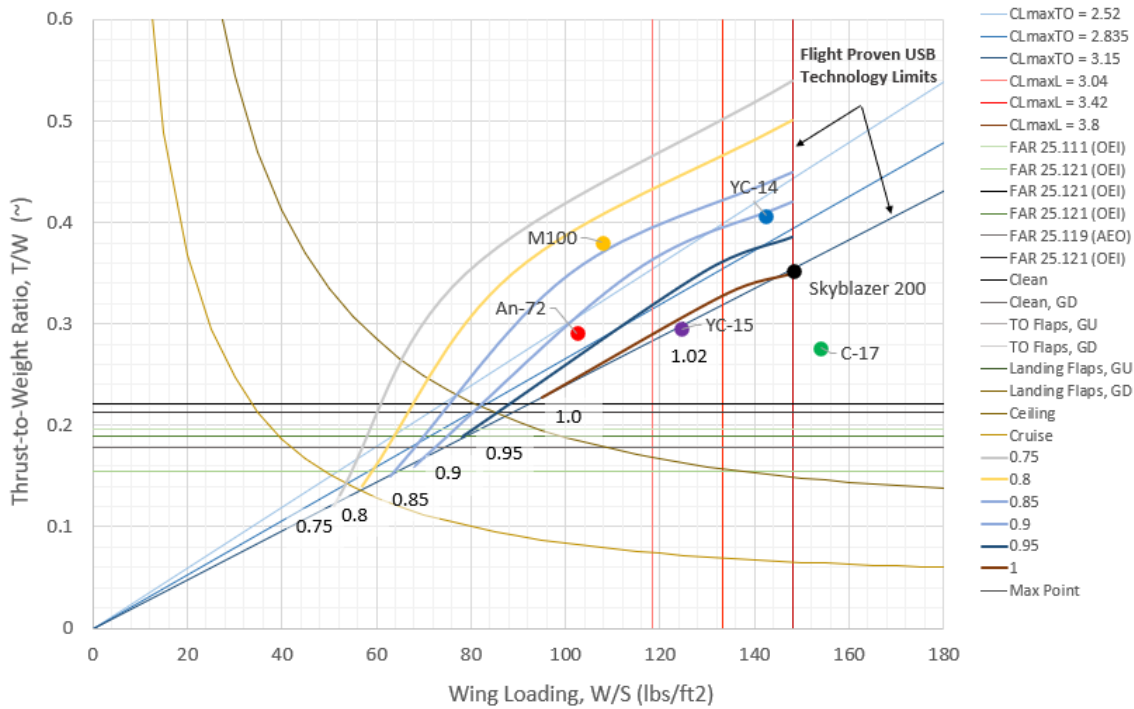


Figure 6-4: Skyblazer 200 Sizing Chart



It is observed that the thrust-to-weight and wing loading are higher than the standard deviation graph previously generated in Figure 4-4 due to having a much smaller takeoff field distance requirement of 4,000 ft. The Skyblazer aircraft wing design has a small area with high lifting mechanisms and complex flaps to achieve a short takeoff distance. The thrust is also higher to be capable of achieving a short takeoff distance, causing a higher thrust-to-weight ratio. Similar aircraft are also plotted for comparison of wing loading and thrust-to-weight.

The design points for the Skyblazer series were placed based on the chosen engine’s thrust to the aircraft weight. The wing loading was also sized based on preliminary wing sizing to achieve varying lift coefficients to meet the short takeoff distance requirement. Wing fuel volume also affected the wing loading design points. Comparable aircraft are also shown to be plotted for comparison in wing loading and thrust-to-weight ratio.

The isoclines are also plotted as curves between the coefficient of lift lines to show the tradeoff between aircraft weight and cost. Both aircraft are observed to be weakly optimized but moving in the right direction.

6.7 Basic Performance Plots

To analyze the aircraft performance at varying Mach, aspect ratios, wing loadings, and altitudes, a series of carpet plots were designed to help make decisions regarding the geometry of the wing and the weight of the aircraft to meet requirements of the RFP. These have been used in combination with the sizing charts to narrow down the specific values for each of those variables that can be used for optimum flight. An aspect ratio between 11 and 12 has been chosen with fuel and performance conditions in mind, while a wing loading of 115 lbf/ft² and 150 lbf/ft² have been chosen for the Skyblazer-100 and 200 respectively. This can help determine the specific range and L/D the aircraft will be achieving during the mission.

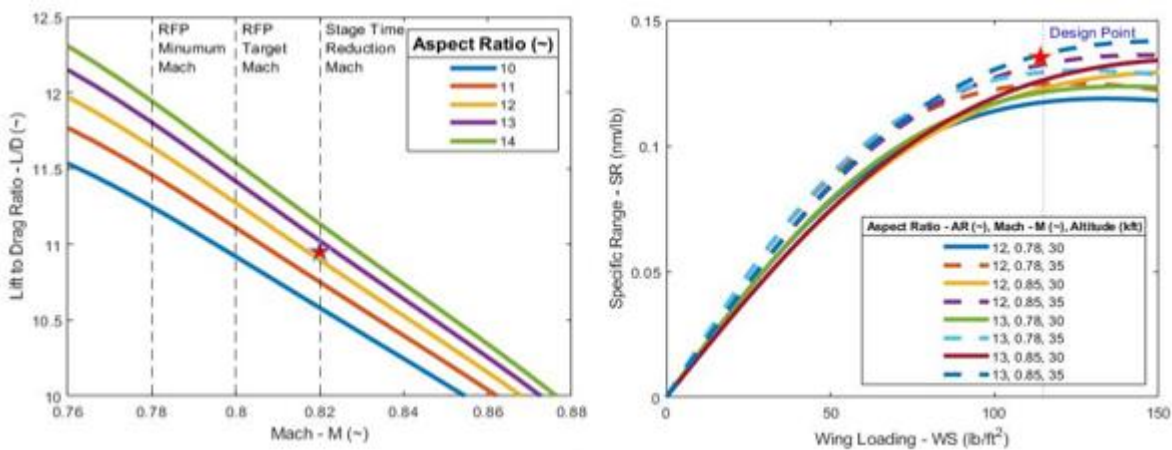


Figure 6-5: Skyblazer-100 Performance Plots



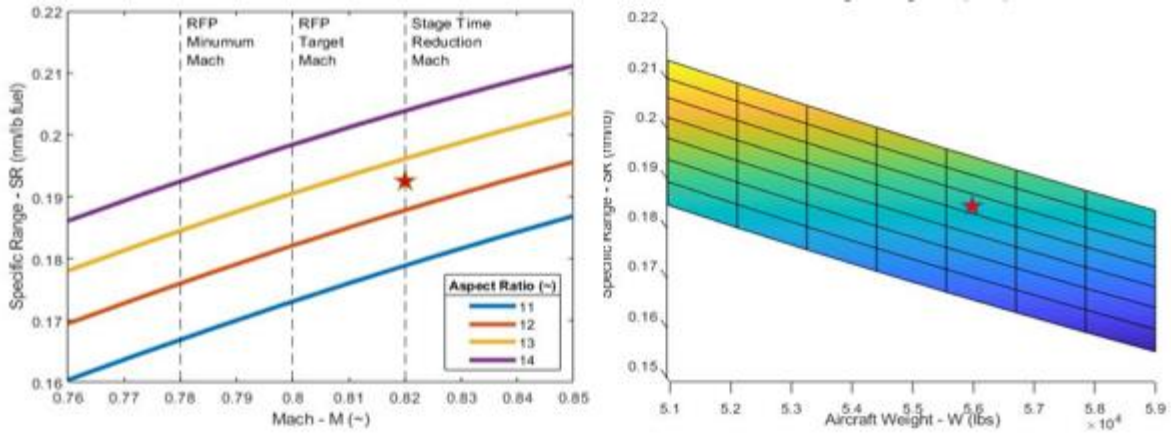


Figure 6-5: Skyblazer-100 Performance Plots (cont.)

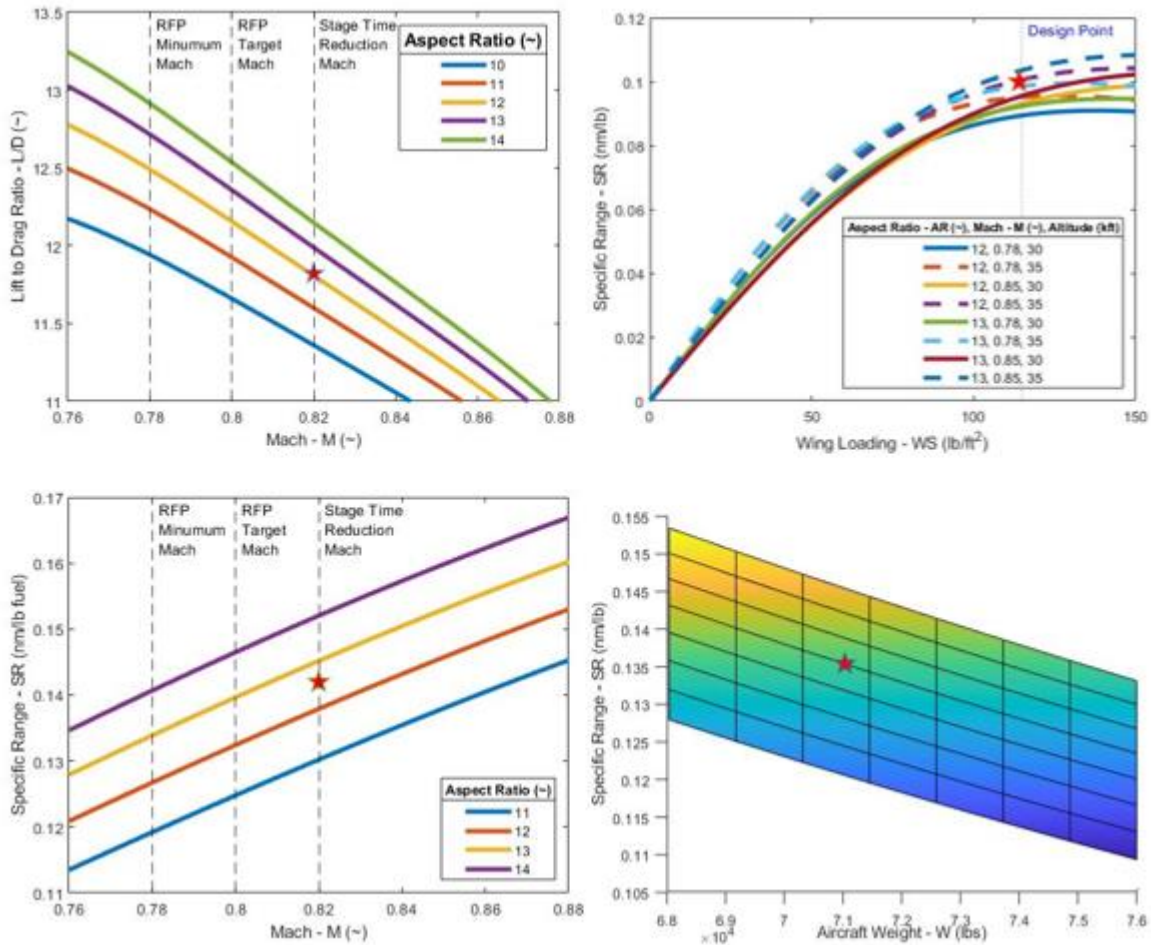


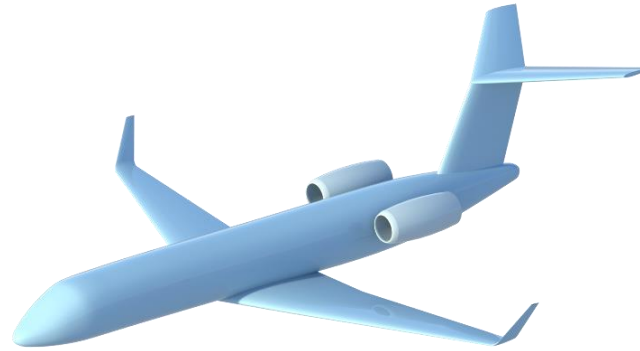
Figure 6-6: Skyblazer-200 Performance Plots

7 **Class I Configuration Matrix**

In order determine the correct design that will fulfill all of the required objective and requirements, it is recommended to perform a preliminary design analysis. Presented in Figure 7-1 are a sweep of configurations considered for a viable regional jet design. The designs considered contains both conventional and radial designs to ensure that all areas are considered before down selection.



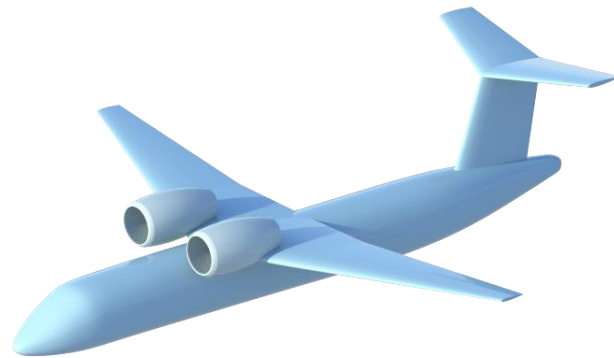
1. High Wing



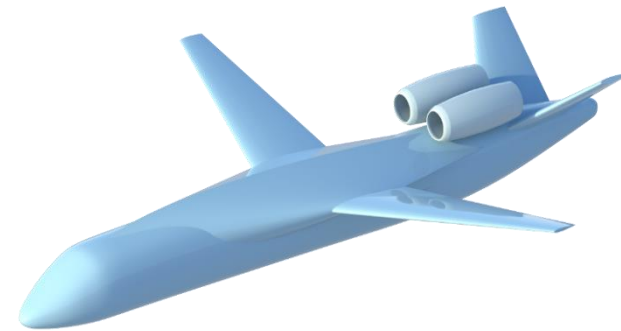
2. Low Wing Aft Engines



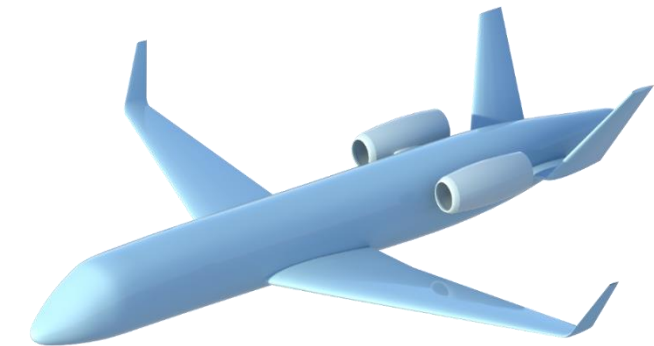
3. Low Wing Low Engines



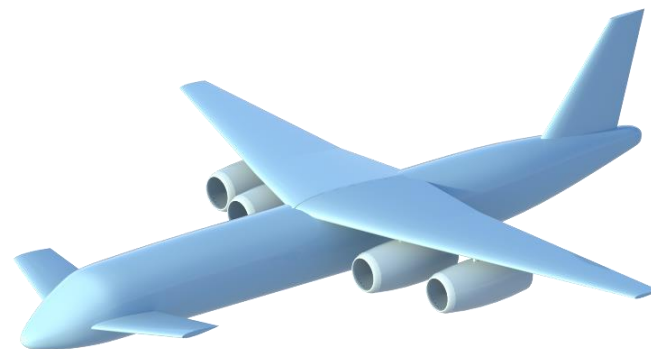
4. High Wings High Engines



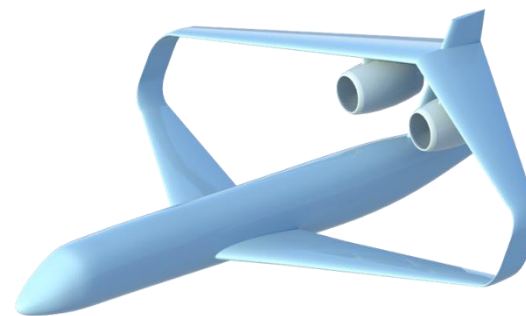
5. Blended Wing Aft Engines



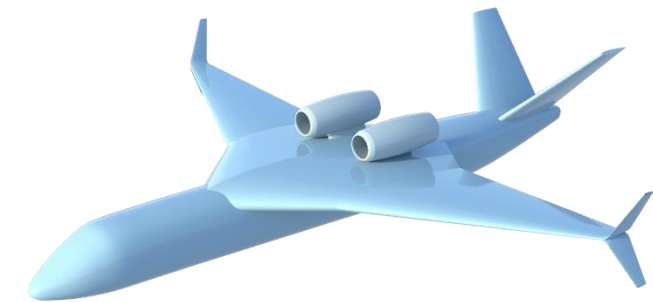
6. Low Wing Dual Tail



7. High Wing Canard



8. Infinity Wing



9. Blended Wing High Engines

Figure 7-1: Configuration Matrix for Class I Design

7.1 Rejected Configurations

This section presents the configurations that were rejected for preliminary design. Configuration pros and cons are listed in the tables below alongside their optimization function (OF) scores.

Low Wing Low Engines: OF = 1.15

- | | |
|--------------------------------|-------------------------|
| + Standard Regional Jet Design | - Not Unique to Market |
| + Low Certification Cost | - Poor engine clearance |
| + Easy Maintenance | - Ground Noise |
| + Ground Effect Lift | |



Figure 7-2: Low Wing/Low Engines

Blended Wing V-Tail: OF = 1.07

- | | |
|--|---------------------------|
| + Light-Weight Empennage Configuration | - High Cabin Noise |
| + Unique to Market | - Unstable Pitch Break |
| | - Unstable Yaw Break |
| | - High Certification Cost |
| | - CG Excursion |

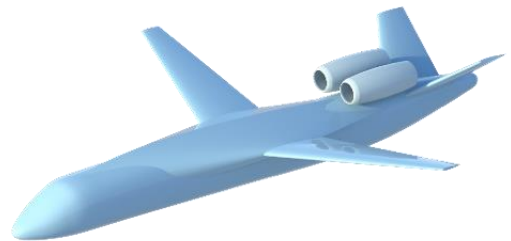


Figure 7-3: Blended Wing Aft Engines

Low Wing Dual Tail: OF = 1.17

- | | |
|----------------------|---|
| + Ground Effect Lift | - High Certification Cost |
| + Unique to Market | - High Cabin Noise |
| | - Engine Thrust Interferes with Empennage |
| | - CG Excursion |

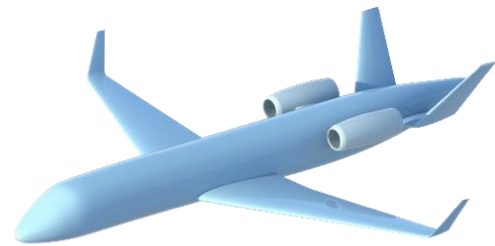


Figure 7-4: Low Wing Dual Tail

High Wing Canard: OF = 1.08

- | | |
|--------------------|---------------------------|
| + CG Balance | - High Engine Count |
| + Unique to Market | - High Certification Cost |
| | - Unstable Pitch Break |

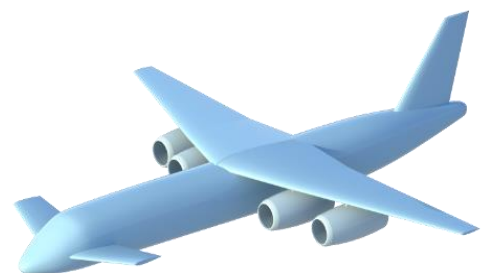


Figure 7-5: High Wing Canard

Infinity Wing: OF = 1.10

- | | |
|--|---|
| <ul style="list-style-type: none"> + Unique to Market | <ul style="list-style-type: none"> - CG Excursion - High Certification Cost - Unstable Pitch Break |
|--|---|

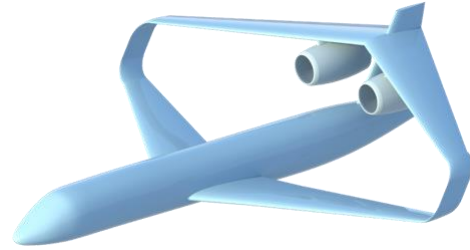


Figure 7-6: Infinity Wing

Blended Wing: OF = 1.06

- | | |
|--|---|
| <ul style="list-style-type: none"> + Unique to Market + Reduced Ground Noise | <ul style="list-style-type: none"> - High Certification Cost - Unstable Pitch Break - Unstable Yaw Break - High Cabin Noise |
|--|---|

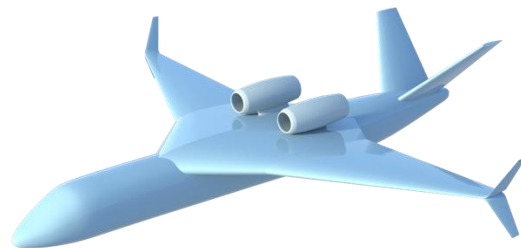


Figure 7-7: Blended Wing High Engines

7.2 Accepted Configurations

The three most competitive configurations are presented in the tables below alongside their pros and cons.

High Wing: OF = 1.19

- | | |
|--|--|
| <ul style="list-style-type: none"> + Standard Regional Jet Design + Low Certification Cost + Improved Ingress/Egress + Improved Passenger Visibility | <ul style="list-style-type: none"> - Not Unique to Market - High Engine Count - High Engine Noise |
|--|--|



Figure 7-8: High Wing

A high-wing design shown in Figure 7-8 allows for the integration of more ingress and egress locations. This minimizes ground time and improves evacuation times in the event of an emergency. The high wing configuration is not unique to the regional jet market, which lowers certification costs. However, because this design is not unique, it does not offer enough significant advantages over existing regional jet aircraft.

High Wing High Engines: OF = 1.29

- | | |
|--|---|
| <ul style="list-style-type: none"> + Ingress/Egress + Improved Passenger Visibility + Unique to Market + High CL + CG Balance + Maintenance and Servicing + Reduced Ground Noise + Shorter Runway Requirements | <ul style="list-style-type: none"> - Certification Cost - Increased Wing Weight - Powerplant Improvement |
|--|---|

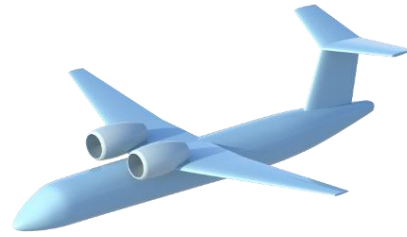


Figure 7-9: High Wing/High Engines

This high-wing high-engine configuration observed in Figure 7-9 is based off of the YC-14 and AN-74 aircraft. Placing the engines on top of the wings increase the C_L during takeoff due to the upper surface blowing (USB) effect. While this design suffers from a high certification cost, its unique layout offers a variety of advantages over existing regional jets, as listed above. Some drawbacks to placing the engines on the wings include a higher wing weight, increased noise, and difficulty in growing powerplant size.

Low Wing Aft Engines: OF = 1.27

- | | |
|--|---|
| <ul style="list-style-type: none"> + Standard Regional Jet Design + Low Certification Cost + Ground Effect Lift | <ul style="list-style-type: none"> - Not Unique to Market - CG Excursion - Powerplant Improvement - Cabin Noise |
|--|---|



Figure 7-10: Low Wing/Aft Engines


The low-wing aft-engine design in Figure 7-10 is already widely used in the regional jet market. This design is proven and would have a low certification cost, but it does not offer any advantages over existing aircraft.

7.3 Final Configuration Selection

Analyzing the configuration matrix revealed the high-wing high-engine configuration observed Figure 7-11 as the optimal design. This configuration offers

“The high wing makes a lot of sense.... On the flight line, there was a general principle involving ground equipment: If a thing can hit a wing, it WILL hit a wing.”

-R. Paul Barrett, Saudi Arabian Airlines Superintendent of Flight Safety on the Flight line, Jeddah, Saudi Arabia



several advantages over other regional jets. The engine placement offers improved performance through the USB effect. Increased lift makes the aircraft more efficient and allows the aircraft to operate on shorter runways, making

it compatible with airports other regional jets may not have access to. The high engines also keep the center of gravity of the aircraft further forward in comparison to other configurations. Furthermore, a high wing also enhances the passenger experience through increased visibility and improved ingress and egress times. Overall, this configuration provides a unique design with several performance and passenger benefits, separating itself from the rest of the market.

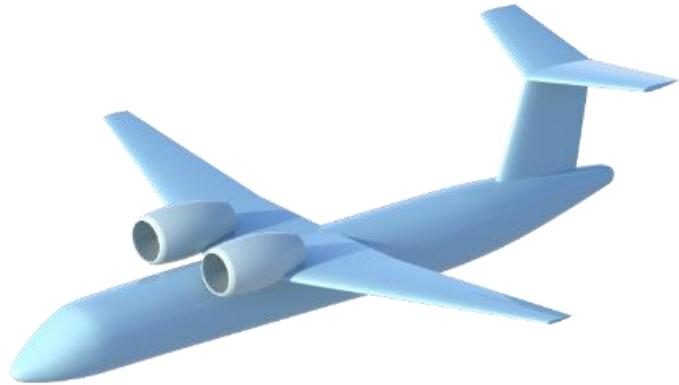


Figure 7-11: High Wing/ High Engine Final Selection

7.4 Configuration Features and Airline Operations Experts’ Observations

A preliminary design was presented to experts in the aerospace field which allowed possible problems to be raised. These perceived challenges are covered along with the current market solutions and Skyblazer solutions. Some quotes are also presented from the expert comments on the preliminary Skyblazer design.

One issue that was brought up after the preliminary design review was the over wing engine mounting configuration with respect to difficult maintenance and replacement requiring specialized equipment. This over wing engine mounting height coincides with current engine mounting equipment, and the configuration would utilize a U-truss for simplified engine replacement and maintenance shown in Figure 7-12.



Figure 7-12: Easy Line Maintenance for Engine at 10 ft off Ramp like Skyblazer, DC-9, EMB-145, and CRJ [31]

There was also a comment questioning our ingress/egress time reduction and compliance. However, this configuration will use multiple door boarding and will be ADA compatible for proper ingress and egress operations. Current RJ’s struggle with ADA compatible ramps due to their taller nature requiring more expensive solutions. Figure 7-13 shows the Skyblazer cabin door layout for ingress/egress and emergency operations.

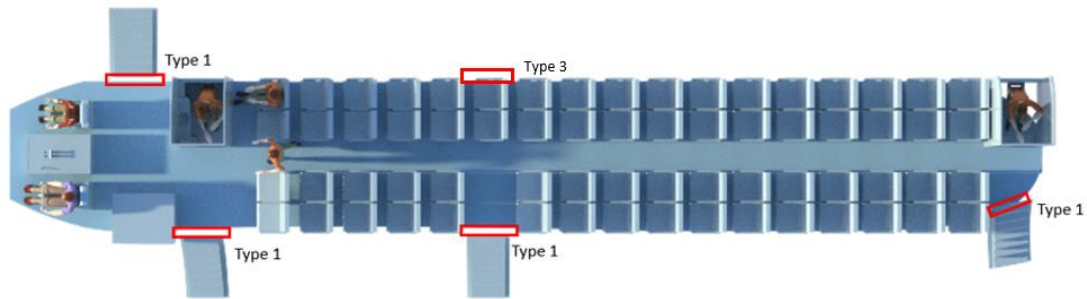


Figure 7-13: Skyblazer-200 Cabin Door Locations for Normal and Emergency Operations

Some experts questioned the aircraft ability to integrate landing gear and fuel storage. With the selected configuration for the design, sponsons will house both main landing gear and additional fuel tanks. They will provide needed space for additional systems, and the benefits outweigh drag drawbacks. Current aircraft load all fuel into the wing to reduce the additional drag, but this places aircraft further off the ground compared to an aircraft with sponsons. Figure 7-14 shows sponsons with landing gear and fuel tank integration for a C-17 Globemaster II.

For refueling time and capability, sponson and wing fuel tanks will allow for distributed fuel. With multi-hose capabilities, refueling time may be reduced. Current aircraft are usually only fueled from one location on the wing, taking much longer during turn around.

An aerospace expert questioned the reductions in direct operating costs. To achieve this, increases in aircraft operation tempo (flight legs per day) will be performed, which would decrease the number of airplanes per fleet. Current aircraft require more time during turn arounds reducing the amount of turns they can make a day. Using a magic carpet, the loading times are also much faster shown in Figure 7-15 when compared against manual loading and unloading



Figure 7-14: C-17 Globemaster II Landing Gear and Fuel Sponsons [32]

After the preliminary design review, the Skyblazer cabin loading time reduction capabilities were questioned. However, this configuration will utilize cabin luggage bins to reduce overhead storage congestion and reduce boarding times. Current aircraft are often congested with a large number of people waiting to get their

carryon from overhead bins. With the unique regional configuration, the water emergency and egress/ingress capabilities needed to be clarified. Current regional jets have over wing exits during water emergency ditching. Sponsons would help float a Skyblazer aircraft during emergency ditching. Floatation tubes could be added to a Skyblazer for flights over large bodies of water. Exits above the sponsons could be used for emergency egress while preventing water ingress.

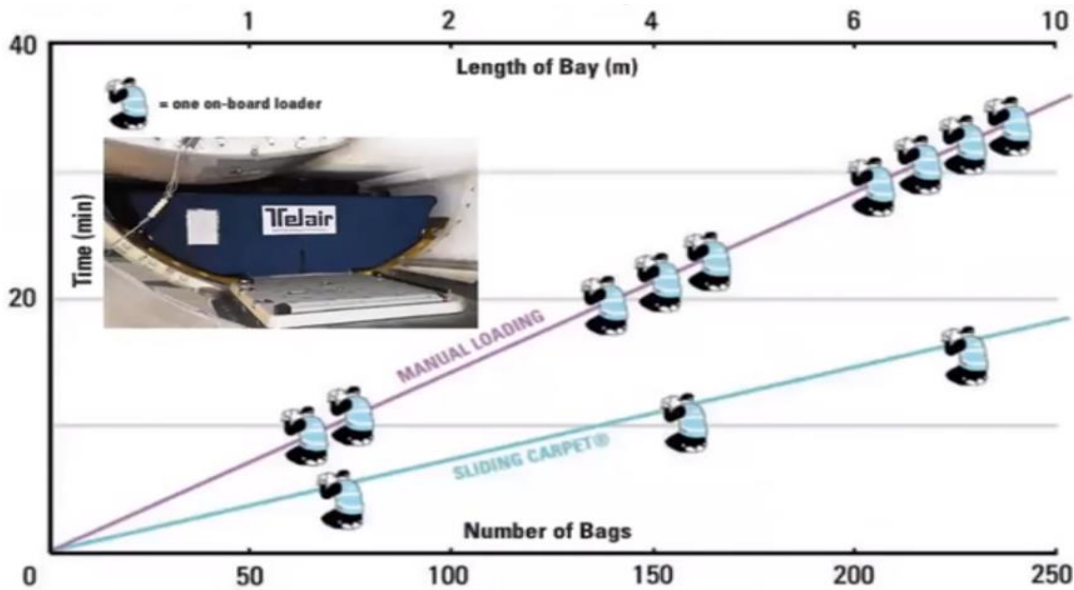


Figure 7-15: Number of Baggage Unloaders with Manual vs. Sliding Carpet [33]

Figure 7-15 contains a plot of collected data from Telair that compares loading times of manual luggage loading to an automatic luggage carpet. Figure 7-16 contains an image of the magic carpet system that will be implemented into the Skyblazer configuration. The magic carpet will continuously run from nose to tail.

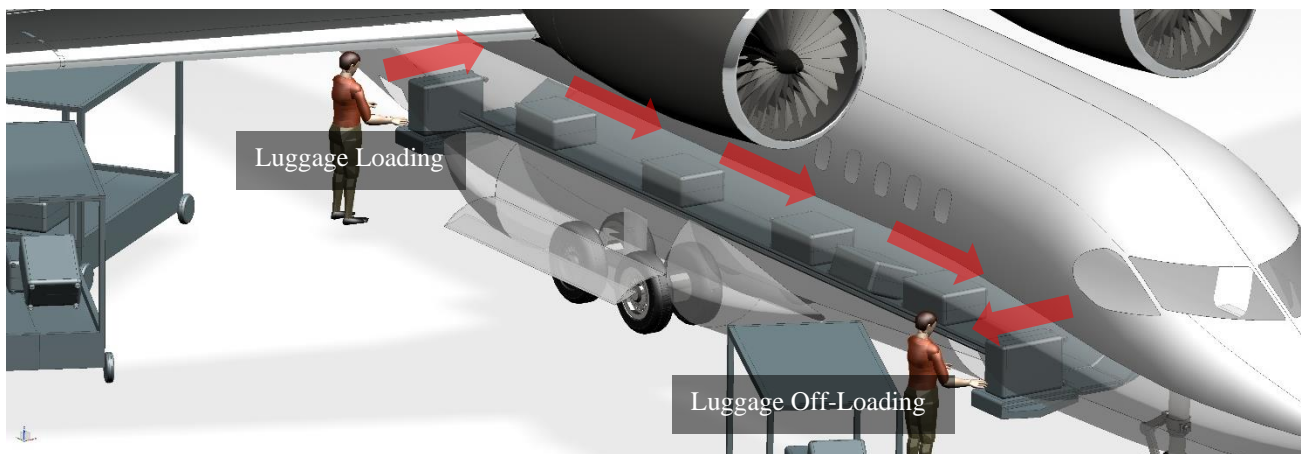


Figure 7-16: Continuous Nose-to-Tail Magic Carpet System

8 V-n Gust and Maneuver Diagram and Flight Envelope

The gust and maneuver V-n diagrams for both aircraft are generated and discussed in this section and are based on FAR 25 requirements. The V-n diagrams shown below provide the limits of the of the aircraft by showing which load factor is being applied at different speeds. The speeds analyzed are +1g stall speed (V_{S1}), cruise speed (V_c), dive speed (V_d), mauver speed (V_a) and the designed speed for maximum gust intensity (V_b). The maximum load factor is 2.5g's while the negative value is at -1.0g's from the cruising speeds to diving speeds. Loads associated with vertical gusts are also evaluated over velocity in the gust diagrams. The gust and maneuver diagram is shown for the 50-seat aircraft in Figure 8-1: 50-Seat V-n Maneuver and Gust Diagram

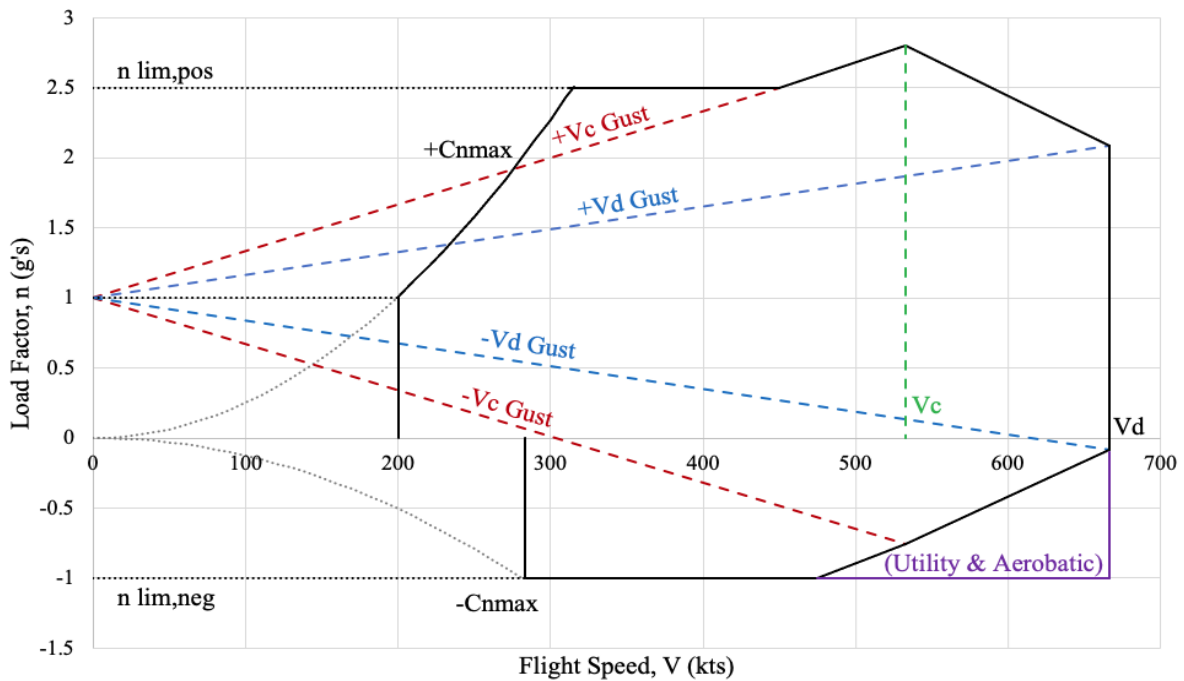


Figure 8-1: 50-Seat V-n Maneuver and Gust Diagram

The flight envelope is shown in Figure 8-2 with altitude plotted against flight speed in Mach. The service ceiling limit shown at 42,000 ft, 1g stall line is shown in black, and maximum Mach limit on the right at 0.85 Mach. The various rates of climb are plotted as labeled in the legend.

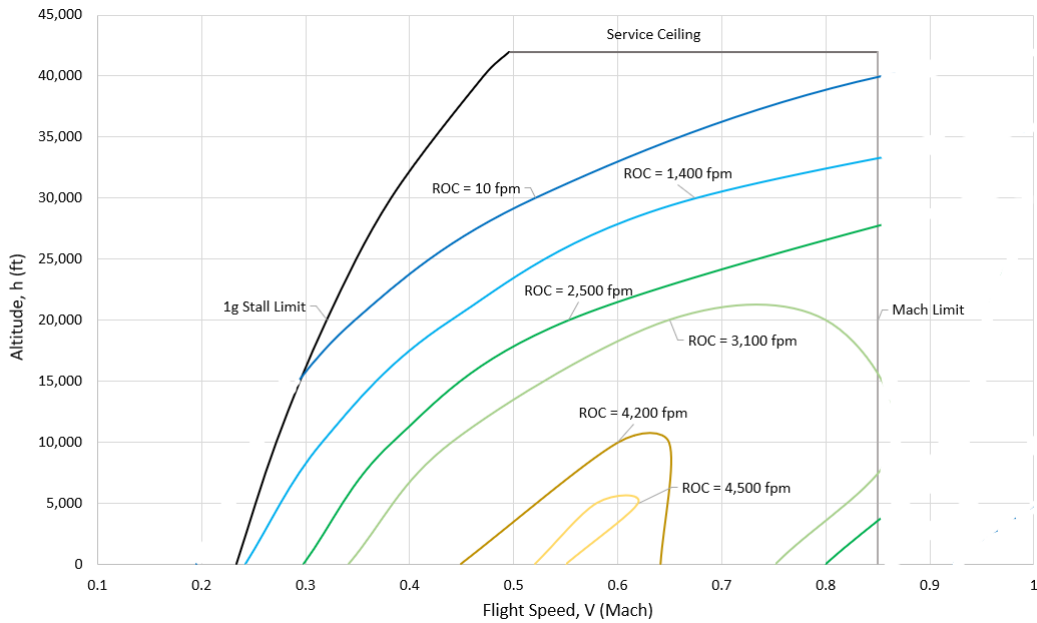


Figure 8-2: 76-Seat Flight Envelope

9 **Payload-Range and Fuel Burn**

A payload-range diagram uses various parameters that affect the aircraft efficiency to calculate ranges based on different payloads. The Breguet Range equation used to generate the plot in Figure 9-1 with both the 100 and 200 series shown. Eqn. 9.1 is shown below with the observed inputs used to calculate range. The weight fraction is altered for each point on the plot depending on the different payload load cases shown on the plots including maximum zero fuel weight, maximum takeoff weight at maximum payload with tanks full, and maximum ferry range. Each of these payload scenarios provide insight for the customer on the tradeoff relationship between the range available under a certain payload. Three different cruise speeds are also used to show the range possibilities for values of Mach 0.78, Mach 0.8, and Mach 0.85 shown in black, red, and blue respectively on the diagrams. The range at MTOW with maximum payload is the structural limit payload range. The 50-seat aircraft is observed to have a longer structural limit payload range based on

$$R(nmi) = \left(\frac{V(fts)}{c_j(lbf/lbf - hr)} \right) \left(\frac{L}{D} \right) \ln \left(\frac{W_{i+1}}{W_i} \right) \quad \text{Eqn. 9.1}$$

the RFP requirement and size.

Table 9-1 shows the calculated fuel burns per trip and seat for the Skyblazer series and an ERJ-145 based on the 500 nmi and 1000 nmi range. The Skyblazer series has a lower fuel burn per seat and higher fuel burn per trip when compared with the ERJ fuel burn.

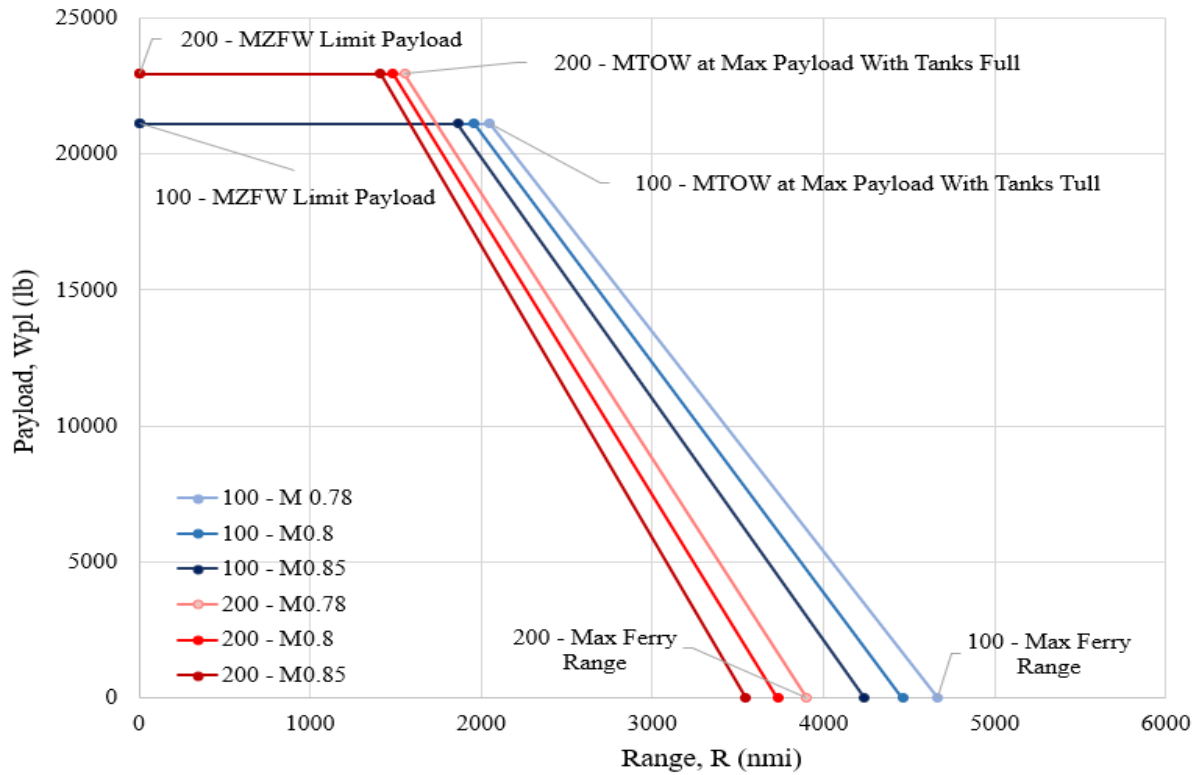


Figure 9-1: Payload-Range Diagram for Varying Cruise Velocities

Table 9-1: Fuel Burn Comparison

	Skyblazer-100	ERJ-145	Skyblazer-200	ERJ-170
Fuel Burn/Trip - 500 nmi (lbf)	3,310	3,650	5,000	4,900
Fuel Burn/Seat - 500 nmi (lbf)	66.2	73.0	65.8	68.1
Fuel Burn/Trip - 1000 nmi (lbf)	6,620	7,310	10,000	9,800
Fuel Burn/Seat - 1000 nmi (lbf)	132	146	132	136

10 Design and Sizing

The overall final design characteristics and specifications sized in this section are shown below in Table 10-1. It includes some characteristics that are shared between the aircraft including the wing and cockpit designs. The fuselage, cabin, and empennage vary between the aircraft due to the size differences and requirements.

Table 10-1: Skyblazer 100 and 200 Series Salient Characteristics

Fuselage Characteristics			
	Fuselage (100 Series/200 Series)	Cabin Interior (100 Series/200 Series)	Overall Aircraft (100 Series/200 Series)
Length, l (ft)	79.5 / 88.8	44 / 59	85.4 / 96
Maximum Height, h_{max} (ft)	11.3 / 10.2	9.17 / 9.17	22 / 22
Maximum Width, w_{max} (ft)	10.2 / 11.4	9.17 / 9.17	83.9 / 83.9
Planform Characteristics			
	Wing	Horizontal Tail (100 Series/200 Series)	Vertical Tail
Area, S (ft ²)	537	85 / 70	121
Span, b (ft)	77	16.35 / 13.435	11.2
Mean Geometric Chord, \bar{c} (ft)	7.7	5.7 / 5.71	10.9
Aspect Ratio, AR	11	3.14 / 2.59	1.04
Inboard Sweep Angle, Λ_{is} (deg)	0	33 / 33	30
Outboard Sweep Angle, Λ_{os} (deg)	28	-	-
Taper Ratio, λ	0.4	0.3 / 0.3	0.8
Thickness to Chord Ratio, t/c	0.14	0.12/0.12	0.12
Airfoil	Supercritical SC(2)-0714	NACA 0012	NACA 0012
Anhedral Angle, Γ (deg)	2	2 / 2	-
Incidence Angle, i (deg)	0	0 / 0	0
Control Chord Ratio	0.25	0.25 / 0.25	0.25
Control Span Ratio	0.26	0.875 / 0.875	.97
Flap Chord Ratio	0.25	-	-
Flap Span Ratio	0.57	-	-

10.1 Cockpit Layout and Design

The cockpit was sized using the methods outlined in Roskam’s Airplane Design Part III. Two main design criteria were considered in the cockpit design: 1) Pilot compatibility and 2) visibility requirements. The Skyblazer series features a glass cockpit.

The overall layout in Figure 10-1 remains similar to current market leaders (ERJ 145 and CRJ200) to make the pilot transition to the Skyblazer aircraft smoother. To account for pilots of various sizes, the seats can be adjusted 3.5 inches in each direction, so all pilots achieve the required visibility. Figure 10-2 demonstrates a 95th and 20th percentile male and female operating the aircraft. Pilots have maximum viewing angles of



Figure 10-1: Cockpit Layout



Figure 10-2: 95th and 20th Percentile Male and Female in Cockpit

52.4° upwards and 31° downward as shown in Figure 10-4. A more detailed analysis of pilot viewing angles was conducted to verify the cockpit design achieves all FAR 25 viewing angle requirements. The analysis was conducted using the captain side pilot eye view Figure 10-4. The Skyblazer viewing angles achieve or surpass the FAR 25 recommendations at all measured points seen in Figure 10-5.

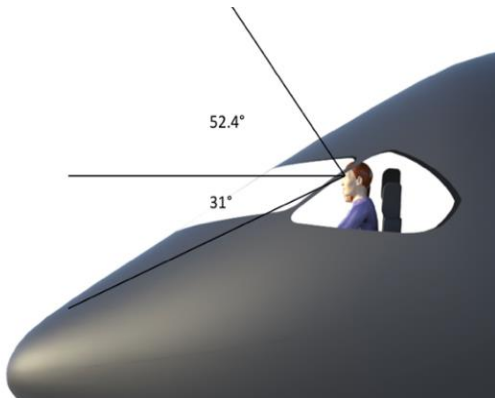


Figure 10-4: Pilot Maximum Viewing Angles



Figure 10-4: Cockpit Side View

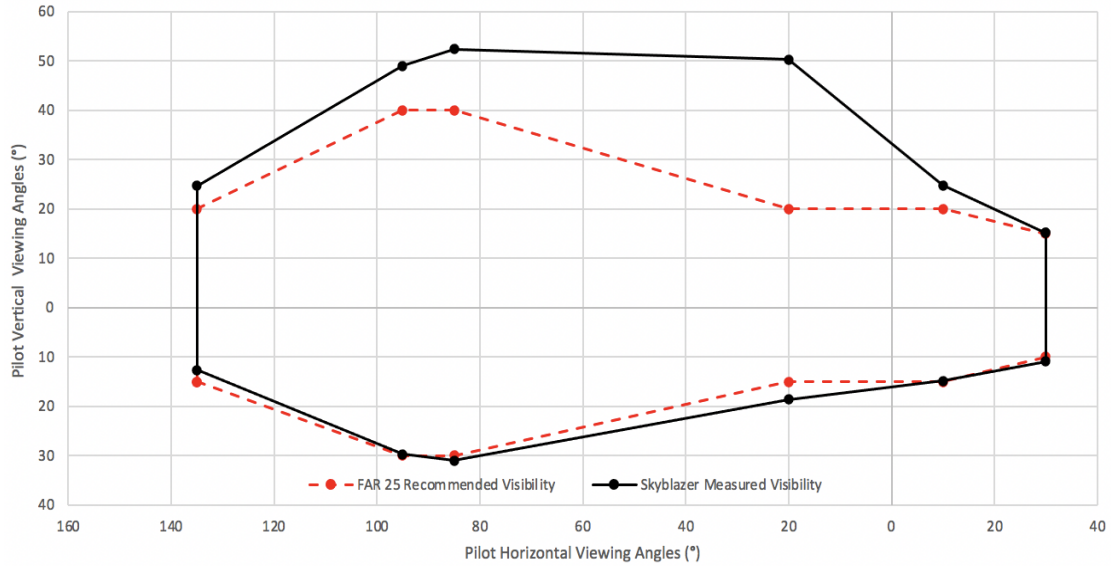


Figure 10-5: Skyblazer vs. FAR 25 Recommended Cockpit Viewing Angles

10.2 Fuselage Layout

The fuselage dimensions were sized using the ratio of the total fuselage length to the maximum fuselage diameter shown in Figure 10-6.

$$\text{Fuselage Fineness Ratio} = \frac{l_f}{d_f} \quad \text{Eqn. 10.1}$$

A fineness ratio ranging from four to nine is ideal when selecting the fuselage lengths. An increase in fuselage length will be the major discrepancy between the 50-seat and 76-seat configurations. Keeping the diameter of the fuselage the same for each configuration the fineness ratios will be 7.02 and 9.72 blank for the 50-seat and 76-seat designs respectively. The seating configuration

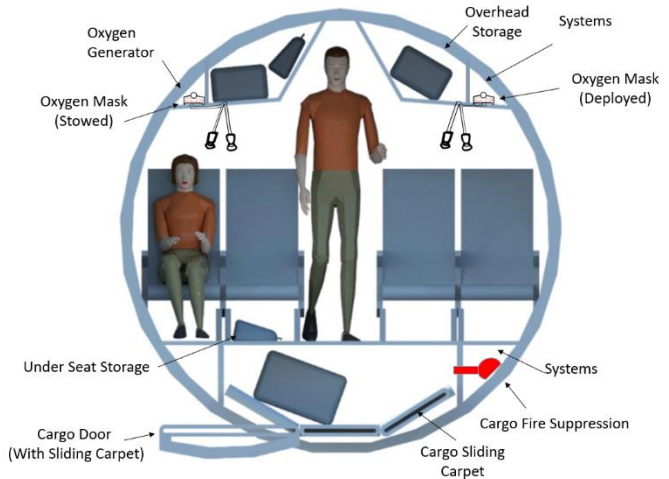


Figure 10-6: Fuselage Cross Section

was based on the passenger capacity requirements. The cross-section shown in Figure 10-6 has a diameter of 100 inches.

As seen in Figure 10-7 and Figure 10-8, a two and two configuration was chosen for the seat layout. This configuration was chosen to maximize the fuselage fineness ratio. Using a two and one would yield a design that would be too long to be aesthetically pleasing and cause take-off tail strike issues. Figure 10-7 and Figure 10-8 depicts the 2x2 fuselage layout of the 2x2 50 and 76 seat variant respectively. The cabin is easily able to accommodate a 95% percentile male and a 20% percentile female with plentiful space for amenities. Figure 10-7 and Figure 10-8 displays the internal features of the fuselage for the 50-seater variant of the design. The internals of the fuselage contain one lavatory for the 50-seat configuration and 2 lavatories for the 76-seater. The fuselage also requires a galley from storage of hot meals and other amenities, this is placed at the rear of the 50-seat configuration and at the front for the 76-seat configuration.

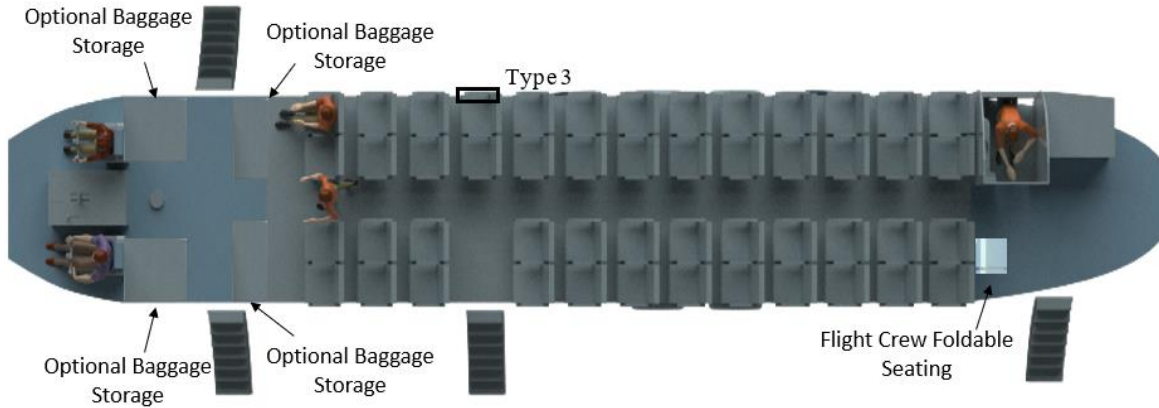


Figure 10-7:50 Seat 2x2 Cabin Layout Top view

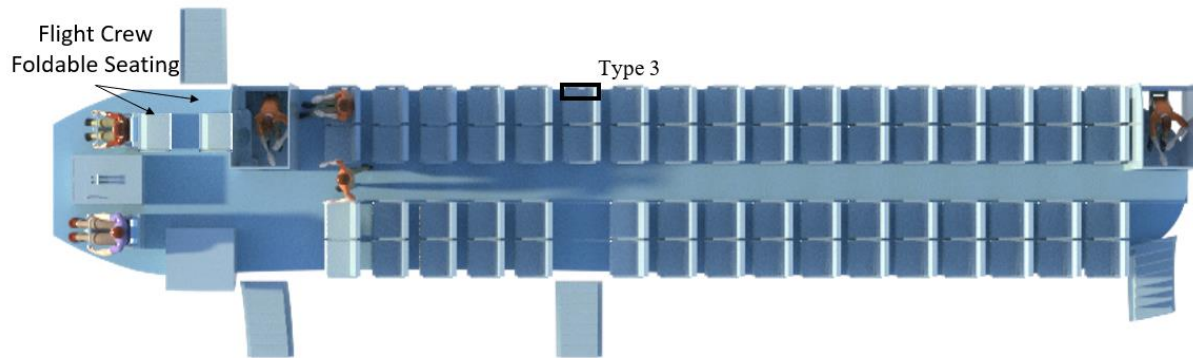


Figure 10-8:76 Seat 2x2 Cabin Layout Top view

In order to improve the overall efficiency of the aircraft during normal operation and emergency operation, three exit locations are placed on the right side of the aircraft. The primary exit locations are at the front and rear of the aircraft with the center exit reserved for emergency or high passenger instances.

10.3 Engine Selection and Installation

Using the thrust requirements for optimal performance based on the weight and wing sizing, the two engines for the 50-seat and 76-seat aircraft are General Electric CF34-3 and GE CF34-8C respectively. Following the configuration previously outlines, the engines will be mounted on top of a high wing. This configuration allows simpler methods for installation and maintenance for less hassle and risk of damaging the engine or aircraft. A “U” truss is used on the outside of the engine to hold the engine in place and connect it to the wing. A winch will also be used to allow the lowering of the engine without outside equipment in order to conduct maintenance on the engines, this will save in costs and time as seen in Figure 10-12. A CAD model showing this method of engine mounting is shown below in Figure 10-11.

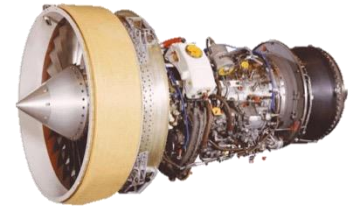


Figure 10-10: GE CF34-3 [34]

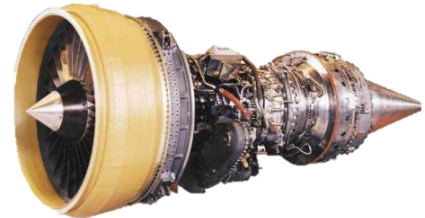


Figure 10-10: GE CF34-8C [35]

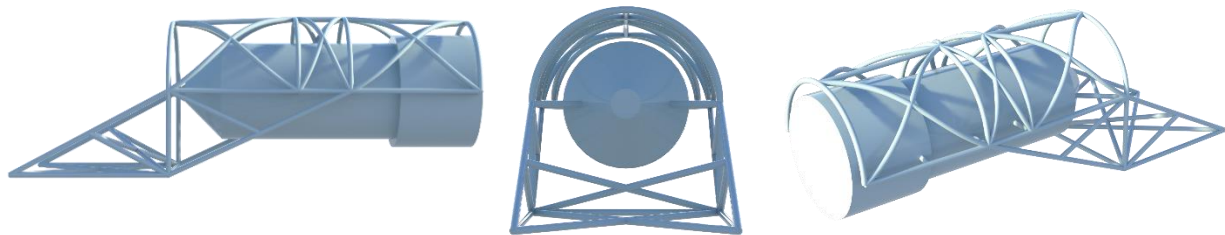


Figure 10-11: Three-View of the Engine Mounting Structure

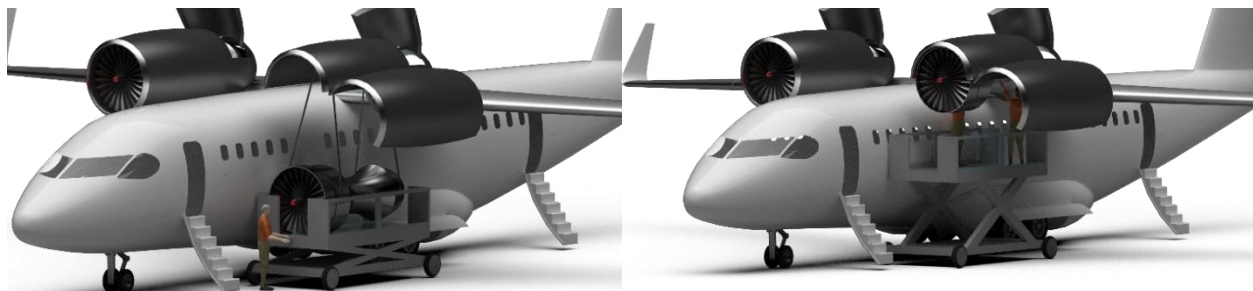


Figure 10-12: Integrated Winch System and Maintenance

10.4 Wing Layout

The wing characteristics to develop the wing layout design are determined in this section. As previously discussed, the overall wing-fuselage arrangement is a high-wing with high mounted engines. This arrangement reflects

high lateral stability and high visibility from the cabin but includes drawbacks of high landing gear weight and increased interference drag.

The preliminary wing thickness was sized using a 13% thick airfoil to meet wing fuel volume requirements. Using this thickness, a cruise Mach of 0.80, and a calculated cruise lift coefficient of 0.31, the quarter chord sweep angle was estimated to be 28°.

A wingspan of 77 ft was determined to fit the ICAO gate spacing requirement for code B. Using STAMPED data, a preliminary average mean chord of 7 ft was determined which results in an aspect ratio of 11.

The inboard dihedral was determined to be 0° to support the engine mounting, while the outboard dihedral has an angle of 2° as shown in Figure 10-13. Although, after consideration the outboard section of the wing will include an anhedral deflection to account for roll stability for a high wing configuration. The incidence angle was based on historical aircraft with the same configuration and was determined to be 0°. The taper ratio was also determined based on historical data and was selected to be 0.40. A supercritical airfoil was selected based on the aircrafts high Reynolds number and high cruise Mach that the aircraft will experience in cruise flight. However, supercritical airfoils can lead to high trim drag and can cause problems with high lift sizing which will be discussed in the next section.

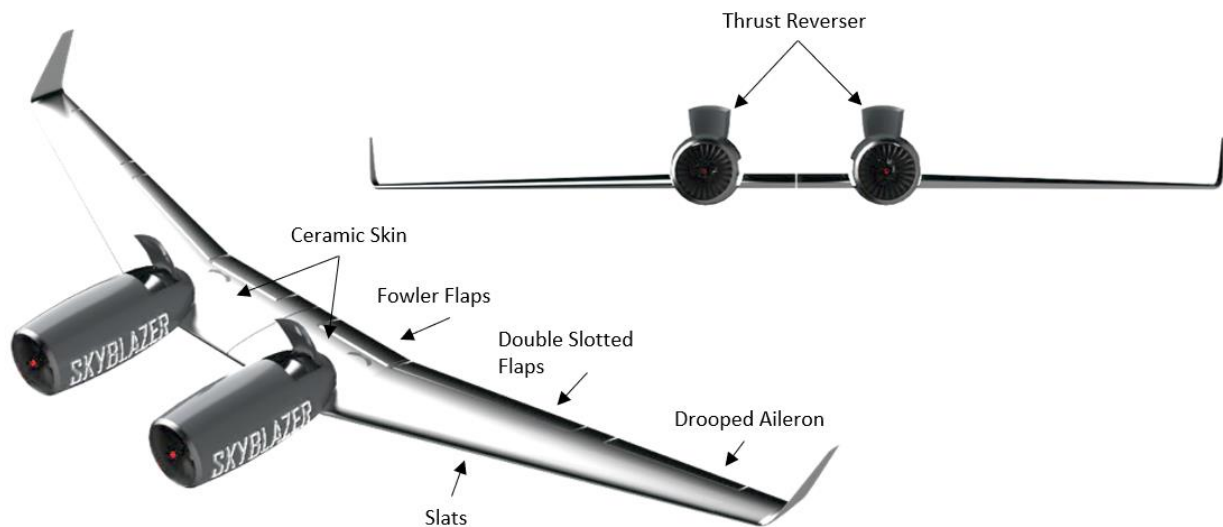


Figure 10-13: Wing Front and Isometric View

Ceramic skin will be applied to the inboard section of the wing that the engine is mounted on. This will be used to avoid ablation and limit the need for charring. This will increase the life span of the fowler flaps used in the most inboard section of the wing. The ceramic skin has the risk of impurities in the heating process of the ceramics

required to fire the material. It also will require structural test and regular checks. To mitigate these risks, regular structural tests will be performed to ensure quality. This may also save on the cost of replacing wings damaged due to charring.

10.5 High Lift Devices

Using material outlined in Roskam's *Airplane Design Part II* in Chapter 7, the high lift devices were sized and determined that the wing area and airfoil selection will have to be reviewed in order to insure enough lift from these sizes can be achieved. A fowler flap was chosen due to the amount of C_L necessary for takeoff and landing flight conditions calculated in the wing design portion. This section will need to be iterated in order to achieve an accurate wing size, airfoil, and sizes of the high lift devices.

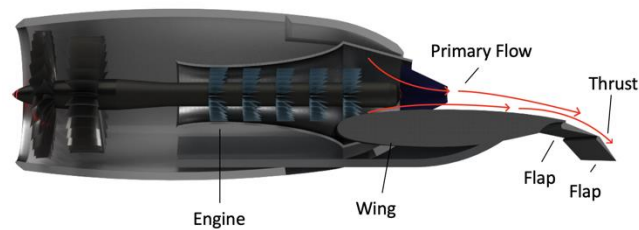


Figure 10-14: Upper Surface Wing Blowing

The Skyblazer 100 series was determined to have the critical CL_{max} needed due to the shorter field length it has to take off within. The wing produces a C_L of around 2.3 determined using VSPAero to create a simulation of the wing's provided lift at landing conditions.

The needed $C_{L_{max}}$ for landing (the most critical case) was determined to be around 5.2. This means complex high lift devices need to be able to create a ΔC_L of about 3.1 to generate enough lift for a safe landing. This can be reduced to about 4.5 using the slip stream and Coanda effect provided by the over wing engines. With a reasonable flapped wing area to wing area of 0.3, this requires a high lift device that provides a localized C_L of 7.3 with a slip stream angle of 60° . This was determined to require a flap deflection angle of greater than 90° to produce a safe amount of lift for landing. All other flight regimes are safely within reasonable safety margins. The aircraft is unable to provide enough lift for landing with just the wings, so this is where the upper surface blowing will become a major player and provide the aircraft with the proper amount of lift to land safely in OEI scenarios.

10.6 Empennage Sizing

Table 10-2 shows the calculated horizontal tail and vertical tail volume coefficients of three similar aircraft configurations. Each of these aircraft had significantly higher volume coefficients due to their enormous size and configuration. These volume coefficients were calculated by geometrically analyzing three-view drawings and

estimating their approximate CG locations. Using their wingspans as a reference, other geometric characteristics were calculated, such as area, span, mean geometric chord, and approximate CG to quarter-chord of the mean geometric chord for the horizontal and vertical tail.

Table 10-2: Horizontal and Vertical Tail Volume Coefficients of Similar Aircraft




			
Aircraft	Boeing YC-14 [36]	McDonnell Douglas YC-15 [37]	Antonov An-72 [38]
Horizontal Tail Volume Coefficient, \bar{V}_h	1.31	1.25	1.28
Vertical Tail Volume Coefficient, \bar{V}_v	0.115	0.113	0.151

Table 10-3 contains the projected empennage characteristics for both Skyblazer series aircraft. The volume coefficients were an average of the volume coefficients found in Table 10-2. The approximate CG locations of the horizontal tail and vertical tail were estimated with a three-view CAD drawing of the Skyblazer-100 and 200. Finally, the horizontal and vertical tail areas were solved using the known wing area, wingspan, and mean geometric chord of the wing. The horizontal and vertical tail volume coefficients were used to give general estimates of the empennage sizing for the Skyblazer series aircraft.

Table 10-3: Skyblazer Series Projected Empennage Characteristics

Skyblazer Variant	100 (50 Seat)	200 (76 Seat)
Horizontal Tail Volume Coefficient, \bar{V}_h	1.28	1.28
CG to the Quarter-Chord of the MGC on the Horizontal Tail, X_h (ft)	37.8	38.5
Horizontal Tail Area, S_h (ft ²)	108	106
Incidence Angle of the Horizontal Tail, i_h (°)	-2	-2
Sweep Angle of the Horizontal Tail, Λ_h (°)	30	30
Vertical Tail Volume Coefficient, \bar{V}_v	0.126	0.126
CG to the Quarter-Chord of the MGC on the Vertical Tail, X_v (ft)	38.5	38.5
Vertical Tail Area, S_v (ft ²)	121	121
Dihedral Angle of the Vertical Tail, Ψ_h (°)	90	90
Sweep Angle of the Vertical Tail, Λ_v (°)	30	30

The incidence angle of the horizontal tail will be chosen to be about -2° to pitch the aircraft down to counter the pitch up from the wing. The horizontal tail sweep angle will be about 30°, which is greater than the wing sweep to ensure our horizontal stabilizer does not stall before the wing to maintain control. This same idea will be applied to

the vertical tail, which will ensure the vertical stabilizer remains in control. The vertical tail sweep was therefore chosen to be 30°. The dihedral angle of the vertical tail for the Skyblazer-100 will be 90°.

Table 10-4 contains the selected empennage sizing values for each Skyblazer variant. The selected horizontal and vertical tail areas were decided using Figure 10-15, Figure 10-16, and Figure 10-17. The Munk shift values were calculated below using Multhopp Integration.

Table 10-4: Empennage Selected Sizing Values

	Skyblazer-100 (50 Seat)	Skyblazer-200 (76 Seat)
Lift Coefficient due to Angle of Attack on the Wing, $C_{L_{\alpha_w}}$ (rad ⁻¹)	4.15	4.15
Lift Coefficient due to Angle of Attack for the Wing-Fuselage, $C_{L_{\alpha_{wf}}}$ (rad ⁻¹)	4.15	4.15
AC Wing Location from the LE of the Wing MGC, \bar{X}_{ac_w} (fr. \bar{c})	0.25	0.25
Lift Coefficient due to Angle of Attack on the Horizontal Tail, $C_{L_{\alpha_h}}$ (rad ⁻¹)	4.15	4.15
AC Horizontal Tail Location from the LE of the Wing MGC, \bar{X}_{ac_h} (fr. \bar{c})	5.65	9.92
Horizontal Tail Area, S_h (ft ²)	85	70
Downwash on the Horizontal Tail due to Angle of Attack, $\frac{\partial \epsilon_h}{\partial \alpha}$	0.0195	0.0193
Change in AC Location due to Fuselage (Munk Shift), $\Delta \bar{X}_{ac_f}$ (fr. \bar{c})	-0.92	-1.21
AC Location of the Aircraft from the LE of the Wing MGC, \bar{X}_{ac_A} (fr. \bar{c})	0.13	0.25
Vertical Tail Area, S_v (ft ²)	121	121
Yawing Moment Coefficient due to Sideslip for the Wing-Fuselage, $C_{n_{\beta_{wf}}}$ (rad ⁻¹)	-0.00132	-0.00150
Lift Coefficient due to Angle of Attack on the Vertical Tail, $C_{L_{\alpha_v}}$ (rad ⁻¹)	3.64	3.64
Yawing Moment Coefficient due to Sideslip, $C_{n_{\beta}}$ (deg ⁻¹)	0.0020	0.0034

Figure 10-15 and Figure 10-16 contain plots that track AC and CG Location as a function of the horizontal tail area for the Skyblazer-100 and Skyblazer-200, respectively. The most forward and aft CG location lines were superimposed on each figure to visualize the desired static margin range. The horizontal tail areas were selected at the intersection with the most aft CG line to maintain neutral to positive stability.

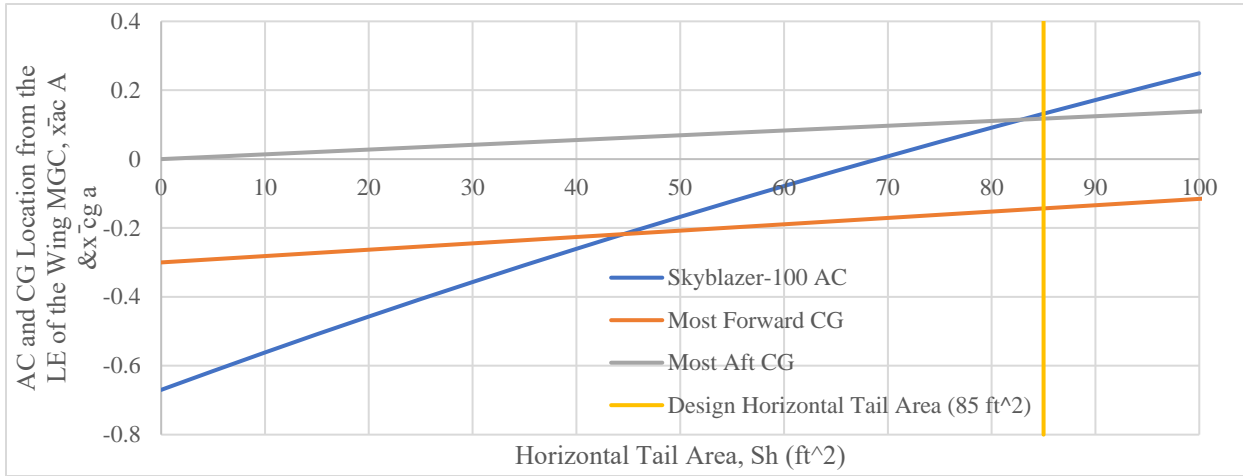


Figure 10-15: Skyblazer-100 AC and CG Location Plot with Horizontal Tail Area

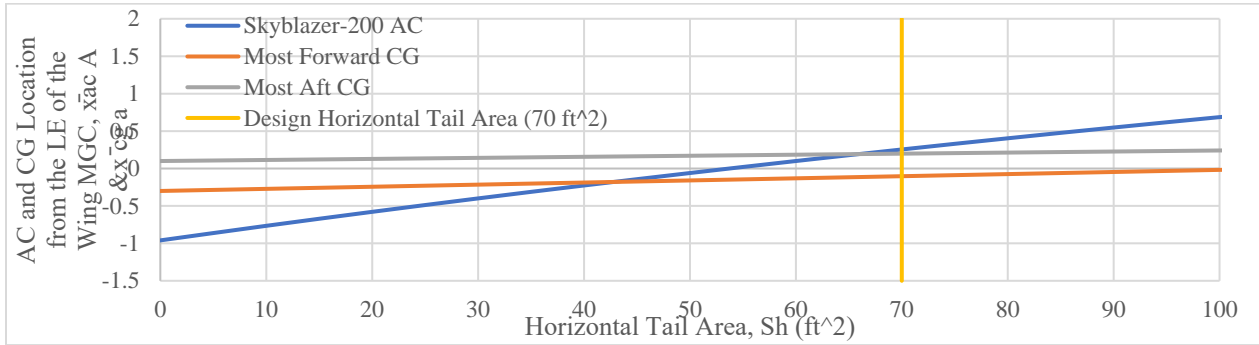


Figure 10-16: Skyblazer-200 AC and CG Location Plot with Horizontal Tail Area

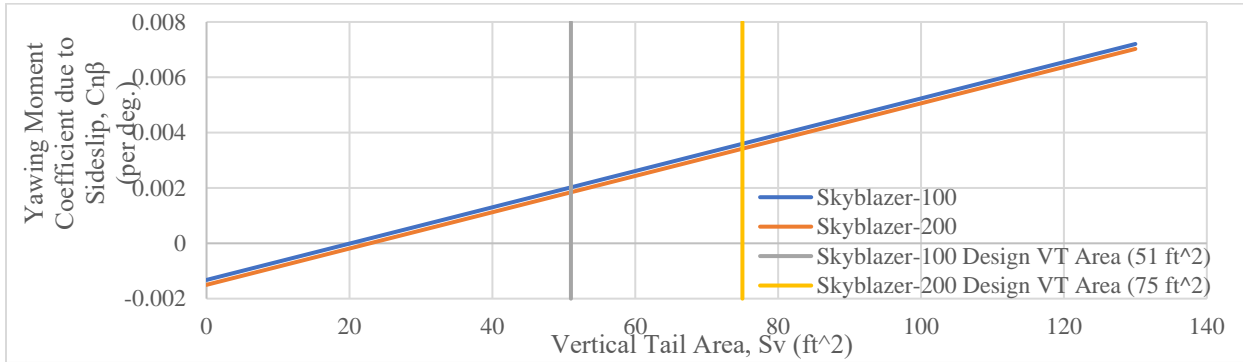


Figure 10-17: Yawing Moment Coefficient Plot with Vertical Tail Area

Figure 10-17 contains a plot that tracks yawing moment coefficient as a function of the vertical tail area with safe areas plotted. Table 10-5 outlines the Critical Engine Out Rudder Deflection needed to maintain a steady heading on take-off. The values of $\sim 11^\circ$ and $\sim 15^\circ$ for the Skyblazer 100 and 200, respectively, are reasonable for landing

allowing for rudder use when landing in a high crosswind during an engine-out condition as well. This allows for the tail to be reduced in size if allowed by directional stability and provides a safe condition during OEI. When taking all of these in consideration, the tail appears to be much smaller than aircraft with similar designs. To be safe the team chose to use the largest of the tail areas, which is the benchmarked size of 120 ft². This helps take unknown and complicated aerodynamic effects into consideration.

Table 10-5: Critical Engine Out Rudder Deflection Values

	Skyblazer-100	Skyblazer-200
Distance to Engine, d_{eng} (ft)	37.5	38.5
Take off OEI Thrust, $T_{TO(1engine)}$ (lbs.)	9200	13790
Critical Drag Induced Yaw Moment, N_D (ft-lbs.)	345000	530915
Minimum Control Speed, V_{mc} (ft/s)	153	185
Yawing Moment Coefficient due to Rudder Deflection, $C_{n\delta_r}$ (deg ⁻¹)	-0.331	-0.340
Rudder Deflection, δ_r (deg)	-10.5	-15

10.7 Landing Gear Designs

The basic landing gear configuration for the Skyblazer 100 and 200 series aircraft were designed with minimal differences to allow for easier manufacturing. The aircraft both feature identical nose and main landing gear wheels. Wheel sizes were based on the landing gear of aircraft with similar takeoff weights. Nose gear assemblies for both aircraft have two wheels on the nose gear. Regarding the main gear assemblies, the 50-seat aircraft has two sets of wheels on each gear, with a total of eight wheels on the main landing gear in Figure 10-19. The 76-seat aircraft has three sets of wheels on each gear, with a total of 12 main landing gear wheels, shown in Figure 10-18. The longitudinal placement of the main gear allows the aircraft to achieve the required 15° of takeoff clearance.

Table 10-6: Landing Gear Wheel Dimensions

	Nose Gear	Main Gear
Wheel Diameter (in.)	21	34
Wheel Thickness (in.)	7.25	9.25



Figure 10-19: 50-Seater Side View and Clearance Angle

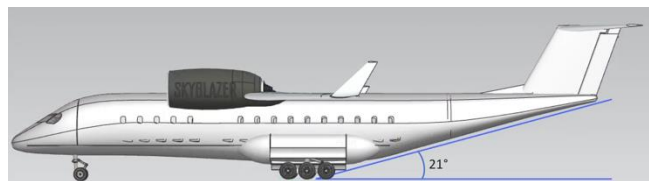


Figure 10-18: 76-Seater Side View and Clearance Angle

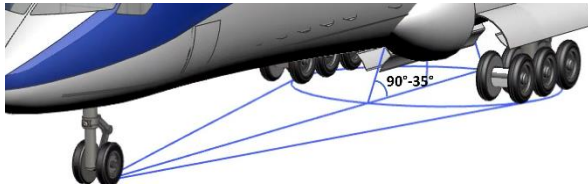


Figure 10-21: Landing Gear Placement Method



Figure 10-20: Landing Gear Front View

The main gear was placed using a 35° half-angle as shown in Figure 10-21. This placement method allows the aircraft to achieve lateral stability. The nose landing gear height was designed to provide adequate lateral ground clearance; the Skyblazer series aircraft achieve a lateral ground clearance angle of 21° shown in Figure 10-18 and Figure 10-19.

The 50-seat aircraft distributes 91% of the static load to the main gear while the 76-seat aircraft distributes 93% of the static load to the main gear.

The sponson design was heavily influenced by the main landing gear integration and fuel storage. When the landing gear is fully extended, the landing tires lie outside of the fuselage structure as seen in Figure 10-20. This provides the aircraft with greater stability during ground operations compared to inboard landing gear. The main landing gear is designed to retract into the sponsons with the use of hydraulic pistons in order to maximize space and avoid any landing gear system failure. The tube-like sponsons will protrude into the cargo space reducing the overall cargo volume; however this will allow for external storage in the sponsons. Since the wings have inadequate space for fuel, the sponsons provide an ideal location for fuel storage, since they are away from the cabin.

Table 10-8 contains the determined static and dynamic tire loads for both the Skyblazer-100 and Skyblazer-200. The maximum tire loads were more critical for the tire selection. The maximum static and dynamic tire loads were grown by 25% as a factor of safety for a more conservative sizing. These expanded maximum tire loads were used for the tire selection in Table 10-10. The Skyblazer-100 and Skyblazer-200 will have one strut for the nose landing gear and two struts for the main landing gear.

Table 10-7: Landing Gear Loads

	100 Series (50 Seat)	200 Series (76 Seat)
W_{to} (lb)	55,000	71,000
I_n (in)	299	424
I_m (in)	30.0	31.7
P_n (lb)	5015	4950
P_m (lb)	49985	66050
P_n/P_{total}	0.09	0.07
P_m/P_{total}	0.91	0.93

Table 10-8: Determined Static and Dynamic Tire Loads for the Skyblazer Series

	Skyblazer-100	Skyblazer-200
Max Static Main Gear Load, P_M ($\times 10^3$ lbf)	26.7	42.3
Max Static Nose Gear Load, $P_{NS\ max}$ ($\times 10^3$ lbf)	4.85	11.8
Min Static Nose Gear Load, $P_{NS\ min}$ ($\times 10^3$ lbf)	1.62	8.56
Dynamic Nose Gear Load, P_{ND} ($\times 10^3$ lbf)	8.13	15.0
Dynamic Main Gear Load, P_{MD} ($\times 10^3$ lbf)	48.6	57.8
Main Max Static Tire Load, $P_{MST\ max}$ ($\times 10^3$ lbf)	6.67	7.06
Main Max Dynamic Tire Load, $P_{MDT\ max}$ ($\times 10^3$ lbf)	12.2	9.64
Nose Max Static Tire Load, $P_{NST\ max}$ ($\times 10^3$ lbf)	2.42	5.90
Nose Max Dynamic Tire Load, $P_{NDT\ max}$ ($\times 10^3$ lbf)	4.07	7.50
Main Static Tire Load with 25% Growth, $P_{MST\ 25\%}$ ($\times 10^3$ lbf)	8.34	8.82
Main Dynamic Tire Load with 25% Growth, $P_{MDT\ 25\%}$ ($\times 10^3$ lbf)	15.2	12.0
Nose Static Tire Load with 25% Growth, $P_{NST\ 25\%}$ ($\times 10^3$ lbf)	3.03	7.38
Nose Dynamic Tire Load with 25% Growth, $P_{NDT\ 25\%}$ ($\times 10^3$ lbf)	5.08	9.37

Table 10-9 contains the landing gear strut and tire deflection values and their intermediate, influencing variables. The touchdown rate is known FAR 25 requirements. The shock absorption and tire efficiency were taken from a table in Roskam Part IV [39]. The Skyblazer series of aircraft will use oleo-pneumatic struts. The landing gear load factor was selected to be 2.0 for the short takeoff and landing operations and its FAR 25 certification.

Table 10-9: Landing Gear Strut and Tire Deflection for the Skyblazer Series

	Skyblazer-100		Skyblazer-200	
	Main Gear	Nose Gear	Main Gear	Nose Gear
Touchdown Rate, w_t (ft/s)	12			
Landing Weight, W_L (lbf)	5.34E+04		8.47E+04	
Touchdown Kinetic Energy, K_t (ft-lbf)	1.19E+05		1.89E+05	
Allowable Tire Deflection, \dot{s}_{tire} (in)	2.7	1.1	1.4	1.4
Shock Absorption Efficiency, η_{shock}	0.80			
Tire Absorption Efficiency, η_{tire}	0.47			
Landing Gear Load Factor, \bar{N}_g	2.0			
Strut Stroke Deflection, \dot{s}_{ss} (ft)	1.35	2.82	1.41	2.81

Table 10-10 contains the tire selection and specifications for the main and nose land gear for each Skyblazer aircraft. The tires were selected from tables in Roskam Part IV [39]. The exact table where each tire was found was listed in Table 10-10. The tire dimensions, type, maximum loading, and uninflated tire pressure were considered when selecting the tires. The clearance radius and width required for each tire were also calculated and shown below.

Table 10-10: Tire Selection and Specifications for the Skyblazer Series

	Skyblazer-100		Skyblazer-200	
	Main Gear	Nose Gear	Main Gear	Nose Gear
Manufacturer	Goodrich	Goodrich	Goodrich	Goodrich
Tire Outer Diameter, $d_{out\ tire}$ (in)	32	20	30	24
Tire Width, w_{tire} (in)	8.8			
Tire Type	VII			
Maximum Loading, P_{max} (lbf)	1.58E+04	5.15E+03	1.295E+04	9.70E+03
Unloaded Inflation Pressure, F_{ui} (psi)	200	225	320	275
Static Loaded Radius, r_{sl} (in)	13.3	8.9	13.6	10.6
Table No. in Roskam Part IV	2.9	2.7	2.9	2.8
Clearance Radius, r_{cl} (in)	1.35	1.18	1.26	1.22
Clearance Width, w_{cl} (in)	4.2	3	4	3.4

The nose strut-wheel layout is shown in Figure 10-22. This strut wheel is both statically and dynamically stable. To do so, the relationship between the wheel hub and rotational axis and ground contact point are appropriately configured so that the rake and trail are favorable. For static stability, the relationship between the hub and the pivot axis lead to the centroid of the rotational axis being ahead of the centroid of the ground contact point. For dynamic stability, positive trail must be achieved.

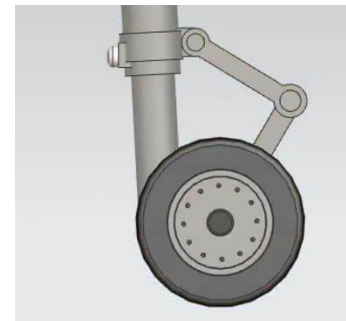


Figure 10-22: Nose-Wheel Strut Layout

11 Weight and Balance

For final weight and balance, the weights were calculated based on methods from Roskam’s *Airplane Design Part V: Component Weight Estimation*

[40]. The percentages of each component are divided by the total weight and should sum to 100%. The sum of all weights were calculated to be 95% of the total weight for the 50-seat aircraft and 92% for the 76-seat aircraft. An extra 1,000 lb was added to the empty weight structure to account for cargo hold flooring and carpet. The rest of the weight was split between the wing structure and fuselage structure to hit to

Table 11-1: : 50-Seat CG Excursions and Weights for Load Cases

50-Seat					
Load Case CGs					
Load Case	Weight (lb)	W*Xcg (lb-in)	W*Zcg (lb-in)	Xcg (in)	Zcg (in)
We	28606	11835864	1813358	414	63
Woe	29266	11913854	1721097	407	59
Woe + Fuel	42831	17202848	2392565	402	56
Wto	54921	22280648	3099580	406	56
Woe + Pass	41356	16991654	2946165	411	71
Woe	29266	11913854	1721097	407	59

Table 11-2: 76-Seat CG Excursions and Weights for Load Cases

76-Seat					
Load Case CGs					
Load Case	Weight (lb)	W*Xcg (lb-in)	W*Zcg (lb-in)	Xcg (in)	Zcg (in)
We	37598	16805922	3790478	447	101
Woe	38258	16898322	3839978	442	100
Woe + Fuel	53754	24506858	4897580	456	91
Wto	72084	34232995	6259184	475	87
Woe + Pass	56588	26624459	5201582	470	92
Woe	38258	16898322	3839978	442	100

total weights for both aircraft to get the final weight within 5% of the overall takeoff weights and preliminary weight and balance. The resulting finalized CG excursion diagrams are shown below for 50-seat and 76-seat aircraft Figure 11-1 and Figure 11-2 respectively with updated weights and longitudinal excursion. It is observed that the main landing gear is located behind the centers of gravity for each weight case. The final and overall CG excursion for both the X and Z directions are shown with the respective weights for each load case in Figure 11-1 and Figure 11-2 for each aircraft below.

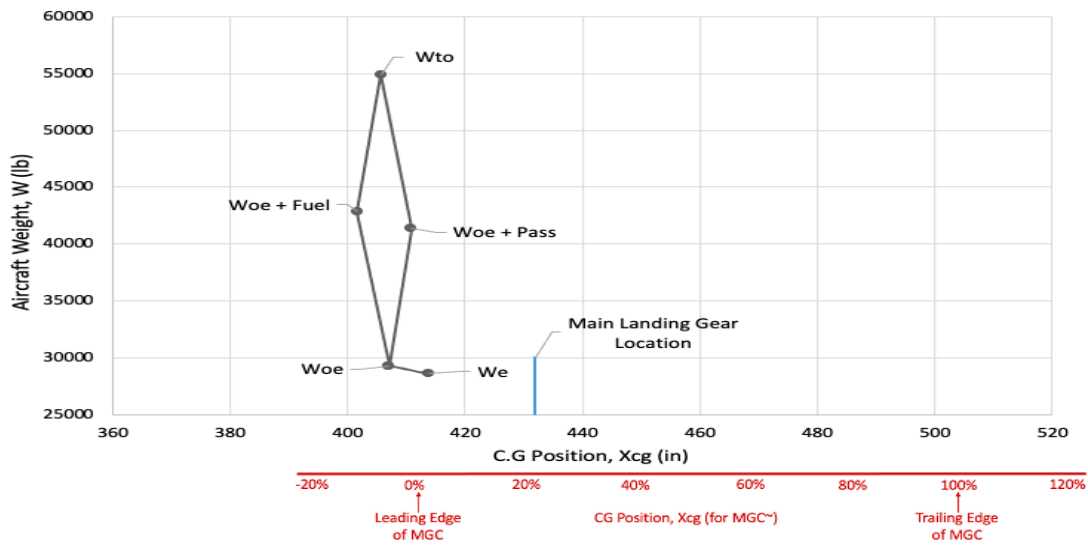


Figure 11-1: 50-Seat Class II CG Excursion Diagram

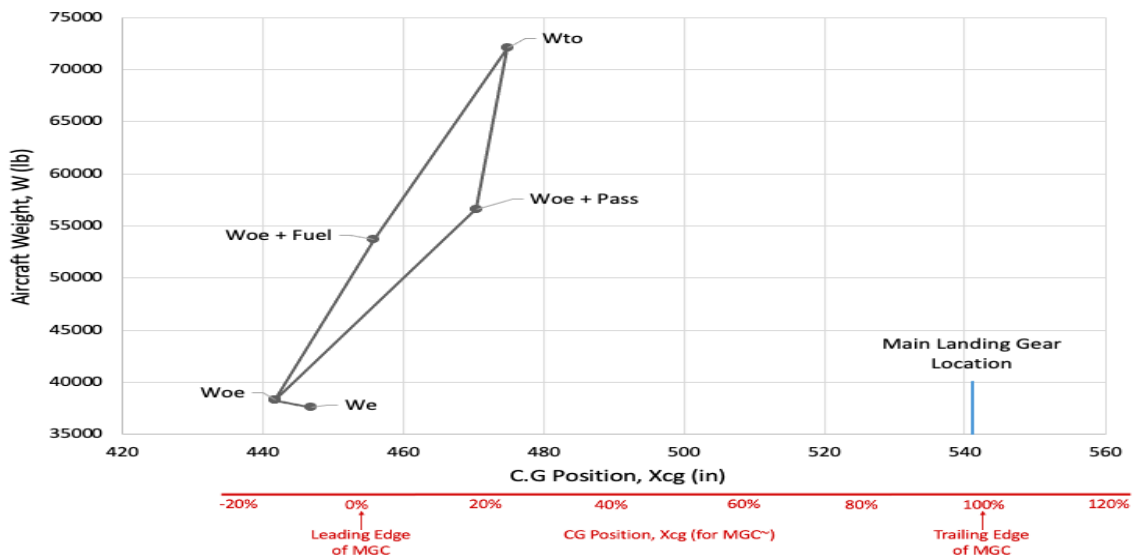


Figure 11-2: 76-Seat Class II CG Excursion Diagram

11.1 CG Excursion and Effects on Static Margin and Trim Drag

Center of gravity excursions for the 50 seat and 76 seat aircraft are 1.5 ft and 1.6 ft respectively. The static margin remains positive for both aircraft. There will be an increase in trim drag on the elevator and aileron surfaces due to the CG excursions.

11.2 Items to Account for Static Margin and CG Excursion

Table 11-3 and Table 11-4 display the location of items with respect to their CG in order to balance the aircraft.

Table 11-3: 50-Seat Weight and Balance Sizing

Weight Sizing			50-Seat Balance Analysis								
Component	Weight (lb)	Weight Fraction	Component	Weight Fraction	Weight (lb)	Xcg (in)	W*Xcg (lb-in)	Zcg (in)	W*Zcg (lb-in)		
Takeoff	53000	—	STRUCTURE	Wing	9.3%	5098	482	2457138	128	652593	
Empty	28774	52%		Horizontal Tail	1.0%	553	945	522970	321	177732	
Fuel	13565	25%		Vertical Tail	1.0%	547	887	484828	39	21535	
Payload	12660	23%		Fuselage	9.0%	4927	505	2488310	59	291126	
(Below Included in Above)				Nacelle	2.1%	1135	340	385822	68	76872	
Crew/Bags	660	1%		Landing Gear	3.3%	1802	401	723159	-27	-48655	
Passengers	10000	18%		Cargo Carpet	1.8%	1000	420	420000	20	20000	
Baggage	2090	4%		FUEL	Fuel System	1.90%	1045	350	365580	27	28202
Engines	3340	6%		Wing Fuel	6.2%	3391	510	1728181	117	396776	
				Sponson Fuel	18.5%	10174	350	3560813	27	274691	
			POWER PLANT	Engine	6.1%	3340	320	1068900	68	226260	
			PAYLOAD	Passenger	18.2%	10000	420	4200000	47	470000	
				Overhead Baggage	1.5%	836	420	351120	100	83600	
				Cargo Baggage	2.3%	1254	420	526680	27	33858	
				Crew/Bags	1.2%	660	118	77990	41	27297	
			FIXED EQUIP	Fixed Equipment	14.9%	8185	315	2578299	40	327403	
				Propulsion System	1.8%	974	350	340958	41	40290	
			TOTAL	1.00							

Table 11-4: 76-Seat Weight and Balance Sizing

Weight Sizing			76-Seat Balance Analysis								
Component	Weight (lb)	Weight Fraction	Component	Weight Fraction	Weight (lb)	Xcg (in)	W*Xcg (lb-in)	Zcg (in)	W*Zcg (lb-in)		
Takeoff	71000	—	STRUCTURE	Wing	9.2%	6563	534	3504533	150	984419	
Empty	36604	52%		Horizontal Tail	1.0%	712	1062	756589	258	183804	
Fuel	15496	22%		Vertical Tail	1.0%	723	975	705196	210	151888	
Payload	18900	27%		Fuselage	10.9%	7736	463	3581579	81	626583	
(Below included in Above)				Nacelle	2.3%	1625	376	611000	162	263250	
Crew/Bags	660	1%		Landing Gear	3.1%	2233	450	1004916	17	37963	
Passengers	15200	21%		Cargo Carpet	1.4%	1000	530	530000	41	41000	
Baggage	3130	4%		FUEL	Fuel System	1.5%	1066	500	533235	41	43725
Engines	4900	7%		Wing Fuel	5.5%	3874	614	2378636	150	581100	
				Sponson Fuel	16.4%	11622	450	5229900	41	476502	
			POWER PLANT	Engine	6.8%	4800	350	1680000	162	777600	
			PAYLOAD	Passenger	21.4%	15200	531	8065318	75	1140000	
				Overhead Baggage	1.8%	1252	531	664327	105	131460	
				Cargo Baggage	2.6%	1878	531	996491	48	90144	
				Crew/Bags	1.2%	660	140	92400	75	49500	
			FIXED EQUIP	FIXED EQUIP	14.0%	9953	350	3483582	60	597185	
				Propulsion System	1.67%	1187	350	415293	70	83059	
			TOTAL	1.00							

12 Advanced CAD

The Skyblazer series three-views are shown below in Figure 12-1 and Figure 12-2 with general dimensions.

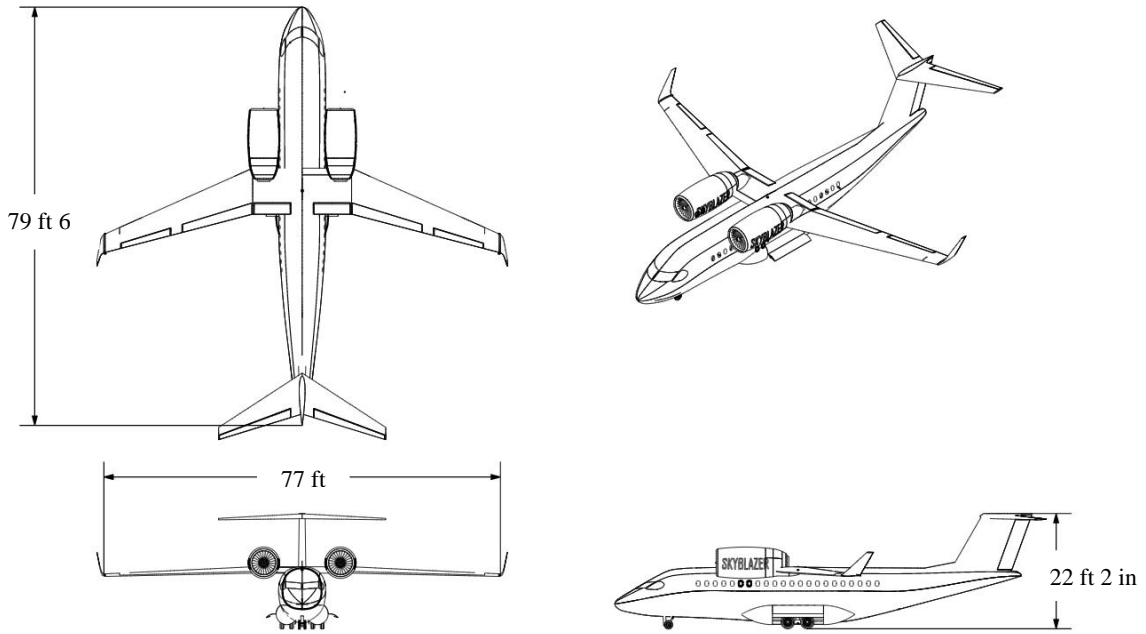


Figure 12-1: Skyblazer 100 Three-View

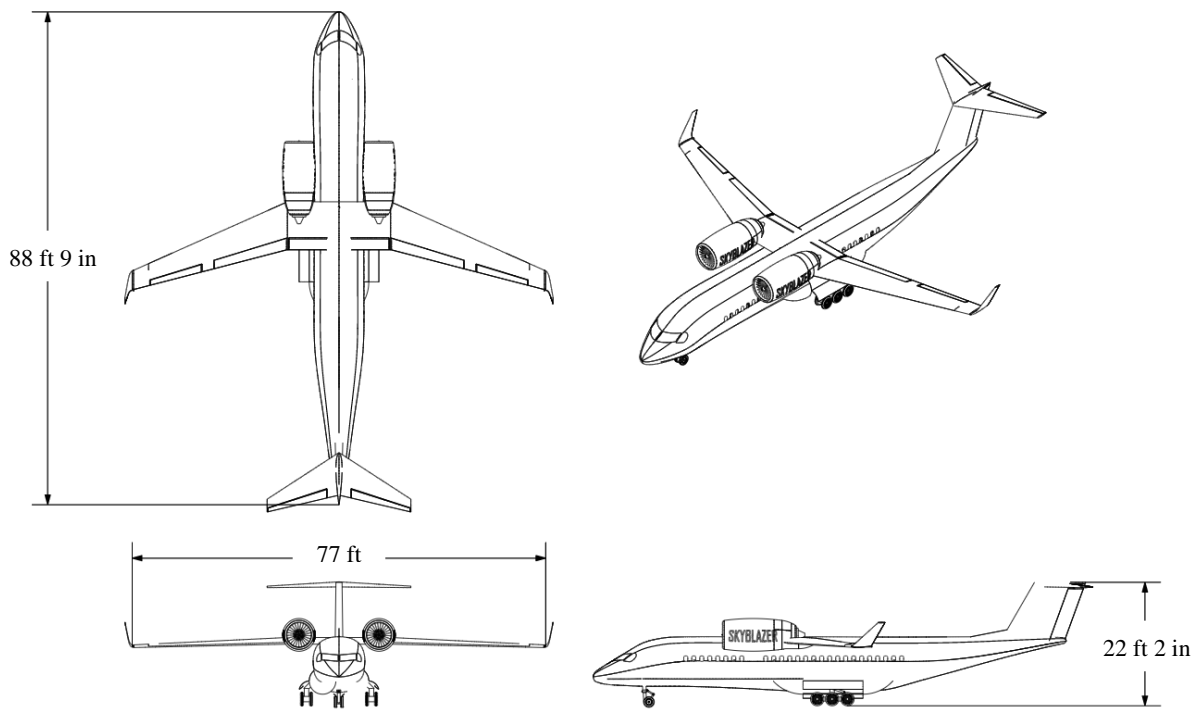


Figure 12-2: Skyblazer 200 Three-View

Figure 12-3 displays the situational rendering of the 100 series. The figure illustrates how the aircraft performs in a hanger environmental. The is also displayed in the boarding configuration with the aircraft steps deployed at the aircraft lowered for ease of access. Figure 12-4 depicts the passenger seating and cabin amenities in relation to various components of the aircraft such as the location of the exists and the lavatory and galley. Table 12-1 lists the materials that will be applied to all major CAD components.

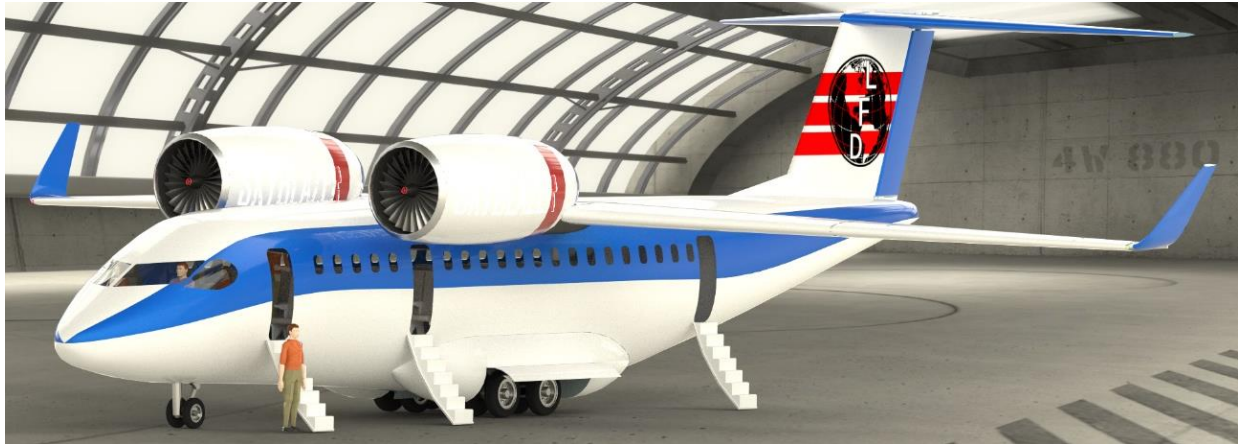


Figure 12-3: Situational Rendering of 100 Series



Figure 12-4: Situational Rendering of 200 Series

Table 12-1: CAD Model Materials

Component	
<u>Airframe/Exterior</u>	
Skin	Carbon-PEEK Composite
Ribs	Aluminum
Spars	Carbon-PEEK Composite
Fuselage Frames	Carbon-PEEK Composite
Engine Structural Support	Titanium
Landing Gear Strut	Steel
Landing Gear Wheel	Aluminum-Titanium Alloy
Landing Gear Tire	Rubber
Exterior Lights	Glass
Forward Bulkhead	Titanium
Aft Pressure Bulkhead	Carbon-PEEK Composite
<u>Interior</u>	
Windows	Plexi Glass
Seat	Cloth or Leather
Floor	Carpet
Interior Walls	Plastic



Figure 12-5: Exploded View of Series 100 and 200

12.1 Substructure

The Skyblazer 100 and 200 series aircraft substructures are pictured in Figure 12-6. Details of each substructure component are outlined in the following subsections.

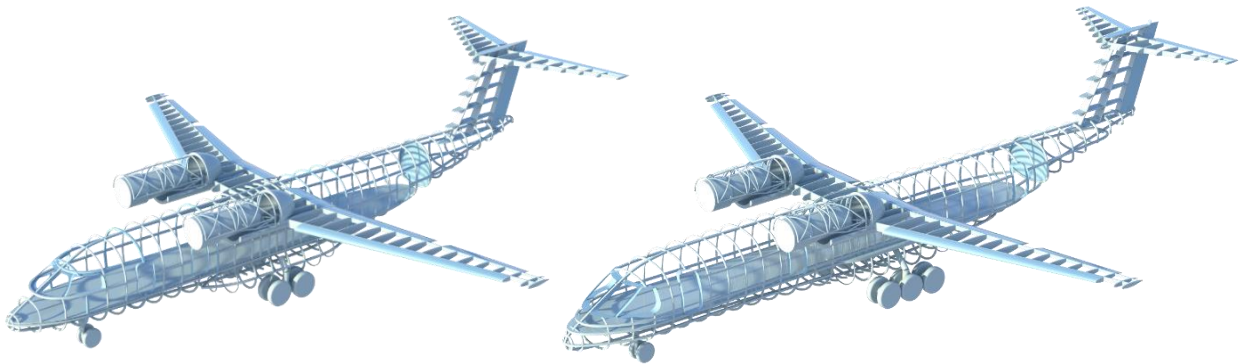


Figure 12-6: Skyblazer 100 and 200 Series Substructure

12.1.1 Fuselage Substructure

The fuselage structure is illustrated in Figure 12-7 for each respective series. The structure is kept relatively simple to avoid any complex geometry. Certain liberties had to be taken to make the structure viable such as the sponsons structure on the series 200 were protruding into the cabin space so they had to be cut and strengthened. The frame was kept at a constant spacing of 30” for class 1 configurations however once the structure becomes more complex certain locations on the structure needs to be heavily strengthened.

The Longeron spacing was also kept as a constant spacing but certain aspect made that impossible such as the sponsons and the tail of the aircraft which presented complex geometry. Presented are the significant values of the structure:

Table 12-2: Fuselage Characteristics

Frame Depth	1.5”
Frame Spacing	30.0”
Longeron Spacing	15.0”

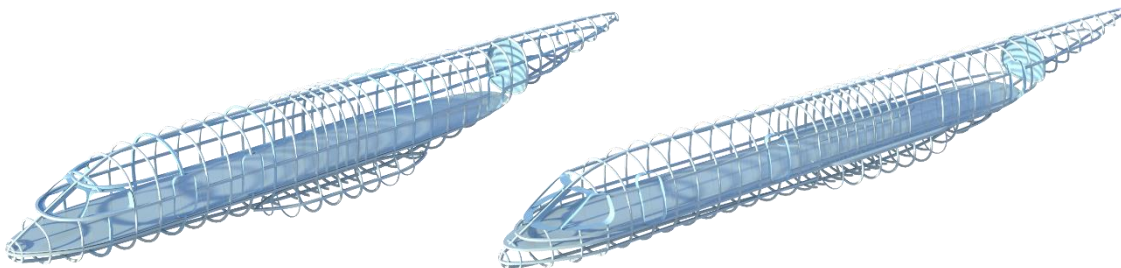


Figure 12-7: Fuselage Substructure for 50-Seat and 76-Seat

12.1.2 Wing Substructure

The wing substructure (Figure 12-8) features a two-spar design. Control surfaces include an inboard flap, outboard flap, and ailerons. Characteristics of the wing substructure are outlined in Table 12-3.

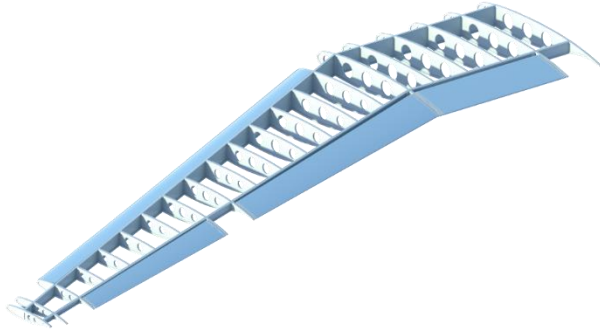


Figure 12-8: Wing Substructure

Table 12-3: Wing Substructure Characteristics

Rib Spacing	2.0 ft
Spar Thickness	0.125 ft
Front Spar Location (% chord)	15%
Rear Spar Location (% chord)	75%

12.1.3 Horizontal Tail Substructure

Similar to the wing substructure, the horizontal tail substructure (Figure 12-9) also features a two-spar design. The elevator is the only control surface on the horizontal tail. Characteristics of the horizontal tail substructure are outlined in Table 12-4.

Table 12-4: Horizontal Tail Substructure Characteristics

Rib Spacing	2 ft
Spar Thickness	0.125 ft
Front Spar Location (% chord)	15%
Rear Spar Location (% chord)	75%

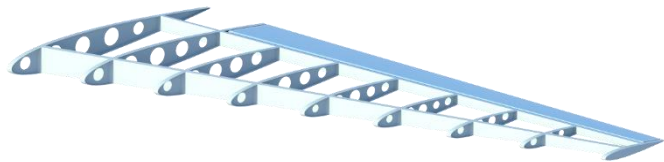


Figure 12-9: Horizontal Tail Substructure

12.1.4 Vertical Tail Substructure

The vertical tail substructure in Figure 12-10 features a three-spar design. The rudder is the only control surface on the vertical tail. Characteristics of the vertical tail substructure are outlined in Table 12-5.

Table 12-5: Vertical Tail Substructure Characteristics

Rib Spacing	2 ft
Spar Thickness	0.125 ft
Front Spar Location (% chord)	15%
Interstitial Spar Location (% chord)	45%
Rear Spar Location (% chord)	75%

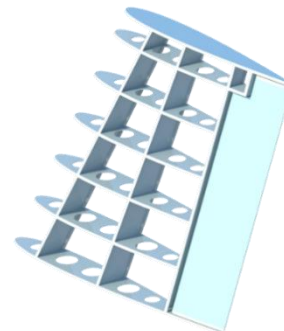


Figure 12-10: Vertical Tail Substructure

12.1.5 Engine Substructure

The engine structure is kept similar to the structure explained in the engine installation section. The addition being the undercover that will slide under the wing thus making the aircraft more aerodynamic and providing structural support. Figure 12-11 depicts the engine mounting structure for series 100 and 200 as there is no virtual change in the engine size and wing structure.

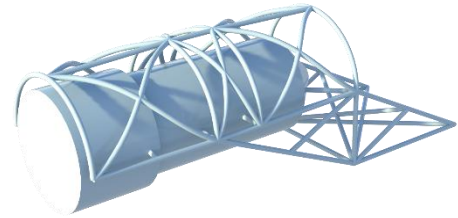


Figure 12-11: Engine Mount Substructure

13 Aircraft Systems

Notable aircraft systems integrated on the Skyblazer series follow in this section.

13.1 Flight Control Systems

The primary flight controls include ailerons, spoilers, elevators, rudder, and stabilizers. The secondary flight controls include trim controls, high-lift devices (flaps), and thrust or power. The system will be fly-by-wire throughout with a combination of hydraulics and electric hydrostatic irreversible control system. The primary flight controls and flaps are sized for individual actuators that are required for the electric hydrostatic system. These are sized based on the wing loading applied to the control surface area rendering a maximum force as shown in Table 13-1 below. Actuators were also selected based on the maximum applied force (in Newtons) and speed requirements [41].

Table 13-1: Actuator Sizing For Control Surface Forces for Both Aircraft

ACTUATOR SIZING: 50-Seat							
Control Surface	S (ft2)	W/S (lb/ft2)	Hinge Dist to Centroid (ft)	Fc (lb)	Moment (ft-lb)	Fc (N)	Actuator w/ Max Force
Aileron	15	115	0.9	1725	1553	7676	D13203-65N-2 (8400 N)
Elevator	12.5	115	1	1438	1438	6397	D13203-65N-2 (8400 N)
Stabilizer	45	115	1	5175	5175	23029	D13105-65N-2 (28400 N)
Rudder	20	115	0.84	2300	1932	10235	D09200-54K-2 (15100 N)
Slats	35	115	0.675	4025	2717	17911	D13105-65N-2 (28400 N)
Fowler Flaps	15	115	1.35	1725	2329	7676	D13203-65N-2 (8400 N)
Double Slotted Flaps	45	115	1.35	5175	6986	23029	D13105-65N-2 (28400 N)
Inboard Spoilers	15	115	0.7	1725	1208	7676	D13203-65N-2 (8400 N)
Outboard Spoilers	10	115	0.7	1150	805	5118	D13203-65N-2 (8400 N)
ACTUATOR SIZING: 76-Seat							
Control Surface	S (ft2)	W/S (lb/ft2)	Hinge Dist to Centroid (ft)	Fc (lb)	Moment (ft-lb)	Fc (N)	Actuator w/ Max Force
Aileron	15	148	0.9	2220	1998	9879	D09200-54K-2 (15100 N)
Elevator	12.5	148	1	1850	1850	8233	D13203-65N-2 (8400 N)
Stabilizer	45	148	1	6660	6660	29637	D13100-65N-2 (38800 N)
Rudder	20	148	0.84	2960	2486	13172	D09200-54K-2 (15100 N)
Slats	35	148	0.675	5180	3497	23051	D13105-65N-2 (28400 N)
Fowler Flaps	15	148	1.35	2220	2997	9879	D09200-54K-2 (15100 N)
Double Slotted Flaps	45	148	1.35	6660	8991	29637	D13100-65N-2 (38800 N)
Inboard Spoilers	15	148	0.7	2220	1554	9879	D09200-54K-2 (15100 N)
Outboard Spoilers	10	148	0.7	1480	1036	6586	D13203-65N-2 (8400 N)

The layout of the flight control system is shown below in Figure 13-1. For redundancy, the rudder and elevators are shown to have three actuator systems, the ailerons and inboard spoilers have two actuator systems, and the outboard spoilers each have one system. The slats and each trim surface also will use electro hydrostatic actuators and will each only require one. They all use “through feel system” for trim and fly-by-wire for signaling using an irreversible electric hydrostatic system. The layout diagram shows the number of actuators on each control surface and how they are connected to the pilot controls and computers.

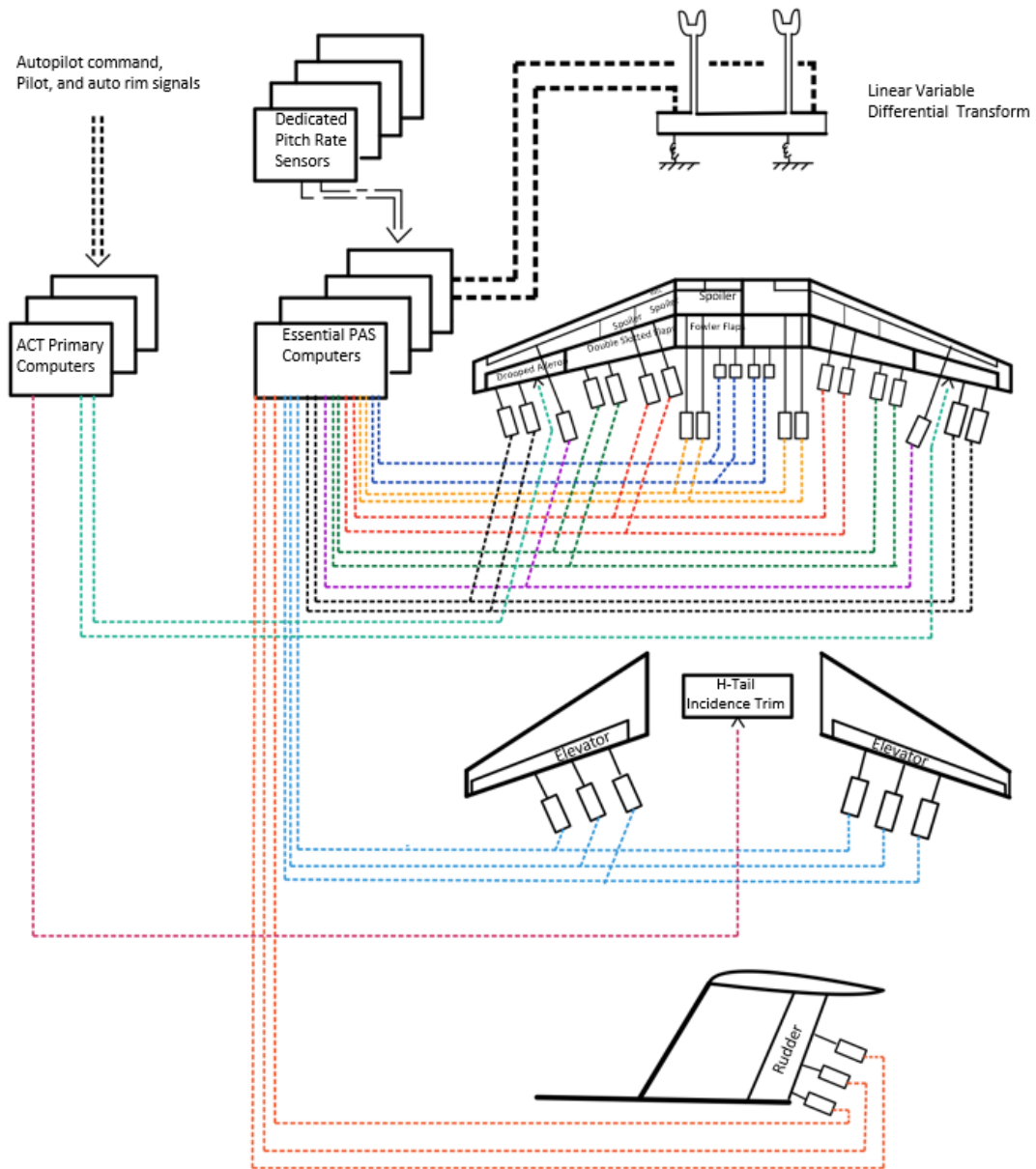


Figure 13-1: Flight Control Systems Layout Diagram

13.2 Propulsion Systems

The thrust reverser control will be used with clam shells on the engine and nacelles using hydraulics. The ignition control and starter system are part of the electric and pneumatic systems described in Section 13.8, while the fuel flow is discussed in the fuel system Section 13.3 below. As previously specified, a winch system will be used to allow the lowering of the engine without outside equipment in order to conduct maintenance on the engines

13.3 Fuel Systems

The fuel system will use six tanks total including one per wing and four sponson tanks with two per side around the landing gear location. All of the tanks will be interconnected, so the fuel can travel to each tank to bypass any issues for the total fuel flow of 12,046 lb. Because the wings are anhedral and the sponsons are located at the belly aircraft, pumps will be used instead of gravity feed to get the fuel up and into the inboard wing sections where the engines are located. A diagram of the fuel system layout is shown below for reference in Figure 13-3, Figure 13-2, and Figure 13-4.

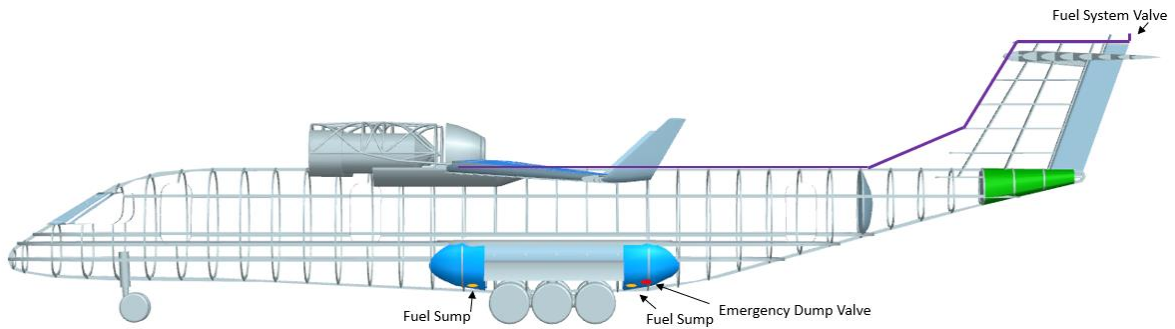


Figure 13-3:Left Side Fuel System

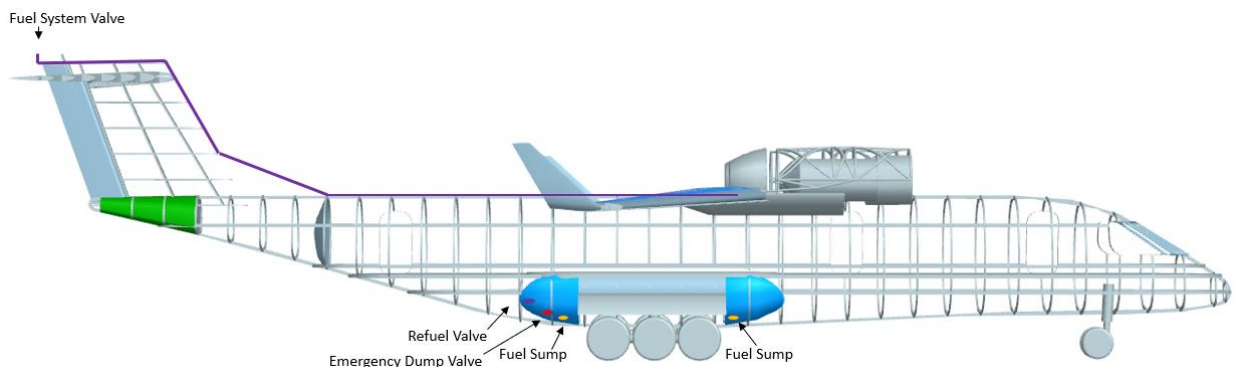


Figure 13-2:Right Side Fuel System

A cross feed valve connected to each of the fuel tanks is also used for redundancy in case of engine failure or fire and to transfer fuel across tanks. Also note that the sponsons are outside of the fuselage outer mold line and are designed to break away in the event of a crash. It is also noted that the sumps will be located in the at the lowest point of each sponson.

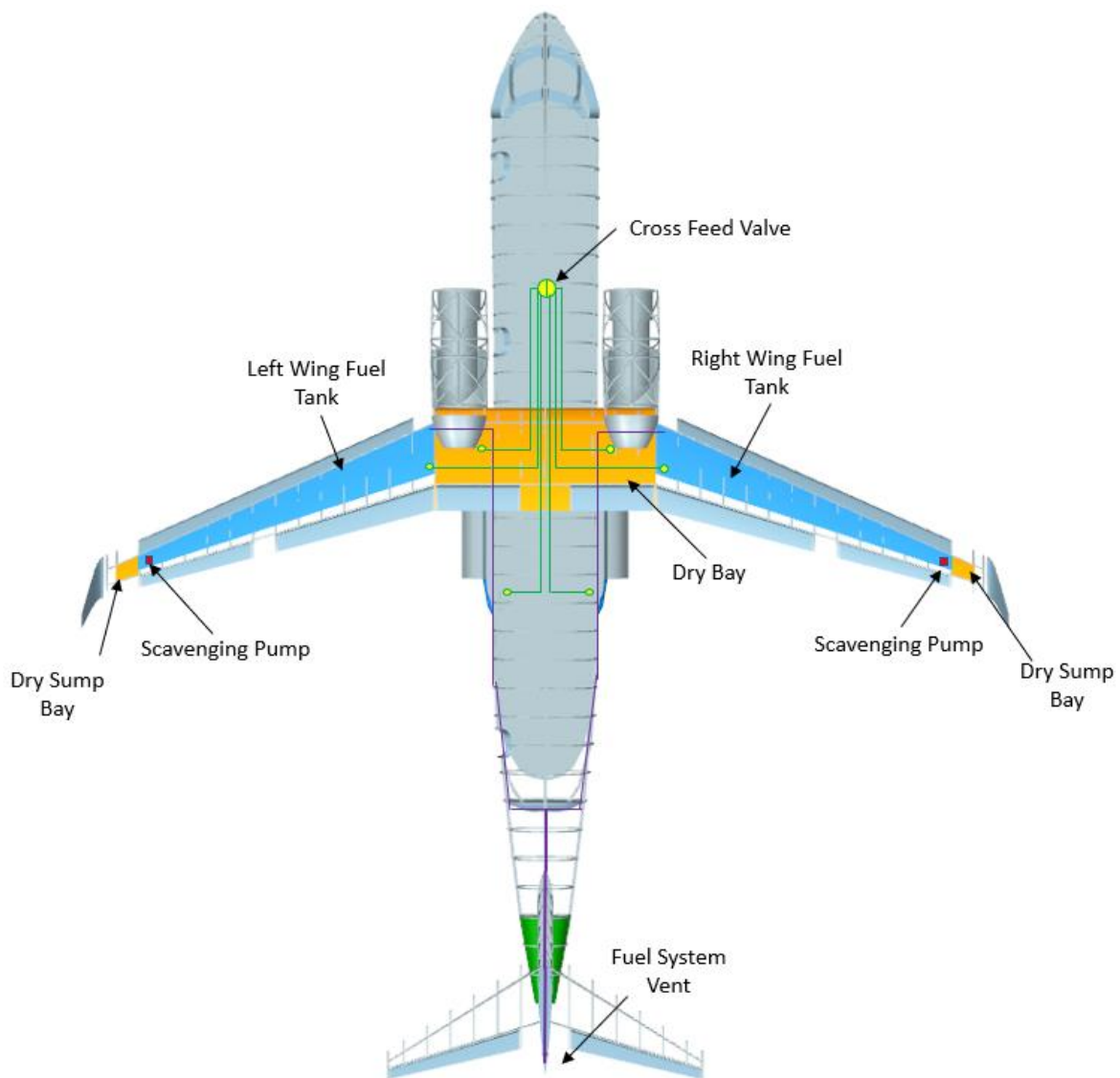


Figure 13-4: Fuel System Layout Diagram Top View

13.4 Hydraulic System

Because the flight controls are electric hydrostatic, they each have their own actuator and hydraulics, so the overall hydraulic system is used to control the landing gear extending, retraction, and steering and also thrust reversing

operations. A layout of the hydraulic systems is shown below in Figure 13-5. It includes connections to the landing gear and brakes. The legend shows all of the components as well for reference.

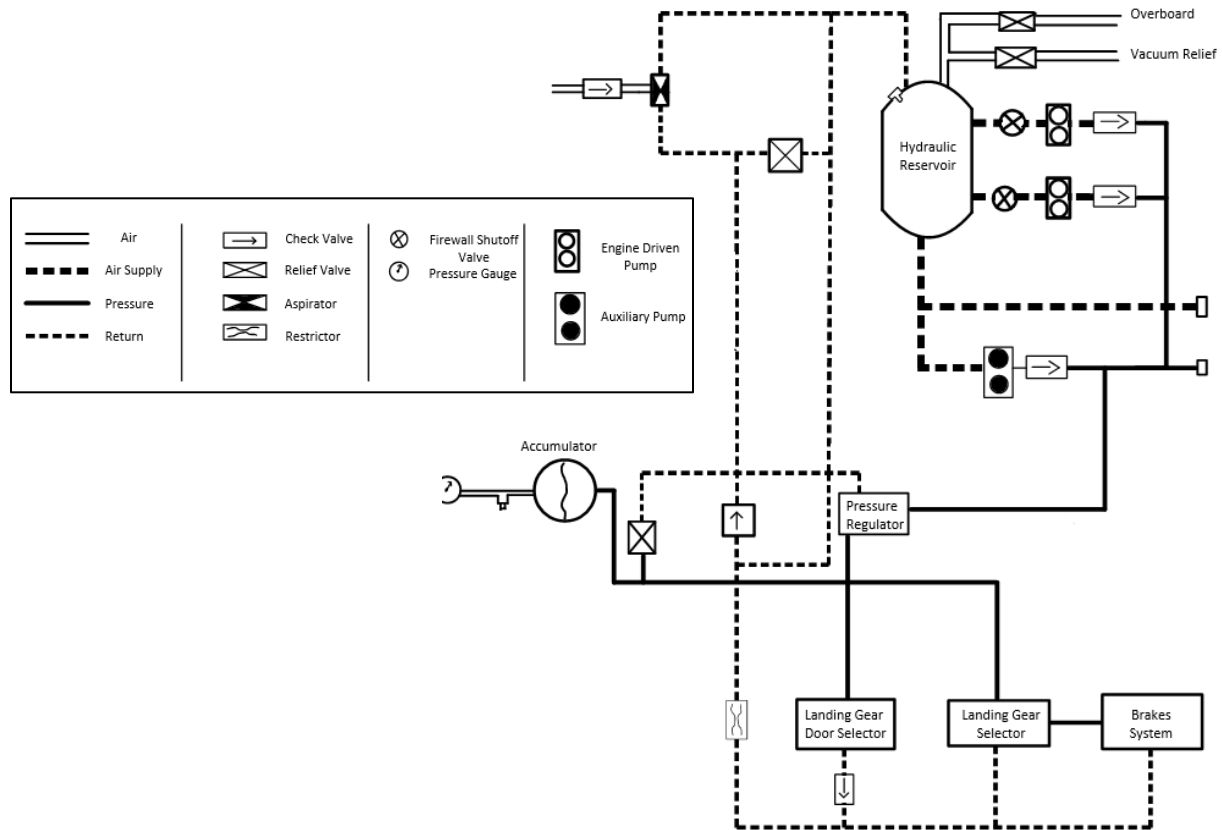


Figure 13-5: Hydraulic System Layout Diagram

13.5 Electric Systems

Using the DC-10 electrical load summary and the ratio of weights between the Skyblazer series to the DC-10, the electrical load summaries were created as shown below. The total power required during takeoff and climb is 18,330 VA for the 50-seat and 23,727 VA for the 76-seat, and the cruise is significantly less power with 7,163 VA for the 50-seat and 9,247 VA and 76-seat. The breakdown of the load summary can be seen in Figure 13-7 for both the Skyblazer 100 and Skyblazer 200.

ELECTRICAL SYSTEM LOAD SUMMARY: Skyblazer 100			ELECTRICAL SYSTEM LOAD SUMMARY: Skyblazer 200		
Load Summary	Power: TO and Climb (VA)	Power: Cruise (VA)	Load Summary	Power: TO and Climb (VA)	Power: Cruise (VA)
Exterior Lighting	492	26	Exterior Lighting	636	33
Flight Compartment Lighting	153	153	Flight Compartment Lighting	198	198
Passenger Cabin Lighting	1816	1880	Passenger Cabin Lighting	2345	2427
Galley	10744	0	Galley	13870	0
Toilets	0	780	Toilets	0	1007
Entertainment	0	384	Entertainment	0	495
Windshild Heating	767	921	Windshild Heating	991	1189
Avionics	947	927	Avionics	1222	1197
Air Conditioning	205	205	Air Conditioning	264	264
Fuel Handling	831	831	Fuel Handling	1073	1073
Hydraulics	1126	0	Hydraulics	1453	0
Flight Control	256	256	Flight Control	330	330
Electrical Power (DC)	1010	767	Electrical Power (DC)	1304	991
Miscellaneous	32	32	Miscellaneous	41	41
TOTAL	18380	7163	TOTAL	23727	9247

Figure 13-7: Skyblazer 100 and 200 Electrical System Load Summary

A high-level interconnect of the electrical system is shown in Figure 13-8 below. It shows the connections between the APU, generators, batteries, and busses. The port bus will serve as the primary bus and will power components such as the fuel quantity indicators, ignition, and pitot heat. The secondary bus will cover avionics and house components such as the radio, navigation, and instrumentation. Inverters will be located on each bus for components that require AC power. Batteries will also be located on each bus to serve as redundancy in case of engine failure, generator failure, and APU failure.

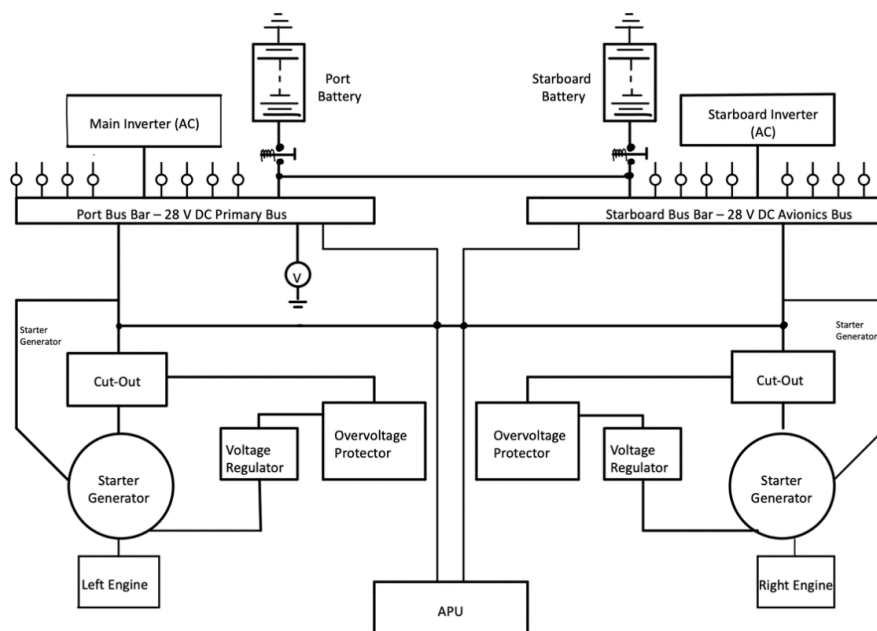


Figure 13-8: Electrical System Layout Diagram

13.6 Escape System, Fire Detection, and Suppression System

For a passenger seating configuration of 41 to 110 seats, there must be at least two exits, one of which must be a Type 1 or larger exit in each side of the fuselage. The Skyblazer 200 is shown in Figure 13-9, and here will be four Type 1 doors in total with three on the port and one on the starboard. The Syblazer 100 will follow the same system principals.

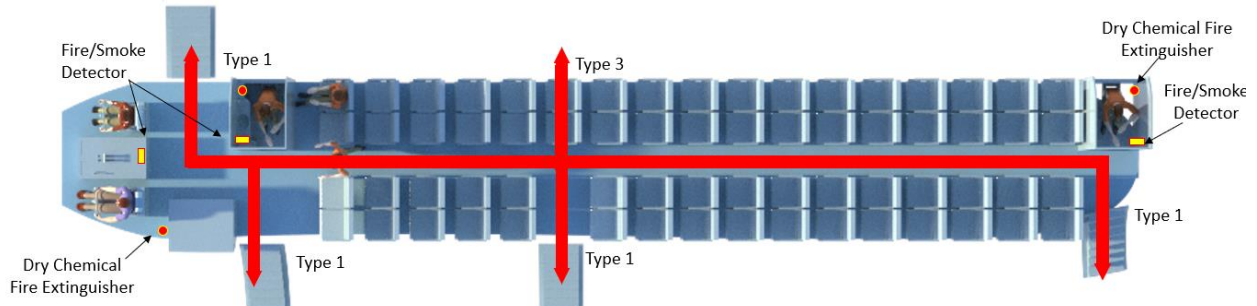


Figure 13-9:Escape System and Fire Extinguisher locations

Fire detection system will be comprised of thermal switches located on the aircraft where a fire is most likely to occur such as the cargo hold and lavatory. Smoke Detectors will also be used to check for smoke ionization of the air to detect very small changes in resistance. Dry Chemical fire extinguishers will be located onboard the aircraft for fire suppression. For the 100-series aircraft there will be 2 onboard and for 200-series aircraft there will be 3. Installed fire suppression systems will also be used on the engine cowling, APU bay, and Cargo and baggage bay. The dry chemical for the installed fire suppression systems will be located along the wall of the fuselage of the cargo bay and will be ran to the engine cowlings and APU.

13.7 Pressurization System

To maintain sufficient cabin air pressure during flight for passenger comfort. The cabin pressurization system includes a source of high-pressure air from the pneumatic system, ambient pressure input, and a control and metering system in the cockpit. This enables positive or negative pressure relief that can be provided to protect the structure. Although the control and metering system will be present in the cockpit, the pressurization schedule with altitude will be automatic to reduce crew workload. The overall pressurization schematic is shown below in Figure 13-10.

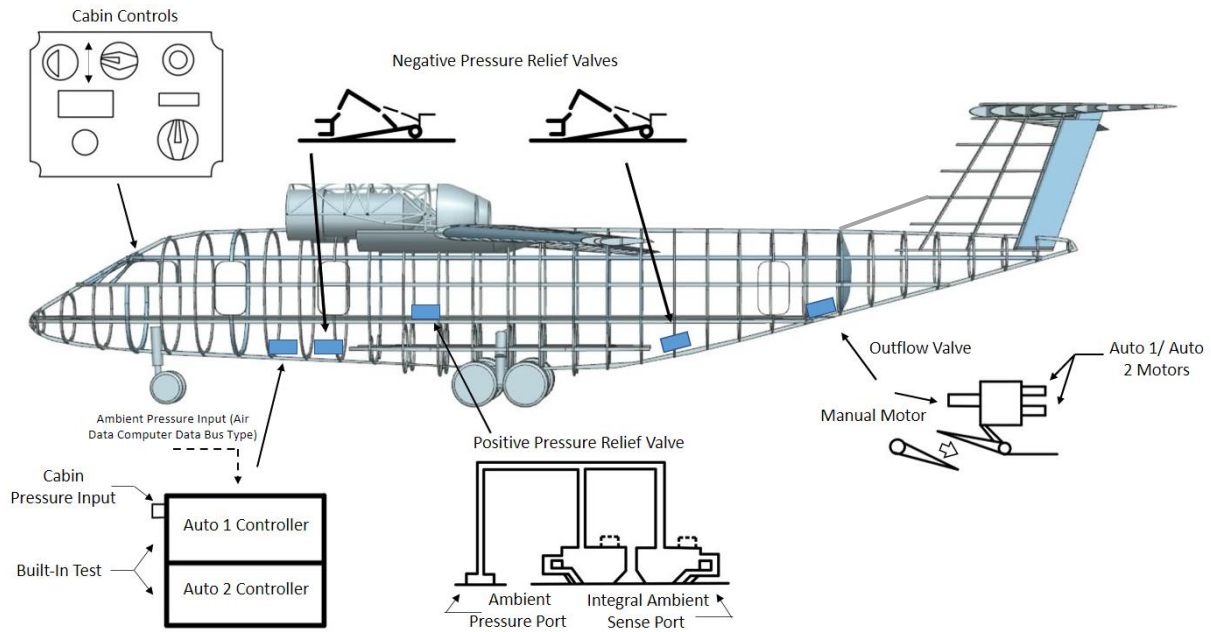


Figure 13-10: Pressurization System Schematic

13.8 Pneumatic System

The pneumatic system will supply air for the cabin pressurization and air-condition system, ice protection system, and cross engine starting. The primary source of air for the system is the engine compressor bleed air, while the secondary source of air is from the APU. The schematic of the overall pneumatic system is shown in Figure 13-11 below.

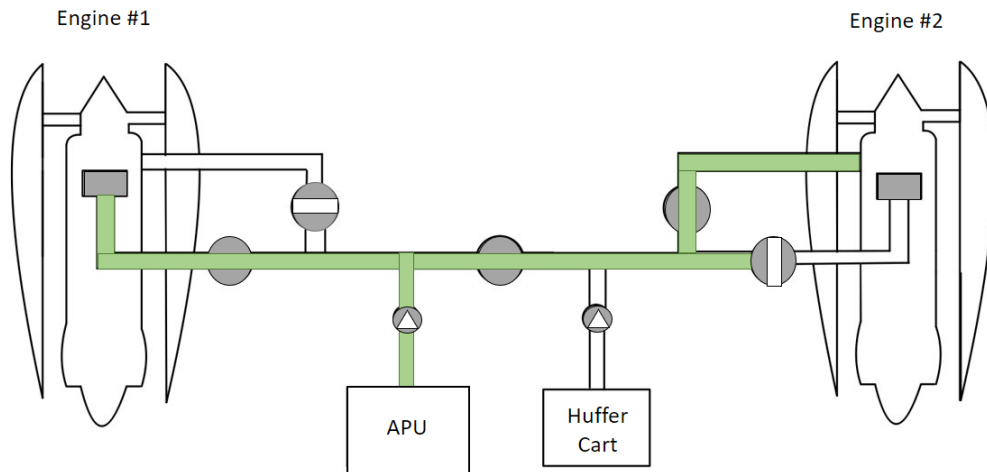


Figure 13-11: Pneumatic System Schematic

13.9 Oxygen System

There will be two oxygen systems onboard the aircraft. For the crew, the oxygen system will be supplied from a gaseous source shown in Figure 13-12. The passenger oxygen will be supplied from a chemical source. The chemical oxygen system will be the larger system for the passengers to avoid the fire hazards during servicing and cylinder replacement. Crew mitigated for the crew as the amount of oxygen needed for the crew is much smaller than the passenger.

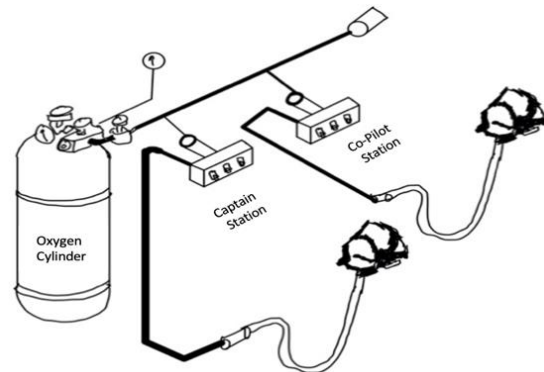


Figure 13-12: Cockpit Oxygen

13.10 Cabin Sterilization System

Cabin sterilization methods will include thermal disinfection. By applying heat to sanitize surfaces effectively kills viruses on hard-to-clean flight equipment. This research has been completed by Boeing as part of its confident travel initiative to support customers and well-being of passengers can crews. Although this testing was completed to disinfect the flight deck, the entire cabin will have the same technology.

13.11 Cockpit Instrumentation

The flight deck is designed accommodate two pilots and adopt avionics platforms used widely amongst the competitors in the regional jet market such as Honeywell’s Primus 1000 and Collins’s Pro Line 4 as well as upcoming avionics suites. This is to ensure smooth transition for pilots as the new fleet of aircraft is integrated. The instrumentation will include a heads-up display that will provide the aircraft CAR III landing capability. As well as at least five electronic displays which include two multifunction displays, two primary flight displays and one in-flight engine condition monitoring system.



Figure 13-13: Cockpit

13.12 De Icing Systems

De-icing will be an important system, as icing has negative effects such as destroying airflow over the wing resulting in disrupting lift, generating drag, and altering pitching moments. Ice can also damage external equipment and clog inlets. Ice detection will be done electrically using an external probe. The probe will sense the change in natural frequency due to occurred mass from the ice development on the probe.

There will be two types of ice removal systems on the aircraft. First being anti-icing. Anti-icing will be used proactively before the aircraft enters into icing conditions. These types include thermal heat, pitot heat, fuel-vent heat, and fluid surface deicers. The next removal system will be De-Icing, this system will be

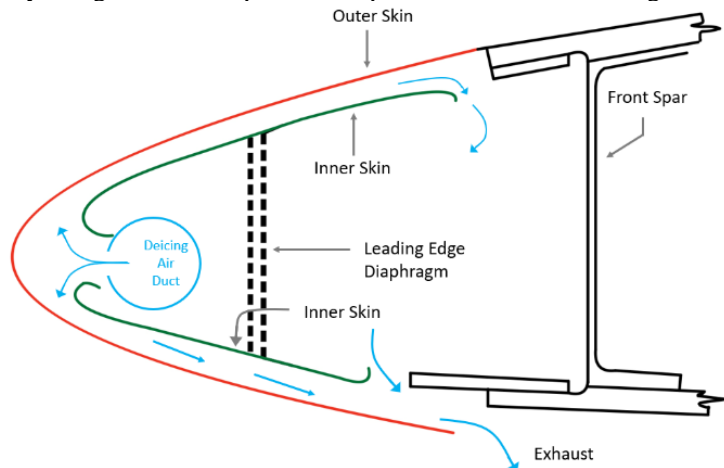


Figure 13-14: Wing and Engine Cowl De Icing Method

reactive and used after significant ice buildup. This method will include sending engine bleed air through deicing air ducts located in the leading edge of the wing shown in Figure 13-14. This method will also be applied to the engine cowls.

13.13 Window Rain, Fog, and Frost Control Systems

Wipers will be used to combat rain on the cockpit windows. A hydrophobic coating will also be applied to the window shield. Will go to the extreme of surface tension will repel the water by keeping the water beaded and will roll off the windshield which will also compliment the windshield wipers. Wind shear warning system will be applied to avoid wind shears and microburst during temperature inversions and thunderstorms.

13.14 Lavatory, Galley, Water, and Waste Systems

The Galley will be equipped with beverage service carts, with locks on every station. The waste system is designed to account for 0.3 gallons per person and will be pressurized by the pneumatic system. The water will be regulated by the EPA.

With a half of a gallon per flush, the waste system will be self-contained. The waste tanks will be flushed with blue disinfectant chemical. After the initial flush, the waste will then meet more chemicals that combines disinfection with a catalytic process that breaks down the solid. The inherent pressurization for the cabin will be enough for the flush and the waste will be serviced every flight from the drain location located at the lowest system points with the final lavatory layout shown in Figure 13-15.

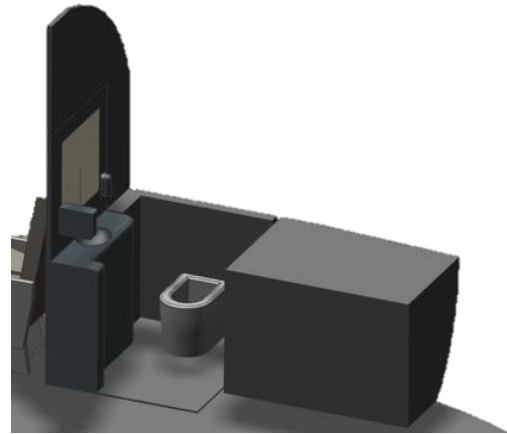


Figure 13-15: Lavatory Layout and Galley

13.15 Safety and Survivability

The sky blazer will be equipped with two flight management systems. First, a Traffic Alert and Collision Avoidance System (TCAS) shown in Figure 13-17 will be used for Collision avoidance and is integrated into the flight control system with input to air traffic control. It automatically notifies ATC and shares that there is incoming traffic and flight crew are working to avoid it. An Enhanced ground proximity warning system (E-GPWS) shown in Figure 13-17 will also be used to keep track on the ground ahead and warn the flight crew of upcoming hazardous terrain to avoid controlled flight into terrain.

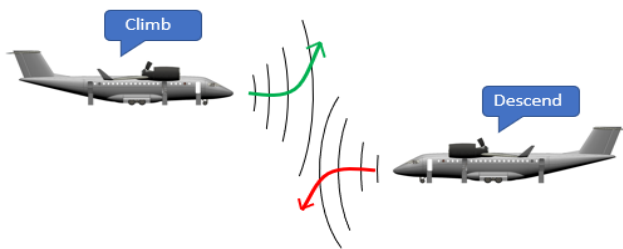


Figure 13-17: Traffic Alert and Collision Avoidance System

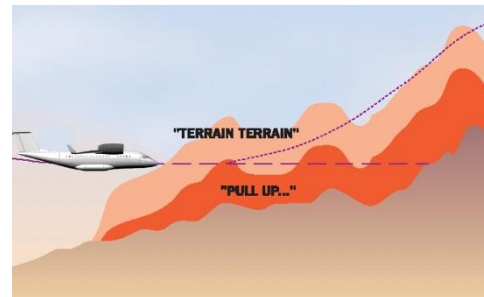


Figure 13-17: Enhanced ground proximity warning system. [42]

Ground Equipment and Servicing Vehicles Compatibility

The high-wing configuration gives ground vehicles 10 feet of clearance, giving them unrestricted access to the entire aircraft in Figure 13-18. This is in contrast to most low-wing aircraft that force vehicles to maintain a safe distance from the wing. Giving all vehicles access to the aircraft at once decreases turnaround times. Air stairs are

used to speed up passenger ingress and egress, however, there will be room for a jetway or exit and entry path leading to the left front door as necessary.



Figure 13-18: Service Vehicle Compatibility

The high-wing high-engine arrangement allows the Skyblazer to achieve a flight line footprint of 650 m². This is in contrast to current market leader Embraer 190, which achieves a flight line footprint of 1760 m², as seen in Figure 13-19. A smaller flight line footprint leads to more aircraft per terminal. Figure 13-20 demonstrates equal capacity terminals at San Diego International Airport harboring a greater number of Skyblazer aircraft than Embraer 190 aircraft.

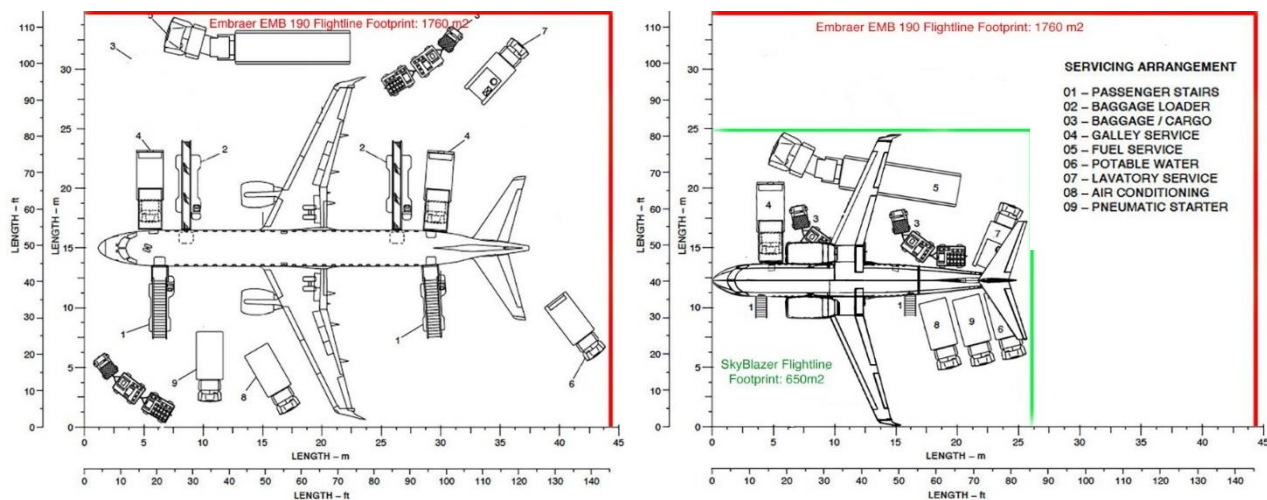


Figure 13-19:Embraer 190 vs. Skyblazer Flight line Footprint Comparison



Figure 13-20: Skyblazer vs. Embraer 190 Terminal Packing

Some of required servicing vehicles for the Skyblazer series include baggage servicing vehicles, fuel service vehicles, potable water, cabin service, galley service, lavatory maintenance, and a towing vehicle for pushback. Connections and carts for ground power and air are also required during servicing.

13.16 Camera System

Camera sensory systems will be installed in strategic locations on the aircraft to achieve semi-automated camera-assisted marshalling for taxing, parking, and also to conduct external visual inspection as needed during preflight operations. The aircraft will be fitted with ultrasonic sensors to assist with taxing and stowing. Cameras will be placed on the nose, each wing tip, and on each side of the horizontal tail to develop a 360-degree view as seen on modern automobiles.

14 Class II Stability and Control

The AAA dynamic modeling software was used to perform final stability and control for the Skyblazer series. Table 14-1 contains the determined metrics from AAA for the Skyblazer series aircraft to evaluate stability longitudinally and lateral-directionally. Table 14-2 contains typical short period damping ratios for various handling qualities and flight phases. Table 14-3 contains a list of typical phugoid damping ratios for varying levels of handling qualities.

Table 14-4 contains the allowable time to double amplitude for roll mode of each flight phase. Table 14-5 contains the time to double amplitude for spiral mode at each flight phase.

Table 14-1: Skyblazer Series Determined AAA Stability Metrics

	Skyblazer-100	Skyblazer-200
Load Factor per Angle of Attack, \dot{n}/α , (g's/rad)	10.3	13.7
Short Period Natural Frequency, $\omega_{n_{sp}}$ (rad/s)	2.54	1.69
Short Period Damping Coefficient, ζ_{sp}	0.353	0.407
Phugoid Natural Frequency, $\omega_{n_{ph}}$ (rad/s)	0.051	0.091
Phugoid Damping Coefficient, ζ_{ph}	0.194	0.110
Feedback Gain due to Angle of Attack, k_α (deg/deg)	0	0.035
Dutch Roll Natural Frequency, $\omega_{n_{dr}}$ (rad/s)	0.979	1.42
Dutch Roll Damping Coefficient, ζ_{dr}	0.185	0.107
Sideslip Feedback Gain due to Aileron Deflection, k_β/δ_a (deg/deg)	0	1.87
Roll Mode Time to Double Amplitude, t_R (s)	1.112	0.579
Spiral Mode Time to Double Amplitude, t_{2S} (s)	25.1	51.6

Table 14-2: Allowable Short Period Damping Ratios for Dynamic Longitudinal Stability [43]

Handling Qualities	Category A and C Flight Phases	Category B Flight Phases
Level 1	$0.35 < \zeta_{sp} < 1.30$	$0.30 < \zeta_{sp} < 2.00$
Level 2	$0.25 < \zeta_{sp} < 2.00$	$0.20 < \zeta_{sp} < 2.00$
Level 3	$0.15 < \zeta_{sp}$	$0.15 < \zeta_{sp}$

Table 14-3: Allowable Phugoid Damping Ratios for Dynamic Longitudinal Stability [43]

Handling Qualities	Phugoid Stability Requirement
Level 1	$\zeta_{ph} > 0.04$
Level 2	$\zeta_{ph} > 0$
Level 3	$t_2 > 55$ sec

Table 14-4: Time to Double Amplitude for Roll Mode Lateral-Directional Stability [43]

Flight Phase	Class	Level I	Level II	Level III
A	I, IV	$t_R < 1.0$ sec.	$t_R < 1.4$ sec.	-
	II, III	$t_R < 1.4$ sec.	$t_R < 3.0$ sec.	-
B	All	$t_R < 1.4$ sec.	$t_R < 3.0$ sec.	$t_R < 10$ sec.
C	I, II-C, IV	$t_R < 1.0$ sec.	$t_R < 1.4$ sec.	-
	II-L, C	$t_R < 1.4$ sec.	$t_R < 3.0$ sec.	-

Table 14-5: Time to Double Amplitude for Spiral Mode Lateral-Directional Stability [43]

Flight Phase and Category	Level 1	Level 2	Level 3
A and C	$t_{2S} > 12$ sec.	$t_{2S} > 8$ sec.	$t_{2S} > 4$ sec.
B	$t_{2S} > 20$ sec.	$t_{2S} > 8$ sec.	$t_{2S} > 4$ sec.

Table 14-6 contains the final longitudinal stability and control values for the Skyblazer-100 and the Skyblazer-200. Table 14-7 contains the final lateral-directional stability and control values for the Skyblazer-100 and the Skyblazer-200.

Table 14-6: Skyblazer Series Class II Longitudinal Stability and Control Derivatives

	Skyblazer-100	Skyblazer-200
Lift Coefficient due to Forward Velocity, C_{L_u}	1.179	0.572
Drag Coefficient due to Forward Velocity, C_{D_u}	0.086	0.082
Pitching Moment Coefficient due to Forward Velocity, C_{m_u}	0.34	0.150
Lift Coefficient due to Angle of Attack, C_{L_α} (rad ⁻¹)	6.55	7.49
Drag Coefficient due to Angle of Attack, C_{D_α} (rad ⁻¹)	0.252	0.336
Pitching Moment Coefficient due to Angle of Attack, C_{m_α} (rad ⁻¹)	-0.91	-1.58
Lift Coefficient due to Angle of Attack Rate, $C_{L_{\dot{\alpha}}}$ (rad ⁻¹)	3.56	3.92
Drag Coefficient due to Angle of Attack Rate, $C_{D_{\dot{\alpha}}}$ (rad ⁻¹)	0	0
Pitching Moment Coefficient due to Angle of Attack Rate, $C_{m_{\dot{\alpha}}}$ (rad ⁻¹)	-28.83	-30.0
Lift Coefficient due to Pitch Rate, C_{L_q} (rad ⁻¹)	40.28	20.4
Drag Coefficient due to Pitch Rate, C_{D_q} (rad ⁻¹)	0	0
Pitching Moment Coefficient due to Pitch Rate, C_{m_q} (rad ⁻¹)	-100.1	-99.0
Lift Coefficient due to Incidence Angle, $C_{L_{i_h}}$ (rad ⁻¹)	0.765	0.670
Drag Coefficient due to Incidence Angle, $C_{D_{i_h}}$ (rad ⁻¹)	0.029	0.026
Pitching Moment Coefficient due to Incidence Angle, $C_{m_{i_h}}$ (rad ⁻¹)	-6.19	-5.10
Lift Coefficient due to Elevator Deflection Angle, $C_{L_{\delta_e}}$ (rad ⁻¹)	0.161	0.253
Drag Coefficient due to Elevator Deflection Angle, $C_{D_{\delta_e}}$ (rad ⁻¹)	0.006	0.010
Pitching Moment Coefficient due to Elevator Deflection Angle, $C_{m_{\delta_e}}$ (rad ⁻¹)	-1.30	-1.94

Table 14-7: Skyblazer Series Class II Lateral-Directional Stability and Control Values

	Skyblazer-100	Skyblazer-200
Side Force Coefficient due to Side Slip Angle, C_{y_β} (rad ⁻¹)	-0.986	-0.735
Rolling Moment Coefficient due to Side Slip Angle, C_{l_β} (rad ⁻¹)	0.076	0.050
Yawing Moment Coefficient due to Side Slip Angle, C_{n_β} (rad ⁻¹)	0.0494	0.103
Side Force Coefficient due to Side Slip Angle Rate, $C_{y_{\dot{\beta}}}$ (rad ⁻¹)	-0.0407	-0.019
Rolling Moment Coefficient due to Side Slip Angle Rate, $C_{l_{\dot{\beta}}}$ (rad ⁻¹)	-0.003	-0.003
Yawing Moment Coefficient due to Side Slip Angle Rate, $C_{n_{\dot{\beta}}}$ (rad ⁻¹)	-0.023	-0.010
Side Force Coefficient due to Roll Rate, C_{y_p} (rad ⁻¹)	0.071	0.069
Rolling Moment Coefficient due to Roll Rate, C_{l_p} (rad ⁻¹)	-0.681	-0.664
Yawing Moment Coefficient due to Roll Rate, C_{n_p} (rad ⁻¹)	0	0
Side Force Coefficient due to Yaw Rate, C_{y_r} (rad ⁻¹)	0.396	0.616
Rolling Moment Coefficient due to Yaw Rate, C_{l_r} (rad ⁻¹)	0.027	0.075
Yawing Moment Coefficient due to Yaw Rate, C_{n_r} (rad ⁻¹)	-0.356	-0.351
Side Force Coefficient due to Aileron Deflection Angle, $C_{y_{\delta_a}}$ (rad ⁻¹)	0	0
Rolling Moment Coefficient due to Aileron Deflection Angle, $C_{l_{\delta_a}}$ (rad ⁻¹)	0.055	0.060
Yawing Moment Coefficient due to Aileron Deflection Angle, $C_{n_{\delta_a}}$ (rad ⁻¹)	0	0
Side Force Coefficient due to Rudder Deflection Angle, $C_{y_{\delta_r}}$ (rad ⁻¹)	0.093	0.148
Rolling Moment Coefficient due to Rudder Deflection Angle, $C_{l_{\delta_r}}$ (rad ⁻¹)	0.007	0.019
Yawing Moment Coefficient due to Rudder Deflection Angle, $C_{n_{\delta_r}}$ (rad ⁻¹)	-0.070	-0.090

Figure 14-1 and Figure 14-2 contain the trim diagrams at cruise conditions for the Skyblazer-100 and Skyblazer-200. The trim diagrams were developed in AAA.

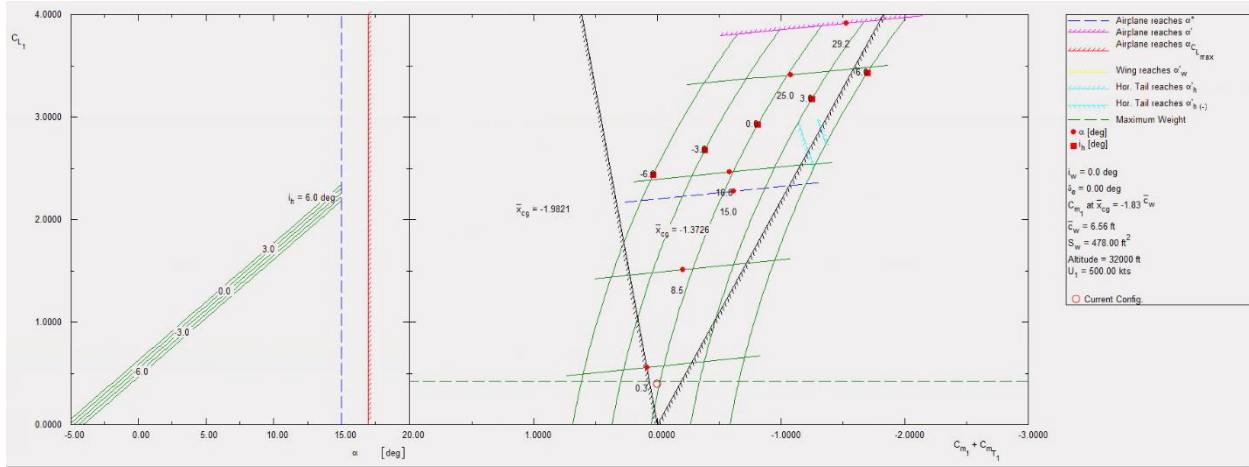


Figure 14-1: Skyblazer-100 AAA Trim Diagram During Cruise

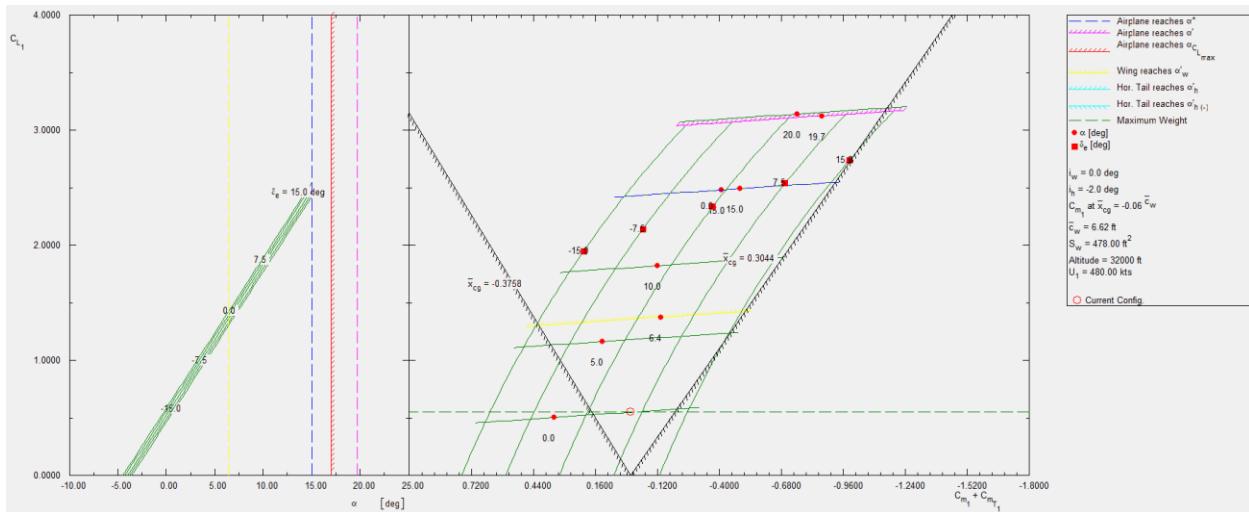


Figure 14-2: Skyblazer-200 AAA Trim Diagram during Cruise

Figure 14-3 shows the short period frequency requirement AAA plot for the Skyblazer during the cruise phase. The Skyblazer-100 appears to meet with level 1 handling qualities with short period frequency during cruise conditions.

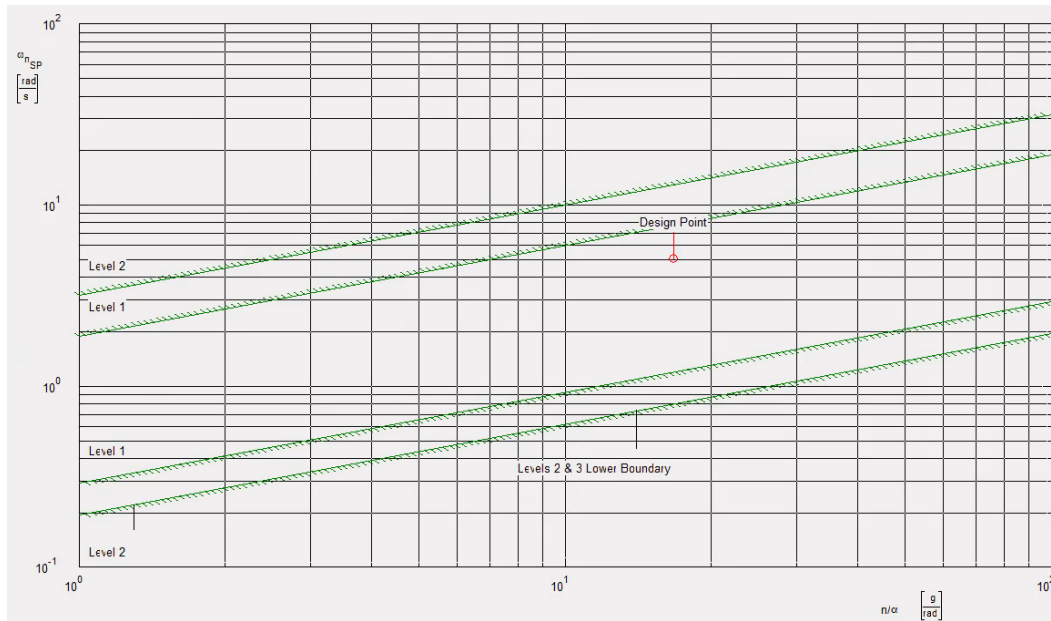


Figure 14-3: Skyblazer-100 AAA Short Period Frequency Requirements during Cruise

Figure 14-4 contains the short period frequency requirement AAA plot for the Skyblazer-200 during the cruise phase. The Skyblazer-200 appears to meet the level 1 flight phase qualities for short period mode during cruise conditions.

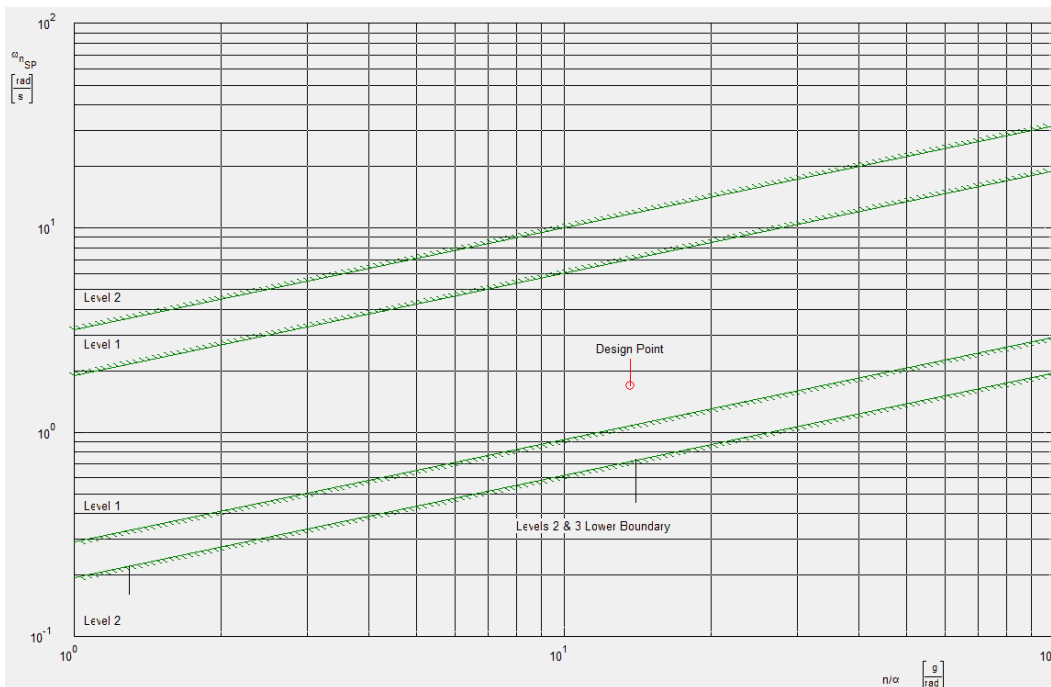


Figure 14-4: Skyblazer-200 AAA Short Period Frequency Requirements during Cruise

Figure 14-5 shows the Dutch roll frequency and damping ratio requirement AAA plot of the Skyblazer-100. The Skyblazer-100 appears to satisfy level 1 handling qualities for Dutch roll mode during cruise conditions.

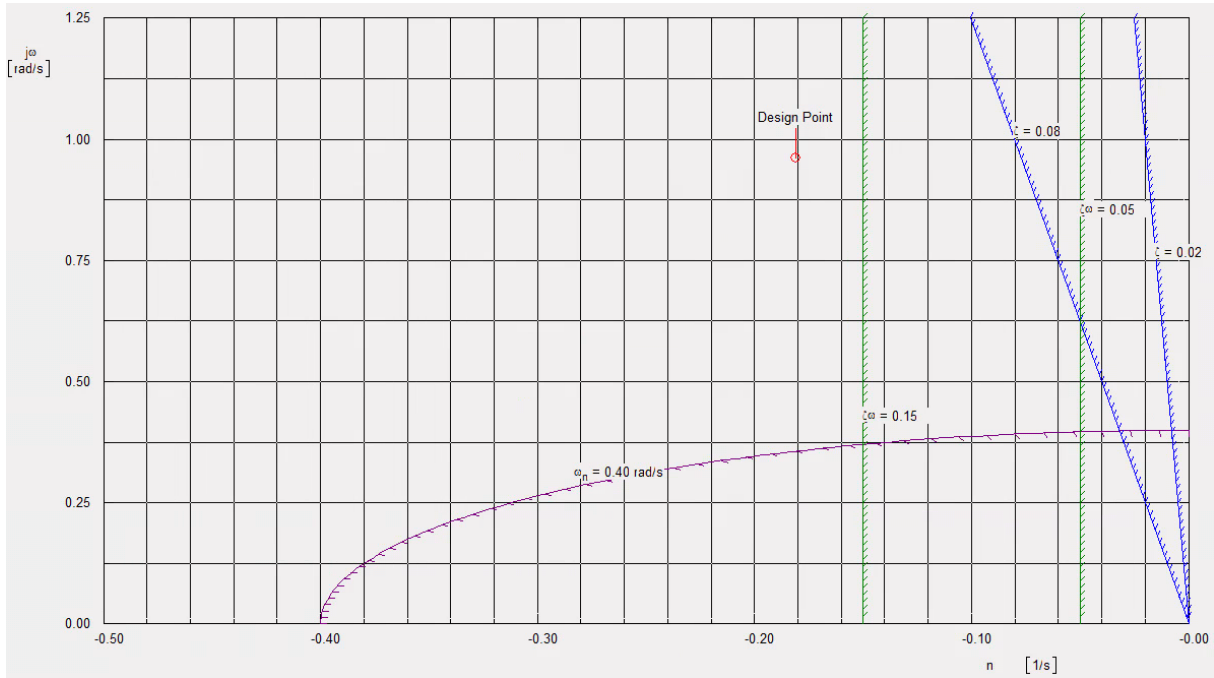


Figure 14-5: Skyblazer-100 AAA Dutch Roll Frequency and Damping Ratio Requirements during Cruise

Figure 14-6 contains the Dutch roll frequency and damping ratio requirement AAA plot for the Skyblazer-200 during cruise conditions. The Skyblazer-200 appears to satisfy the Dutch roll mode frequency and damping ratio level 1 handling qualities during cruise conditions. The sideslip feedback gain due to aileron deflection was used to set a default rolling moment coefficient due to the sideslip angle, which caused the design point in Figure 14-6 to shift in the desired requirement bounds.

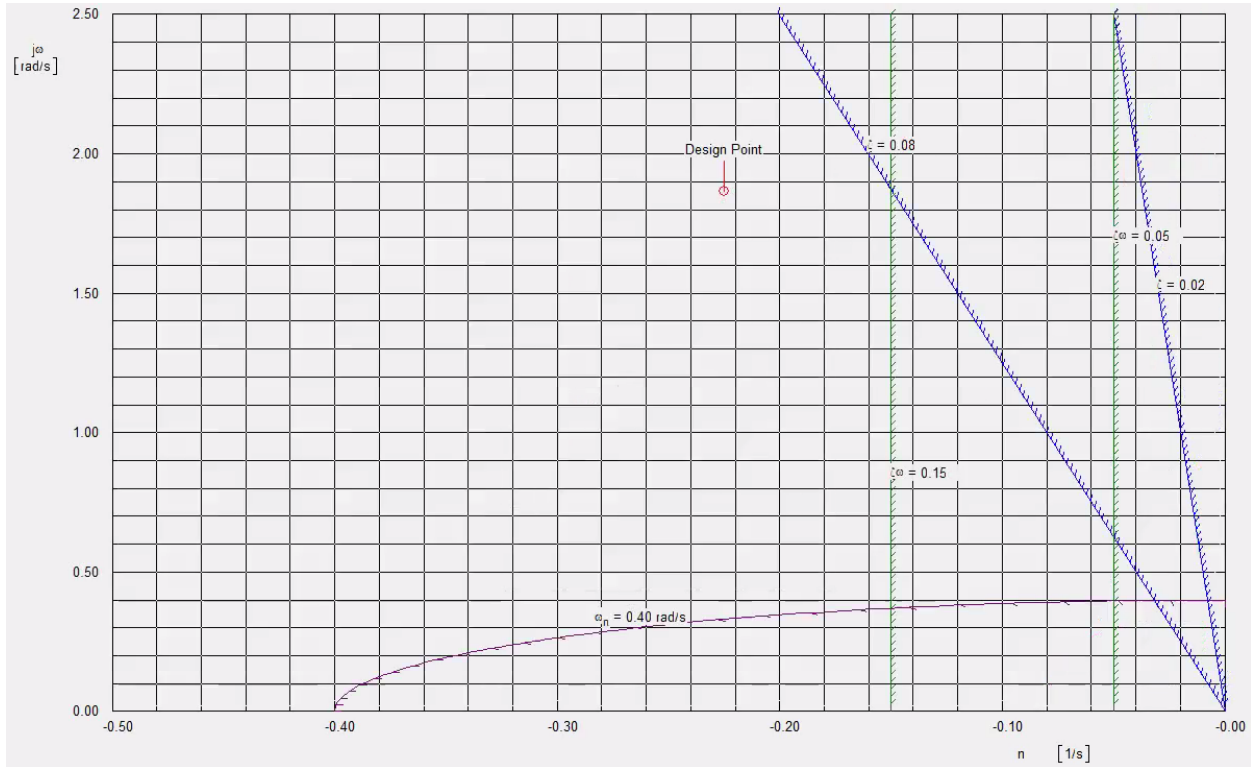


Figure 14-6: Skyblazer-200 AAA Dutch Roll Frequency and Damping Ratio Requirements during Cruise

Table 14-8 contains the ride comfort index values calculated for the Skyblazer-100, Skyblazer-200, and Embraer ERJ-145. The ride and comfort index is used to estimate passenger satisfaction when experiencing gusts of varying intensity. The ride comfort index is a function of the vertical and lateral accelerations of the aircraft in a gust. The accelerations are inversely proportional to the wing loading and are proportional to the lift coefficient due to angle of attack of an aircraft. The Skyblazer series aircraft have a higher wing loading compared to a typical regional jet. Therefore, a greater number of passengers will be satisfied while flying aboard the Skyblazer regional jets at each gust intensity level.

Table 14-8: Ride Comfort Index Values for Skyblazer Series and Competing Regional Jet Aircraft

Turbulence Intensity Probability of Exceedance	Skyblazer-100 Ride Comfort Index	Skyblazer-200 Ride Comfort Index	Embraer ERJ-145 Ride Comfort Index
Light	2.31	2.24	2.42
Moderate	3.41	3.06	3.87
Severe	6.38	5.31	7.82

15 Performance and Acoustics

15.1 Takeoff Performance

Table 15-1 contains the final performance metrics for the Skyblazer-100 and Skyblazer-200. Both Skyblazer series aircraft takeoff well within the required takeoff distances. The performance metrics were calculated assuming takeoff conditions with landing gear down. The ground effect helps the Skyblazer aircraft during takeoff by nullifying induced drag. The podded main landing gear and configuration also help minimize the zero-lift drag coefficient. The Skyblazer aircraft landing distance performance was the same as the takeoff distance. The performance metrics also show how both Skyblazer aircraft can take off and land in STOL runways.

Table 15-1: Class II Performance for the Skyblazer Series

Performance Metric	Skyblazer-100	Skyblazer-200
Takeoff Distance, s_{TO} (ft)	3190	4200
Takeoff Ground Distance, s_{TOG} (ft)	610	740
Balanced Field Length, BFL (ft)	3670	5260

15.2 Stall Performance

Figure 15-1 contains Schrenk’s Approximation plots for the Skyblazer series during clean conditions, respectively. During clean conditions, it appears both Skyblazer variants will stall at the root wing chord before any other place along the wing. The wings will stall at a load 50 times than that of their takeoff weight. The engine mounts disrupt the lift by generating zero lift from about 4.68 ft out to 10.21 ft from the centerline, as seen in Figure 15-1.

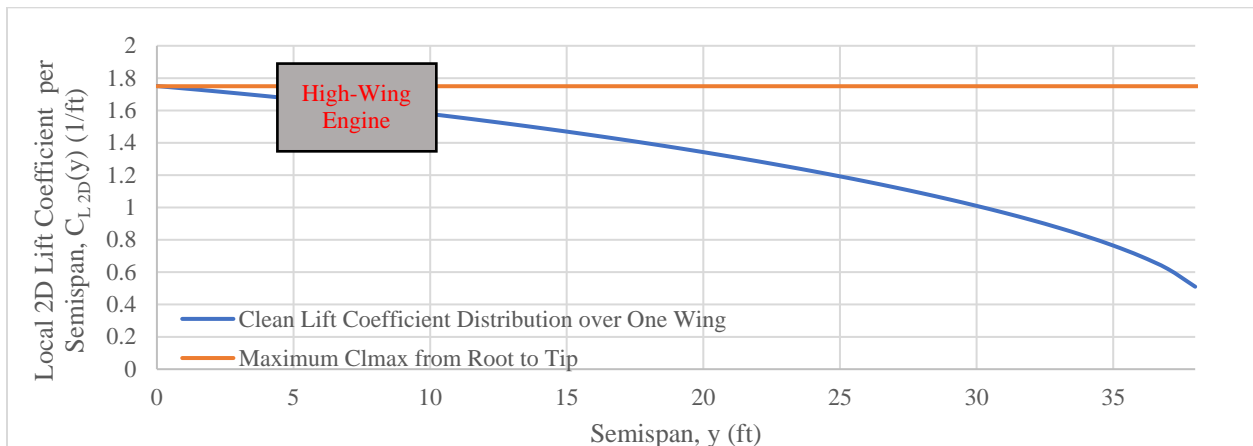


Figure 15-1: Skyblazer Series Schrenk’s Approximation Plot for Clean Condition

15.3 Drag Polar and Wetted Area

The wetted area of each major aircraft component (fuselage, wings, engines, empennage) were calculated to obtain drag polars to a higher accuracy.

15.3.1 Fuselage Wetted Area

For fuselage, the perimeter method is usually the most efficient way to find the wetted area. Eqn. 15.1 displays the mathematical way a finding the wetted area of the fuselage with the assumption that the mid-section of the fuselage

has a circular cross-section. The 50-seat has a calculated fuselage wetted area of 1,896 ft² while the 76-seat has a value of 2,167 ft².

$$S_{wet_{fus}} = \pi D_f l_f \left(1 - 2 \left(\frac{l_f}{D_f} \right)^{\frac{2}{3}} \left(1 + \left(\frac{1}{\frac{l_f}{D_f}} \right)^2 \right) \right) \quad \text{Eqn. 15.1}$$

Figure 15-2 and Figure 15-3 display the fuselage stations with varying cross-sections. By obtaining the perimeter at the selected cross-sections, the data can be plotted to calculate the estimated wetted area of the fuselage. The overall wetted area plot can be seen in Figure 15-4. When comparing the area found from Eqn. 15.1 and the perimeter plots, the area depicted in the perimeter plot is always greater. This is due to the sponsons which are not accounted for in the equation but are included when performing the perimeter plots. The peaks seen in Figure 15-4 are due to the sponson integration which causes the wetted area around the mid-section of the fuselage to be a lot greater when compared to the rest of the fuselage. When calculating the error between the calculated and measured, the 50-seat variant has an error on 14% and the 76-seat has an error of 17%. As stated earlier, this error can be attributed to the lack of sponson intergaration. The perimeter plot area will be used for the drag polar calculatona as this correctly represents the wetted area of the fuselage.

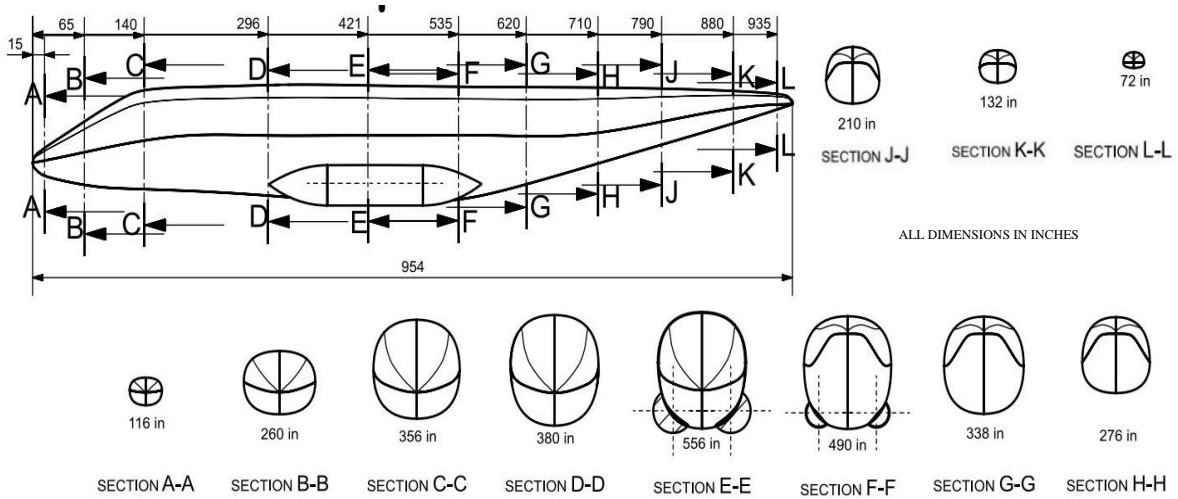


Figure 15-2: 50-Seater Perimeter Cross-section Analysis

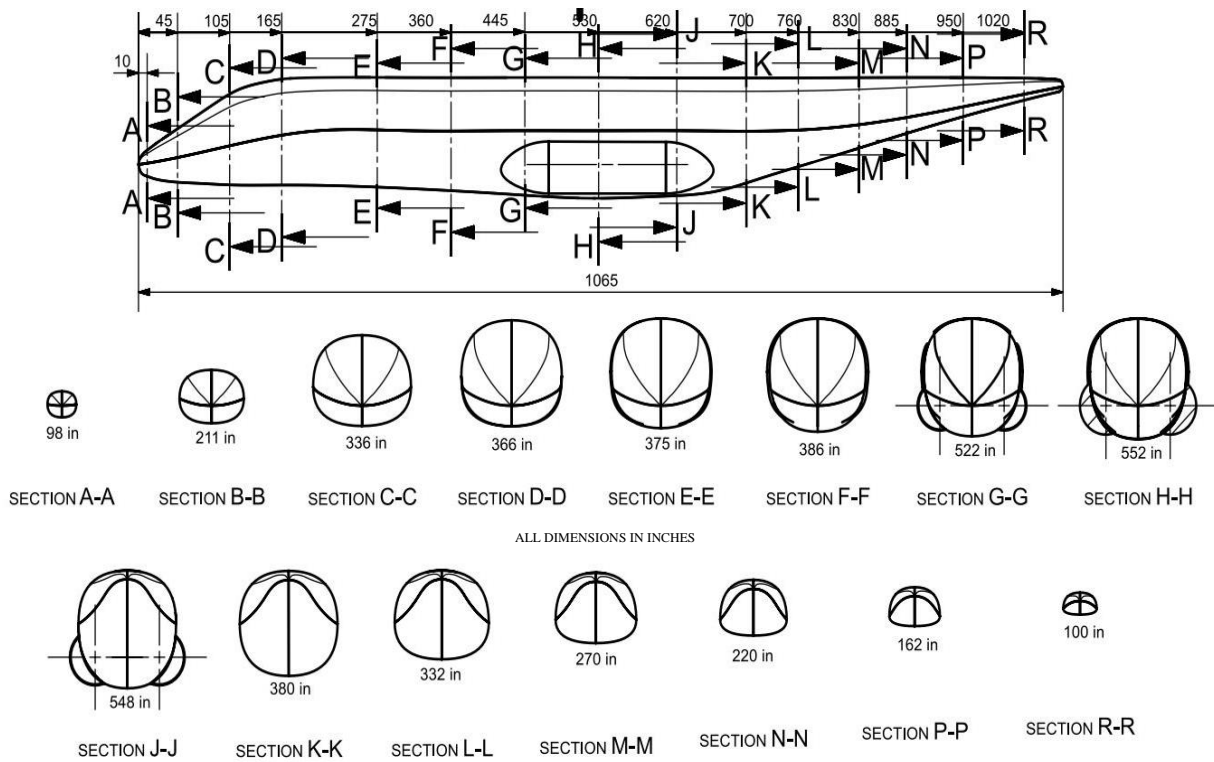


Figure 15-3: 76-Seater Perimeter Cross-section Analysis

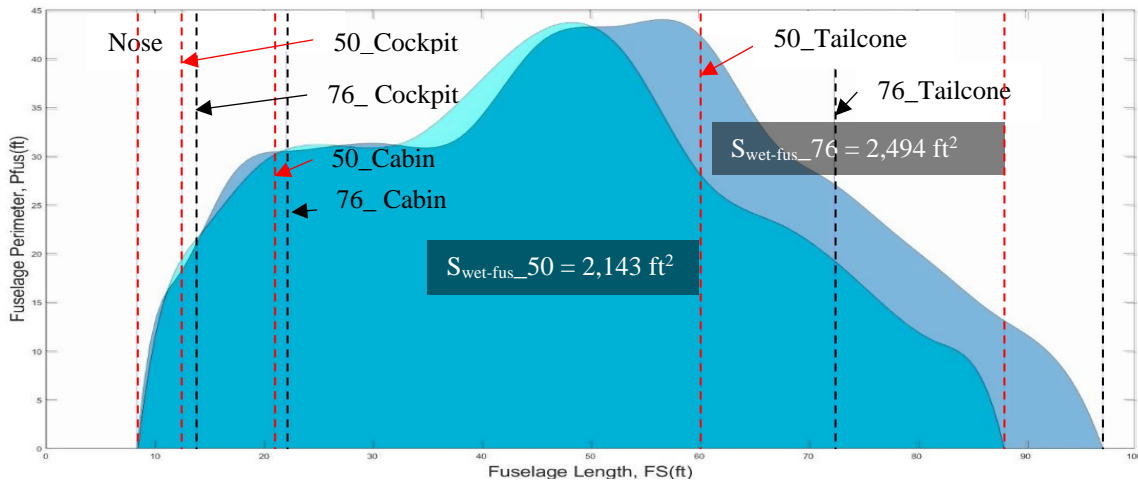


Figure 15-4: 50 Seat and 76 Seat Variant Wetted

15.3.2 Engines Wetted Area

The engine design does not have a gas generator cowling or plug contributing to the wetted area. The only

component contributing to the wetted area is the fan cowling and Eqn. 15.1. Eqn. 15.3

$$S_{wet_{fan}} = D_n l_n \left(2 + \frac{0.35 l_1}{l_n} + \frac{0.81 l_1 D_{h1}}{l_n D_n} + 1.15 \left(1 - \frac{l_1}{l_n} \right) \left(\frac{D_{ef}}{D_n} \right) \right) \quad \text{Eqn. 15.3}$$

can be used to calculate the wetted area of the engine with a calculated final value of 213 ft².

$$S_{wet_{plf}} = 2 S_{exp.plf} \left(1 + \frac{\left(\frac{t}{c} \right)_r \left(1 + \left(\frac{t}{c} \right)_r \left(\frac{c_t}{c_r} \right) \right)}{4 \left(1 + \frac{c_t}{c_r} \right)} \right) \quad \text{Eqn. 15.3}$$

15.3.3 Wing Wetted Area

Wing geometric characteristics are used to calculate the wetted area with the final wing geometry and resulting wetted area is shown in Table 15-2.

Table 15-2: Wing Wetted Area

$S_{exp.wing}$ (ft²)	268.5
Root Chord, c_r (ft)	9
Root Thickness, t_r (ft)	1.25
Tip Chord, c_t (ft)	3.6
Tip Thickness, t_t (ft)	6

15.3.4 Empennage Wetted Area

The planform wetted area equation was also used to find the wetted areas of the horizontal and vertical tails. Characteristics used to solve for the empennage wetted areas are outlined in Table 15-3. The summation of the of the wetted area can be seen in Table 15-4.

Table 15-3: Empennage Wetted Area Characteristics

Characteristic	Horizontal Tail	Vertical Tail
S_{wet} (ft²)	190	266
$S_{exp.planform}$ (ft²)	93.6	130
Root Chord, c_r (ft)	8	12
Root Thickness, t_r (ft)	0.96	1.43
Tip Chord, c_t (ft)	2.4	9.6
Tip Thickness, t_t (ft)	0.288	1.15

Table 15-4: Total Wetted Area

	50-Seat	76-Seat
Total Wetted Area (ft²)	3349	3711



15.4 Acoustics

Jet engine acoustic suppression principles were applied when determining configuration of the aircraft. Acoustic suppression principles include keeping jet exit velocities low, enhancing mixing, observing the direction of reflected noise with respect to passengers, airframe, and observers, damping out vibrations transmitted to airframe, and lastly by limiting fan disk tip speeds to high subsonic.



Figure 15-6: Skyblazer Acoustic Refraction

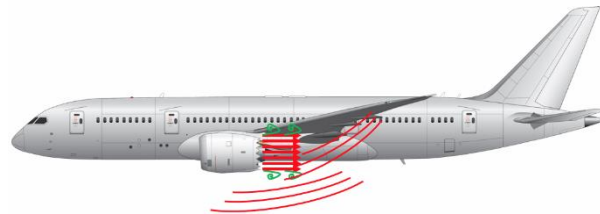


Figure 15-7: EMB-190 Acoustic Refraction

The Skyblazer has taken steps to suppress acoustics through the use of high-bypass engines which reduces the shear layer intensity resulting in smaller vortex sheets. Also, due to the high wing- high engine configuration the acoustic waves will be reflected upwards shown in Figure 15-6 unlike the EMB-190 refracting acoustic waves downward shown in Figure 15-7. This will greatly reduce the acoustics experiences from observers on the ground. In terms of

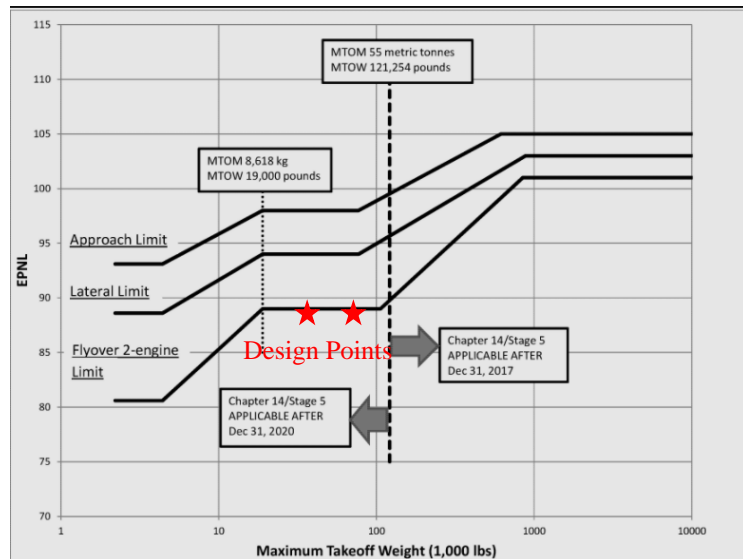


Figure 15-8 Stage 5 Airplane Noise Standards [44]

cabin noise, the Skyblazer will not excite ovality modes, unlike DC-9 configured aircraft due to the engine location which suppresses cabin noise. As a result of these decisions to reduce acoustic suppression the Skyblazer will be compatible with the lowest stage 5 Airplane Noise Standards flyover 2-engine limit shown in Figure 15-8. This is true because as the Skyblazer flies by the noise will only be radiated upwards. This is the business plan, and this is important as it allows for the Skyblazer to takeoff earlier in the morning and fly later at night. This allows for more operations hours during a flight day and compliments the design philosophy of the Skyblazer Series.

16 Cost Analysis

A semi-conventional regional jet configuration was chosen to minimize manufacturing and maintenance costs. A few assumptions were made when preparing the price estimate, this includes a profit margin of 10%, increased safety testing costs due to the sponsors, high The price of the aircraft were estimated using AAA’s cost section and the aircraft price in respect to the number of units manufactured curve is shown in Table 16-1. The price of similar aircraft are shown on the same graph by taking data collected and extrapolating those costs out to 2030 using a 3% inflation rate each year. Taking the considerations from Figure 3-4 and Figure 3-5 leads the team to target selling 800 of each aircraft as an acceptable market size. Using AAA to calculate the Life Cycle Cost, Direct Operating Costs, and Manufacturing Costs, provides the teams with the following graphs and charts of data. This data assumes a 15% profit margin and that all 800 aircraft are manufactured at a rate of 6.67 aircraft/month (80 aircraft/yr).

Table 16-1: Skyblazer Cost and Price

	Acquisition Cost (\$ Millions)	Price Per Aircraft (\$ Millions)
Skyblazer 100	26.3	31.9
Skyblazer 200	37.2	42.7

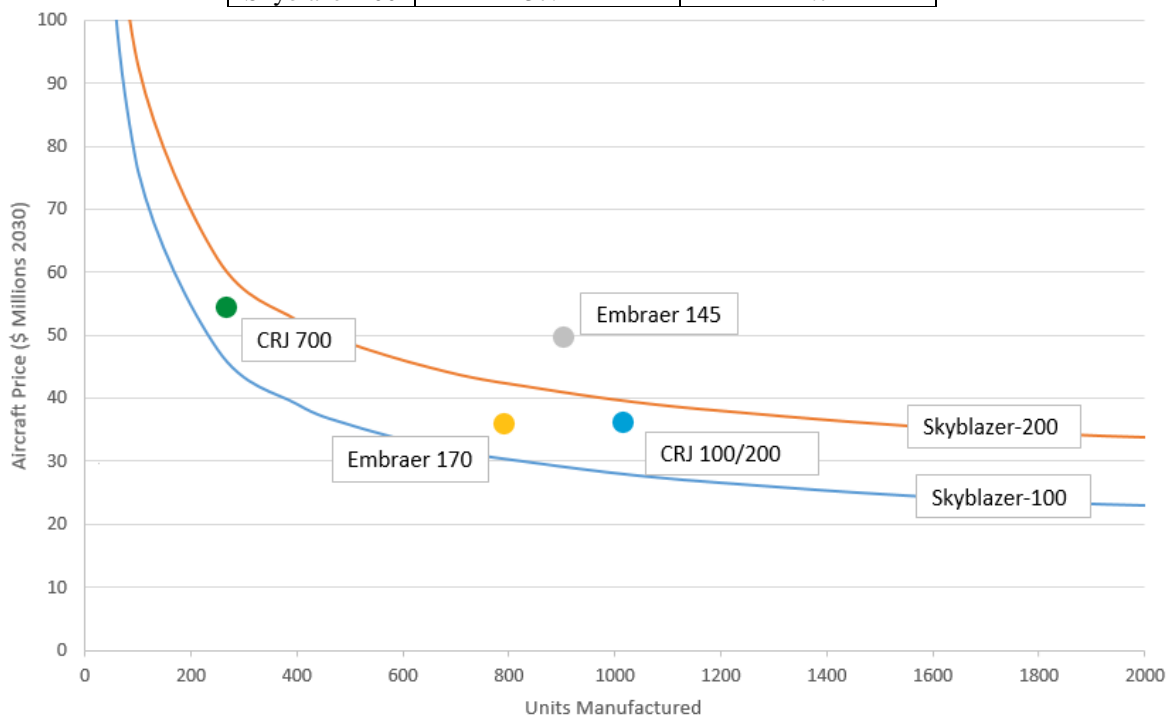


Figure 16-1: Aircraft Price vs Units Manufactured [45][46][47][48]

Table 16-2: Skyblazer General Costs in Millions of Dollars

	Engineering/Design Cost (\$ Millions)	Production Tooling Cost (\$ Millions)	Facilities Cost (\$ Millions)	Labor Cost (\$ Millions)
Skyblazer 100	216	572	894	3,889
Skyblazer 200	420	602	915	5,795

Table 16-3: Skyblazer Direct Operating Cost in Dollars Per Nautical Mile

	Fuel/Oil/Lubricant Cost (\$/nm)	Crew Cost Cost (\$/nm)	Maintenance Cost (\$/nm)
Skyblazer 100	1.95	1.3	2.1
Skyblazer 200	3.34	1.7	2.52

Table 16-4: Skyblazer Direct Operating Cost in Millions of Dollars

	Fuel/Oil/Lubricant Cost (Millions \$)	Crew Cost Cost (Millions \$)	Maintenance Cost (Millions \$)
Skyblazer 100	901	600	971
Skyblazer 200	1,544	785	1,165

Table 16-2 lays out the costs provided by the AAA analysis for engineering and design research and development costs, production tooling costs, facilities costs, and labor costs. The facilities costs is estimated to be higher than average to provide for appropriate safety testing of the emergency and crash safety system designs. The direct operating costs for Fuel/Oil/ and Lubricant Cost, Crew Cost, and Maintenance Costs are shown in terms of dollars/nmi and total cost in millions of dollars in Table 16-3 and Table 16-4 respectively.

To provide the team with knowledge of potential profits the team collected some information from the Bureau of Transportation statistics and American Airlines' investor data. The average seat price of \$353 [49] was adjusted for inflation to \$441 and the average seat fill of 80% [50] was decreased to 70% due to the higher number of turns per day the Skyblazer expects to achieve. The max seat miles per year for the Skyblazer, chosen to be 11 flight hours per day or 4000 flight hours per year, and all previous described assumptions were made in this calculation. This is shown in Table 16-5 with a profit of \$523 million for the Skyblazer-100 and \$623 million for the Skyblazer-200.

Table 16-5: Potential Profit of Skyblazer Aircraft

	Flight Hours Per Year	Seat Miles per Year	Gross Income (\$ Millions)	Life Cycle Cost (\$ Millions)	Profit (\$ Millions)
Skyblazer 100	4000	1,600,000	887	364	523
Skyblazer 200	4000	1,500,000	1,349	716	632

References

- [1] AIAA, "Request for Proposal: Modern Regional Jet Family," 2021, [Online].
- [2] BAE Systems, "De Havilland Comet 1&2," 5 February 2021.
- [3] Smithsonian Magazine, "Comet's Tale," 5 February 2021.
- [4] Embraer, "Embraer Commercial Aviation," 5 February 2021.
- [5] T. Aviation, "Trans State Airlines Taps Universal for ERJ 145 ACARS, Datalink," 5 February 2021.
- [6] L. Linares, "The Bombardier CRJ Family," 10 May 2017.
- [7] The Flight, "Bombardier CRJ-100 SkyWest.," 8 February 2021.
- [8] Ben, "What is the CRJ550?," 7 February 2019.
- [9] Anon, "Fairchild Dornier 328JET," Wikipedia, 2021.
- [10] Delta, "Bombardier CRJ-700," 2021.
- [11] Michelin, "The MICHELIN Air X tire homologated to fit the Embraer E170," 2019.
- [12] Embraer Commercial Aviation, "E170," 2021.
- [13] Mitsubishi Aircraft Corporation, "Introducing Mitsubishi SpaceJet," 2019.
- [14] M. Tyrrell, "Mitsubishi Aircraft Corporation introduces SpaceJet aircraft family," Aerospace Manufacturing, 2019.
- [15] Bombardier, "CRJ Airport Planning Manual," 8 February 2021.
- [16] Aircraft Compare, "Bombardier CRJ 550," 8 February 2021.
- [17] Global Air, "CRJ700," 2021.
- [18] World Airline News, "World Airline News 12 July 2012," 9 February 2021.
- [19] A. Mozdzanowska, J. R. Hansman, J. Histon and D. Delahaye, "Emergence of Regional Jets and The Implications on Air Traffic Management," Air Traffic Management Research & Development Seminar, Budapest, 2003.
- [20] K. Belson, "Increasingly, It's a Tight Squeeze in the Air," *The New York Times*, 6 May 2009.
- [21] "Airline Pilot Forums," MH Sub I, LLC dba Internet Brands, 2017
- [22] J. Dahan, "Cleared to Dream," Air Line Pilots Association, INT'L, 2021
- [23] Barrett-Gonzalez, R., 2021. *AE 522 Regional Jet Lecture April, 8, 2021*
- [24] Barrett-Gonzalez, R, and A. McKinnis, "Statistical Time and Market Predictive Engineering Design (STAMPED) Vector Analysis Techniques," Industry, Engineering & Management Systems Conference, Clearwater Beach, 2019.
- [25] M. Schultz, J. Evler, E. Asadi, H. Preis, H. Fricke and C.-L. Wu, "Future aircraft turnaround operations considering post-pandemic requirements," *Journal of Air Transport Management*, vol. 89, 2020.
- [26] Lewis, P., "SkyWest pursues expansion plans."
- [27] "Skywest – Facts," *Skywest Airlines*, 2021.
- [28] Becker, Helane, and Cunningham, Conor, "Pilot Retirements Accelerate Beginning In 2021 & Peak in 2025" 5 July 2017.
- [29] Tom Boom "How Ryanair Manages Super Tight Turn Arounds" March, 2021
- [30] Roskam, Jan, *Airplane Design Part I: Preliminary Sizing of Aircraft*, DARcorporation, Lawrence KS, 1985.
- [31] Doria, C, "McDonnell Douglas MD-82 (DC-9-82) – American Airlines," *VerticalScope Inc.*
- [32] Anon, "C-17 Globemaster II," *AllOnGeorgia*.
- [33] Anon, "Telair.pdf," *Telair International*,
- [34] *CF34-3 turbofan engine with GE Aviation*, Cincinnati OH, Presentation.
- [35] *CF34-8C turbofan propulsion system with GE Aviation*, Cincinnati OH, Presentation.
- [36] Anon, "Boeing YC-14," Wikipedia, 2021.
- [37] Anon, "McDonnell Douglas YC-15," Wikipedia, 2021.
- [38] Anon, "Antonov An-72," Wikipedia, 2021
- [39] Roskam, J., *Airplane Design Part IV: Layout of Landing Gear and Systems*, Lawrence: DARcorporation , 2010.
- [40] Roskam, J. *Airplane Design Part V: Component Weight Estimation*, Lawrence: DARcorporation , 2010.
- [41] Danaher Motion, "Dynamic Servo Actuators," 2006.
- [42] Veerapaneni, Anilkumar. Simulation of Enhanced Ground Proximity Warning System using VHDL, 2014.
- [43] Roskam, J. *Airplane Design Part VII: Determination of Stability, Control and Performance Characteristics: FAR and Military Requirements*, Lawrence: DARcorporation , 2018.

- [44] Federal Aviation Administration (FAA), DOT, 82 FR 46123, page 46123-46132, 2021.
- [45] Anon, "Bombardier CRJ700 Series," Wikipedia, 11 May 2021.
- [46] Anon, "Bombardier CRJ100/200," Wikipedia, 2 Apr. 2021.
- [47] Anon, "Embraer ERJ Family," Wikipedia, 7 May 2021.
- [48] Anon, "Embraer E-Jet Family," Wikipedia, Wikimedia Foundation, 8 May 2021.
- [49] "First Quarter 2019 Air Fare Data," First Quarter 2019 Air Fare Data | Bureau of Transportation Statistics, 2019.
- [50] "American Airlines Reports Fourth-Quarter and Full-Year 2020 Financial Results," American Airlines, 28 Jan. 2021.